TECHNOLOGY • RESEARCH HIGHLIGHTS • VISIONS • SCIENCE

77

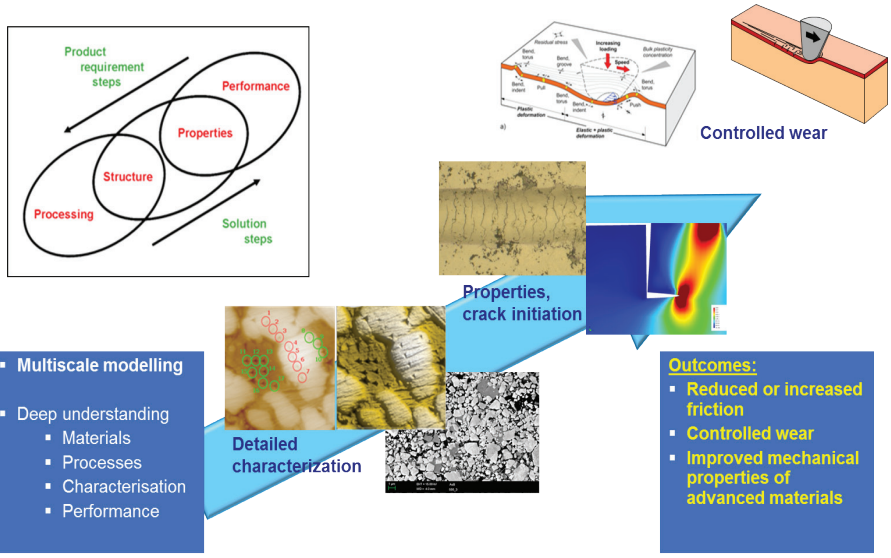

Multiscale modelling and design for engineering application

VTT TECHNOLOGY 77

Multiscale modelling and design for engineering application

Tarja Laitinen & Kim Wallin (Eds.)

ISBN 978-951-38-7913-6 (Soft back ed.)
ISBN 978-951-38-7914-3 (URL: http://www.vtt.fi/publications/index.jsp)

VTT Technology 77

ISSN-L 2242-1211
ISSN 2242-1211 (Print)
ISSN 2242-122X (Online)

JULKAISIJA – UTGIVARE – PUBLISHER

VTT
PL 1000 (Tekniikantie 4 A, Espoo)
02044 VTT
Puh. 020 722 111, faksi 020 722 7001

VTT
PB 1000 (Teknikvägen 4 A, Esbo)
FI-02044 VTT
Tfn +358 20 722 111, telefax +358 20 722 7001

VTT Technical Research Centre of Finland
P.O. Box 1000 (Tekniikantie 4 A, Espoo)
FI-02044 VTT, Finland
Tel. +358 20 722 111, fax +358 20 722 7001

Kopijyvä Oy, Kuopio 2013

Foreword

Utilizing 3D design procedures in manufacturing industry is well matured in industrial R&D. The shape of the components, design of the machine or the vehicle, assembly and finally the whole production are designed virtually through computational methods, which naturally offer flexibility and speed to the design phase. Simulation and virtual verification of the designed components is rapidly increasing and can further shorten R&D phase dramatically.

However, virtual material values or models available for digital design and simulation are still limited. Due to the lack of digital material values the huge potential of tailored performance can not be fully exploited. We at VTT have recognized that for the economic and ecologic use of materials, digital design tools for material design are a necessity of the digital design chain.

Development of new materials and understanding of material and process behaviour is always a complex equation of crossing interactions. Physical and chemical phenomena are affected from the nano- and/or molecular level up to macroscopic level. Interactions between the material performance, properties, microstructure and processing methods need to be understood more deeply. For this purpose, modelling skills have developed rapidly in recent decades, with the support of increased numerical calculation capacity and commercial multi-level and multi-physics software development.

At VTT we have a great capacity and potential for exploiting this competence. It is recognised that there are many activities related to materials and process modelling in various scales, based on various methodologies and targeting various applications. At VTT we have a strong vision to bring this knowledge better together creating opportunities for multiscale approaches as well as to offer a platform for cross learning experiences. At the same time, it is clear that good modelling goes hand in hand with experimental verification. Modelling creates more detailed understanding of phenomena, while experimental verification directs the model to correctly reflect and predict the real world phenomena. Also in this sense VTT can offer a 360° service as VTT's competences are well recognised in many fields combining modelling and in experimental research.

Research programmes play essential roles in VTT's day-to-day operation. They are the main vehicle for implementing VTT's strategy. The programmes produce comprehensive technology-based solutions aiming at industry renewal and thus have a great impact on the society and industries. They also provide a platform for

longer-term interaction and collaboration with VTT's clients, financiers and other stakeholders. Last, but not least, the programmes encourage transdisciplinary research and new openings within VTT.

In this publication we are presenting some highlights from our current modelling activities obtained in VTT's MultiDesign innovation programme. We hope they will inspire new ideas in your mind on what could be done and obtained via digital approach to design. We are happy to discuss your thoughts further as to how we could help you take MultiDesign approaches to the next level for the benefit of industry, research community, and society at large.

Espoo, February 5th, 2013

Erja Turunen, Vice President
VTT Strategic Research, Applied Materials

Contents

1. Multiscale modelling of engineering materials

Anssi Laukkanen, Kenneth Holmberg & Kim Wallin

VTT Technical Research Centre of Finland
Metallimiehenkuja 8, P.O. Box 1000, FI-02044 Espoo

1.1 Abstract

Outline of multiscale modelling and the process-structure-properties-performance (PSPP) concept is presented. Brief description of multiscale modelling methods is provided following their range of application in spatial and temporal ranges. The PSPP concept as a state-of-the-art modelling assisted material design procedure is described. Case examples illustrating the material features incorporated to a PSPP analysis are given, emphasizing the modelling of realistic material structures in the nano to microstructure range and on the other hand the mechanisms responsible for material performance in a component environment.

1.2 Introduction

A trend which has gained momentum during the last decade is a loose integration of computational methods under the banner of multiscale modelling. The core idea of multiscale modelling is not in the effusive complication of materials related modelling tasks, but the realization that present day material modelling means can be effectively used in solving materials related engineering problems and systematically aim towards optimal material solutions on a component specific case by case basis. These abilities were previously unobtainable due to affiliated limitations in available computational methodologies and resources, but have reached a degree of maturity during the last five to ten years. Thus, the argument is that incorporation of material modelling systematically in material development, tailor-

ing and selection processes enables the development of materials with improved performance, better utilization and leads to more cost effective solutions.

Carrying out modelling in a productive manner requires tight integration of experimental and modelling activities, experimental activities being for example material characterization and testing in the context of the desired function. Modeling is a synonym for understanding and quantifying what actually takes place when the material performs the critical functions it is supposed to, and such an activity can not be effectively carried out solely from a modelling standpoint, when the methods being applied to a particular case have not matured to a status with predictive abilities. As such, in an optimal scenario material processing, characterization, testing and modelling activities form a tightly knit cross-linked bundle. In a material design task, one such way of operation is the process-structure-properties-performance (PSPP) methodology, or the VTT ProperTune method. The purpose in utilization of such concepts is to provide tools which integrate the various necessary means and methods into a workable whole, enabling and defining the required interactions between the various manufacturing, experimental and modelling activities.

The interplay between modelling and experimental work, emphasizing the role of modelling in materials research, is presented in the tried and tested Figure 1. The role of building sound mechanistic and physically grounded understanding of the problem is emphasized, and in Figure 1 is demonstrated by levels 1 to 2. Applying modeling as an exploratory tool is extremely laboursome and not recommended at such stages due to its inefficiency. After obtaining a degree of understanding, a typical step is the building of a qualitative or simplified theoretical basis which is in line with available observations. At this point tools such as multiscale modelling become attractive when the understanding of the problem has matured to a state where a quantitative model can be formulated. Thus, the multiscale modelling approach can be best formulated on the basis of early understanding of the problem obtained on an empirical basis, after which the modelling task contains the derivation and validation of a quantitative model first utilizing the available results pool. Being successful, the sound basis provides means for identifying the applicability of the resulting model, and its abilities as far as being able to predict behaviour outside the data contained within the confines of model validation. As the rudimentary division implies, obtaining that predictive ability for a new phenomenon and material does require extensive contributions in terms of labour.

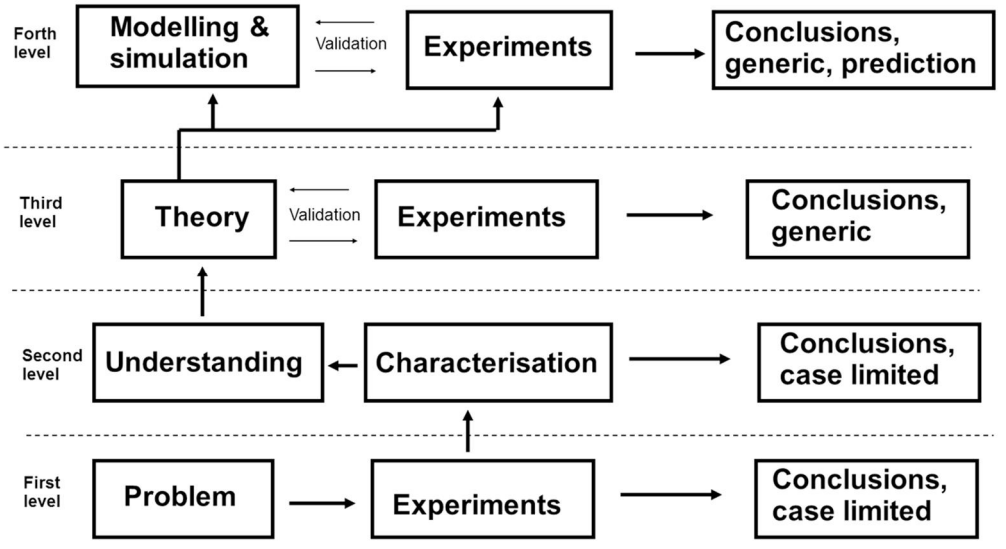

Figure 1. Role of modelling and empirical work in obtaining predictive capability for materials related problems.

Current work is organized to a provide a brief outline of multiscale modelling, primarily arising from experiences with engineering materials such as metallic, hybrid composite (polymer or metal matrix composites), ceramic or polymer materials either as coatings or bulk material. Most of the content is as such fairly general and the means and methods can be generalized to various specific materials, a testament to the applicability of multiscale modelling. Multiscale modelling is explored from two different angles crucial for most modelling tasks – what it in reality contains and how does it describe the material and its behaviour, and how to successfully apply it in finding materials related solutions. The former is a methodology based description, while the latter emphasizes methods of work, concepts, such as the PSPP methodology. Brief selected case examples are provided to demonstrate the sort of material features and phenomena which can be incorporated in multiscale analyses, the emphasis being in meso-scale analyses of mechanical, fracture and wear behaviour.

1.3 Multiscale modelling

Multiscale modelling usually relies on establishing modelling toolkits and packages for solving material related problems by incorporating an array of methods over a vast range of spatial and temporal scales. One way of organizing multiscale modelling methods and demonstrating some of the spatial and temporal linkages is presented in Figure 2. The presentation as given here is inclined towards problems of strength, fracture and wear of materials. The modelling methods can be

roughly divided to two categories, discrete and continuous methods on the basis of how they describe materials. A descriptive synonym often used for discrete methods is atomistic methods. Methods are present which enable the treatment of physical phenomena at small atomistic scales or primarily nanoscale structures, like various ab initio approaches, molecular dynamics or specific topics of interest such as dislocation dynamics of deformation behaviour in ordered materials. Atomistic methods can be applied more effectively to time controlled phenomena, such as diffusion, aging, deformation mechanisms etc. by incorporation of stochastic, usually Monte-Carlo based, methods. The macroscale continuous region is commonly populated by methods arising for example from solid or fracture mechanics. Of note is also the increasing use of discrete methods, such as coarse grained molecular dynamics. The range in between, often referred to as the mesoscale, is for several materials an interesting one since it often contains from a practical solution standpoint many interesting material features, such as microstructures (and it can be directly coupled to component macroscale operating environments). Methods of this intermediate scale typically deal with microstructures and how material properties are affected by mechanisms active in multiphase structures, grain structures, interfaces and various different types of substructures.

The underlying idea is not to perform extremely and overtly complex numerical analyses, but to identify the key features having the greatest impact on a specific material problem or goal and model them quantitatively. Performing analyses with a high degree of concurrence and coupling is usually not the best approach in attacking a specific problem. The most common example for many engineering materials is the structure-properties-performance chain from the PSPP method. In such a context, the problem is typically laid out such that the focus is in understanding what are the features of material microstructure (or nanostructure) which are most prevalent in finding the optimal solution for the material problem at hand, or “simply” understanding what are the features in the current material selection responsible for the observed behaviour and performance of the material in a component setting. As such, a fair way of comprehending multiscale modelling is to view it as a framework having the ability to pick the viewpoint to a material from the “buffet” offered by the available methods which has the greatest impact on the end result, performance requirement, cost or simply the desired outcome. If need be in the long run, coupling and complicating the numerical model as seen appropriate can be performed by incorporation of new features, mechanisms and methods. For many scenarios, certain very specific material qualities are relevant for a set of active mechanisms, and as such a multiscale analysis does not need to be overtly complex in order to yield a desirable outcome. A classic example would be the identification of microstructural features most prevalent to deformation behaviour, as such to discover dependencies responsible and impacting material strength and mechanisms of fracture.

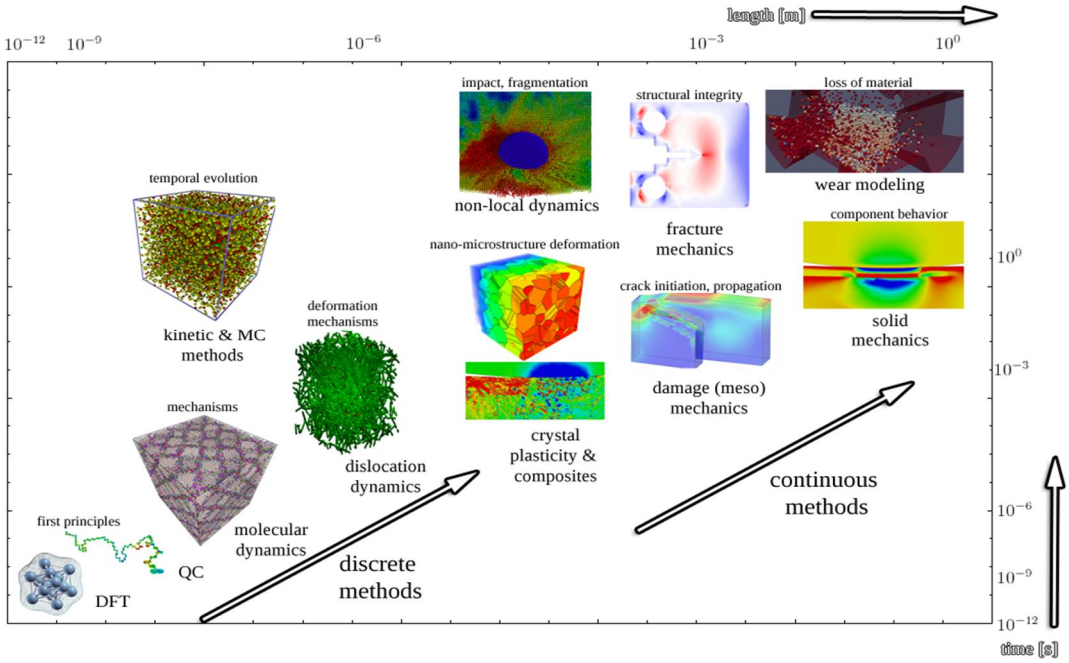

Figure 2. Multiscale modelling methods for deformation, fracture and wear organized according to their nominal spatial and temporal ranges.

1.4 Process-Structure-Properties-Performance, PSPP

Multiscale modelling by way of looking at the various methods and even mechanistic understanding itself does not describe in detail its successful application or how to include it in material design and tailoring tasks, keeping in mind that the whole process effectively entails integration to experimental and characterization activities. For this reason, application concepts have been developed and one of prominent ones is the process-structure-properties-performance concept, or the PSPP concept, which is presented schematically in Figure 3. VTT ProperTune is an implementation of the PSPP concept. The PSPP concept is a template for seeking a solution to material design and optimization tasks. The outline is such that in order to provide the necessary freedom for finding the optimal solution material processing (manufacturing) stage, or stages, with its processes and their parameters is tied to comprehension of the resulting material structure, by way of utilizing modeling and experimental means. The structure followingly yields and is coupled to material properties, this link being established again by combining both experimental and modelling approaches. Properties when the material undergoes the conditions and mechanisms it experiences in a component setting translate to material performance. Modeling and experimental activities are intertwined and coupled throughout the PSPP chain, and the couplings are established in a case

specific manner in order for the overall methodology to support the finding of an optimal solution. However, the crux of the concept is to let go of the dated trial and error founded “let’s see what we can do” or “pipeline” approaches, and initiate the process from performance requirements (typically “performance at a cost”). The processing, experimental and modelling methodologies are adapted to finding the solutions meeting these conditions and identifying the case specific features being able to yield solutions meeting desired criteria and requirements for material use at a component scale.

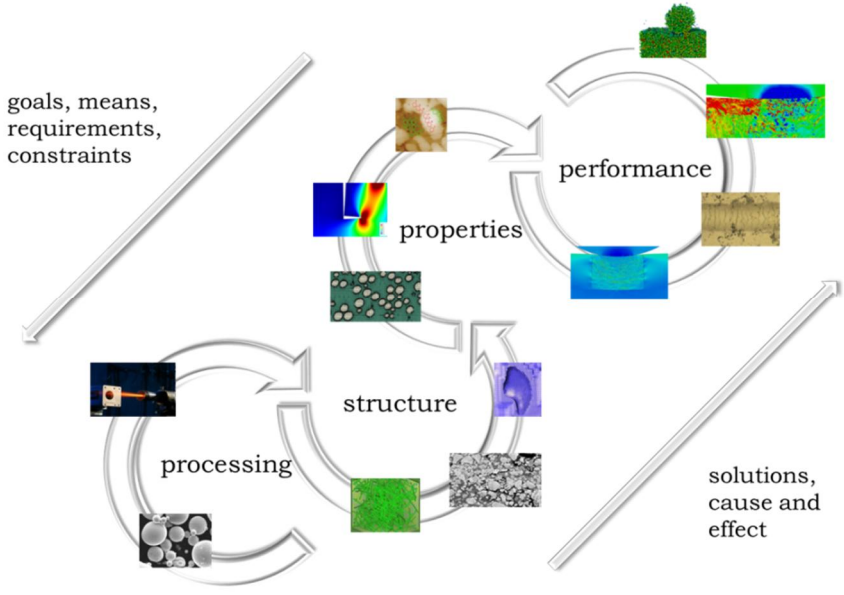

Figure 3. Process-Structure-Properties-Performance concept exploiting multiscale modelling.

1.5 Material structure in multiscale modelling

An example of multiscale modelling incorporating the meso-scale is presented in Figure 4 for microstructures of a metallic material, in this case essentially a 3 different types of steels. Incorporation of the microstructure entails its detailed modelling at the scale of material grains, and incorporation of any additional features and substructures such as precipitates or particles depending on the mechanisms being scrutinized. The basis for modeling the microstructure in a continuous manner is derivation of a 3D image of the different phases. This can be performed directly by way of using 3D imaging or in a mathematical manner utilizing statistical properties of microstructures in question. The resulting aggregates, like representative or statistical volume elements, are then utilized to model and to determine the link between material microstructure and its properties, in the simplest

case its true stress-strain curve. The obtained sub-grain stress-strain fields can be for example further processed to yield information about material performance against a specified set of mechanisms, such as fracture events originating from initiation of local of defects and cracks. A noteworthy feature is to acknowledge that generation of various 3D microstructures is possible within the PSPP framework, and as such, it is possible to devise models of nano- and microscale composites in addition to grain and subgrains structures, interfaces etc.

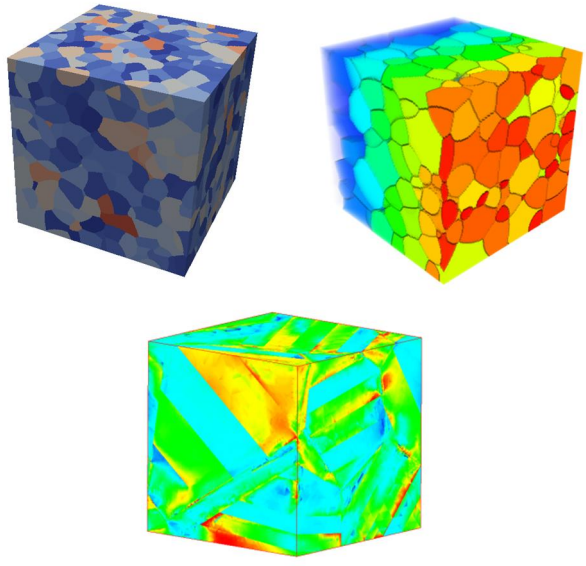

Figure 4. Examples of mesoscale microstructures of a metallic material and the resulting stress state of a representative volume element in a simulated tensile test: aggregate comprised of a grain structure (left), inclusion of grain boundary precipitates (middle), stress state in a lath containing microstructure (right).

1.6 Material properties and performance in multiscale modelling

An example of a modelling case comprising both the structure to properties and properties to performance PSPP modelling routes is presented in Figures 5 and 6 for a thick metal matrix composite coating. The point being made is that in addition to structural modelling, a detailed mechanistic understanding is required in order to consider how the material behaves in terms of performance. The performance in this context being measured by the propensity of the material to initiate and propagate cracks when being subjected to loading by applied external contact. The structure to properties analysis of Figure 5 is carried out by building a finite element model directly on the basis of a scanning electron microscope image, i.e. the microstructural phases are segmented and a numerical model is generated to

the resulting material distribution. The resulting model is then subjected to indentation testing to obtain the mechanical properties and behaviour of the microstructure, and to validate the numerical model.

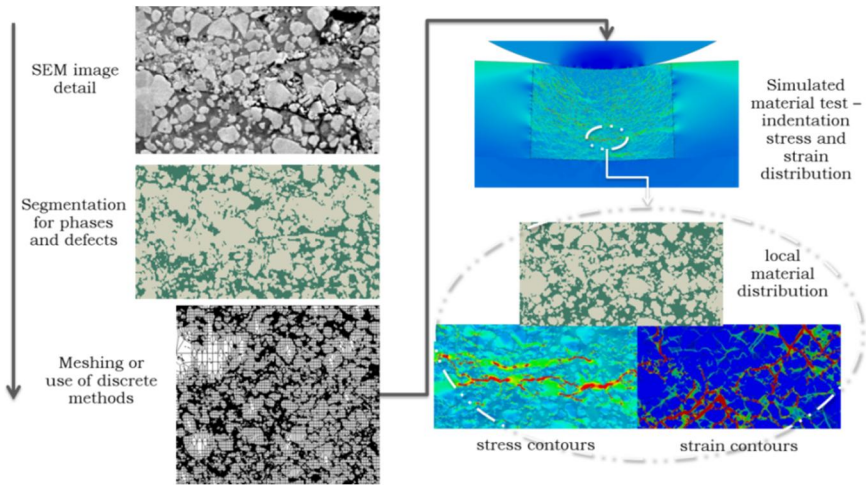

Figure 5. Structure-properties-performance analysis for a metal matrix composite coating.

The stress-strain fields demonstrate the features responsible for the structure-property relationship, but do not contain any other information about performance, unless mechanical strength was the ultimate goal. For this reason, the mechanism critical to performance needs to be incorporated in the modelling chain, and for the current demonstration the measure of performance arises from fracture properties of the composite coating. A fracture mechanical analysis of crack initiation and propagation within the material is carried out as presented in Figure 6. The fracture mechanical analysis yields a measure of performance against material failure, demonstrating the initiation and progression of damage as resulting from the applied external loading.

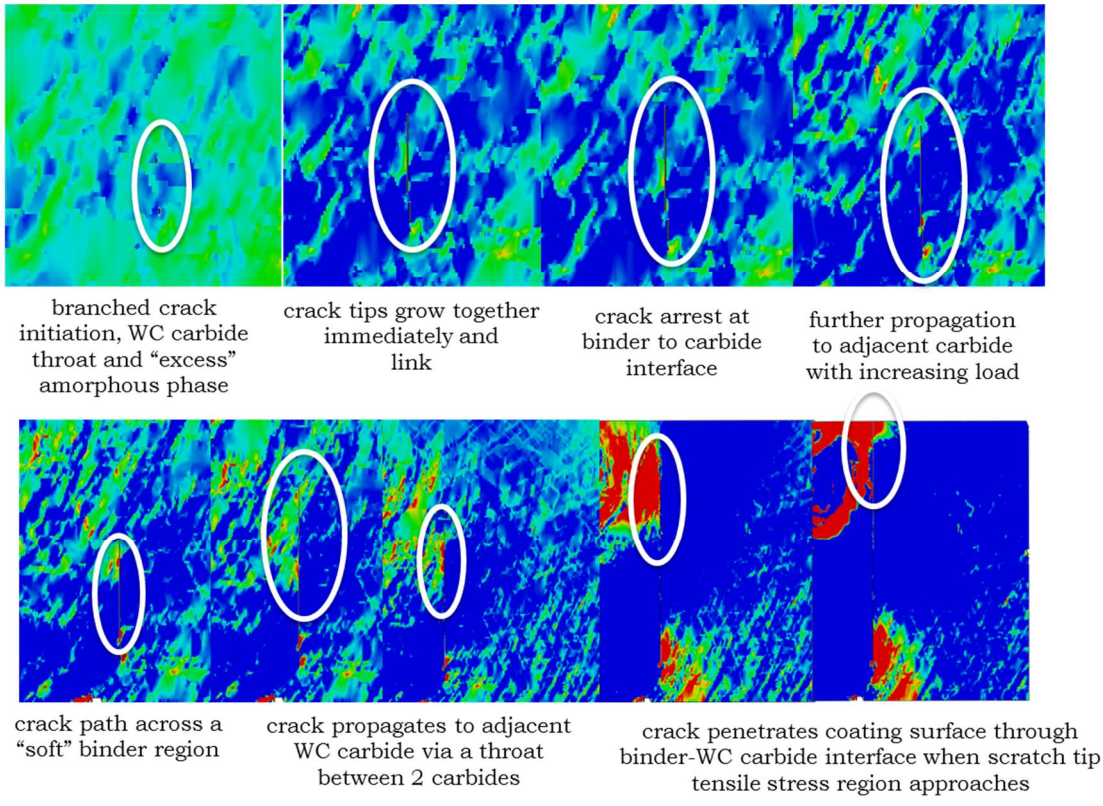

Figure 6. Extended finite element analysis of crack initiation and propagation in a metal matrix composite coating.

1.7 Summary and conclusions

A brief outline of multiscale modelling and the process-structure-properties-performance (PSPP) concept was presented. Multiscale modelling is a family of methods ranging from physics to engineering being able to tackle various material behaviour related problems in a general setting. The PSPP method is a concept for effective application of multiscale modelling and integration of crucial experimental and characterization resources. In addition, the PSPP method is a methodology for modelling assisted material design, for finding optimal material solutions and tailoring materials. Within a specific multiscale modelling application two features were emphasized: the representation of material and the behaviour responsible for critical measures of performance. These are crucial in order to be able to apply the PSPP methodology effectively for a range of materials and in a performance requirement driven and cost conscious manner.

2. Materials modelling research in VTT

Yingfeng Shen, Merja Sippola, Kenneth Holmberg & Kim Wallin

VTT Technical Research Centre of Finland
Tekniikantie 2, P.O. Box 1000, FI-02044 Espoo

2.1 Abstract

This survey was conducted to review present activities at VTT related to materials modelling, used techniques, HW and SW tools as well as problems and visions of the modellers. The results show that materials modelling is actively used at VTT, the materials and phenomena are various and the modelling tasks usually challenging with several phases, phase changes and several size scales. Material degradation and surface/interface phenomena are the most common to model, but also fracture, moisture/heat transfer and thermodynamics are common modelling tasks. The largest material group is metals, but coatings, ceramics, biomaterials, polymers, composites, bentonite and ice are also modelled extensively. The largest modelling categories are material performance and properties. The most used hardware is PC. Linux clusters are used for heavier calculating jobs. The most used commercial software are Matlab, ABAQUS and COMSOL Multiphysics. FactSage and HSC are used in thermodynamics. Several different open source programs are used. VTT researchers also develop subroutines for commercial programs and open source codes. Experimental validation is a general rule at VTT and validation is done at small, medium and full scale. The full scale validation is less common due to large time, size scale or lack of resources.

2.2 Introduction

This survey was conducted to review present activities at VTT related to materials modelling, used techniques, Hard Ware and Soft Ware tools.

Figure 1 shows the thinking behind the survey: modelling is seen as a tool for understanding and in some cases prediction of material behaviour. Reliable modelling is based on understanding previously developed in experiments, but on the other hand the model extends the understanding. Validation of models with experimental data is a must in the extent possible and practical.

The definition for materials modelling used in this survey was: *materials modelling includes all computerised material modelling and simulation activities*:

- from material processing, structures and properties to performance and
- from atomic scale up to component scale; technical systems composed by a number of components are excluded, and
- related to metals, ceramics, polymers, biomaterials, composites and coatings, liquids and gases (all materials and structures are included).

Also analytical modelling was included as a separate point.

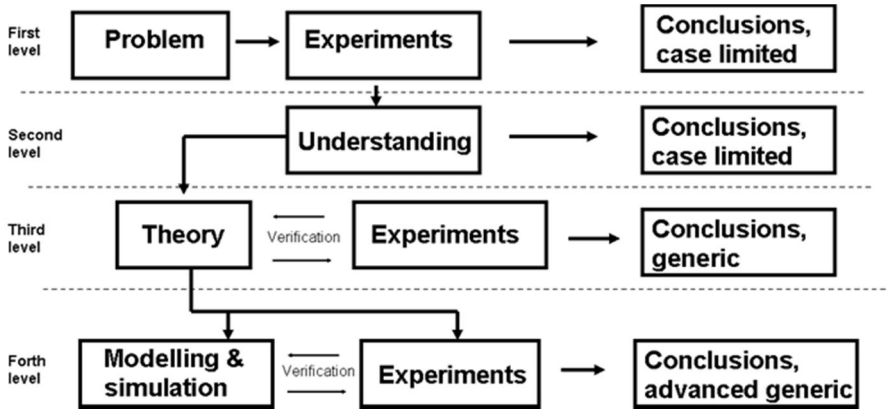

Figure 1. Modelling and its context.

The following categories were reviewed:

- VTT research teams involved in materials modelling
- physical phenomena and their scale, multiscale and transition
- experts on modelling and their skills
- used software tools: commercial, open source and VTT developments
- VTT materials modelling software products
- used hardware tools, databases
- experimental model verification techniques
- descriptions of reference cases
- related VTT publications
- national and international partners
- problems and visions
- large materials modelling projects active in 2011.

2.3 Material models

2.3.1 Materials

Figure 2 summarizes the materials modelled at VTT. The same people work often with several different materials but also many models are multi-material models, often even involving different phases (solid, liquid, gas).

The biggest material group is metals, but also polymers, biomaterials, composites, coatings, liquids and gases are well represented. Some people model bentonite clay, some ice. Then there are a few materials modelled by only one or two people.

The other materials include construction product, concrete, granular frictional materials, functional materials (SMA, MR-elastomers), powders, metal-liquid interface, plasma, metal oxides and foams.

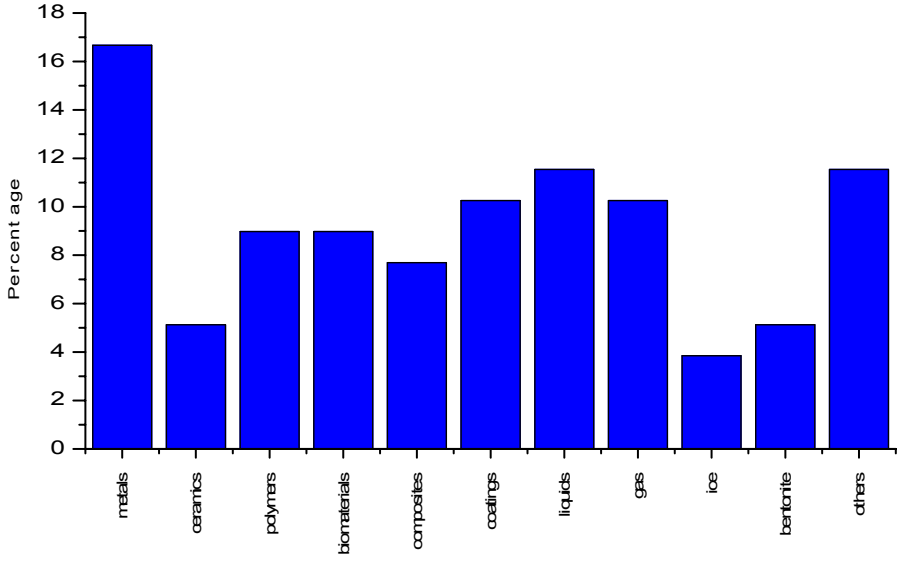

Figure 2. Materials.

2.3.2 Categories

Figure 3 shows what is sought with the models. The biggest is material performance, but material properties and microstructure are also often sought for. Processing is less often the target. Here each person is counted only once even if the modeller has several modelling cases in the same category.

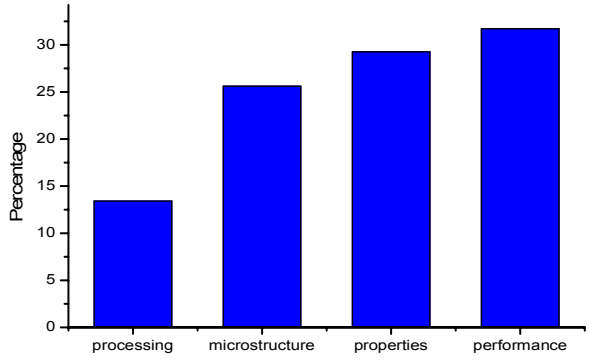

Figure 3. Catergories.

2.3.3 Phenomena

The phenomena modelled by VTT material modellers are extremely varying (see Figure 4). Most people model several different phenomena and several different materials/material combinations, but there are also people concentrating on a few phenomena and/or on one material or a few materials or material combinations.

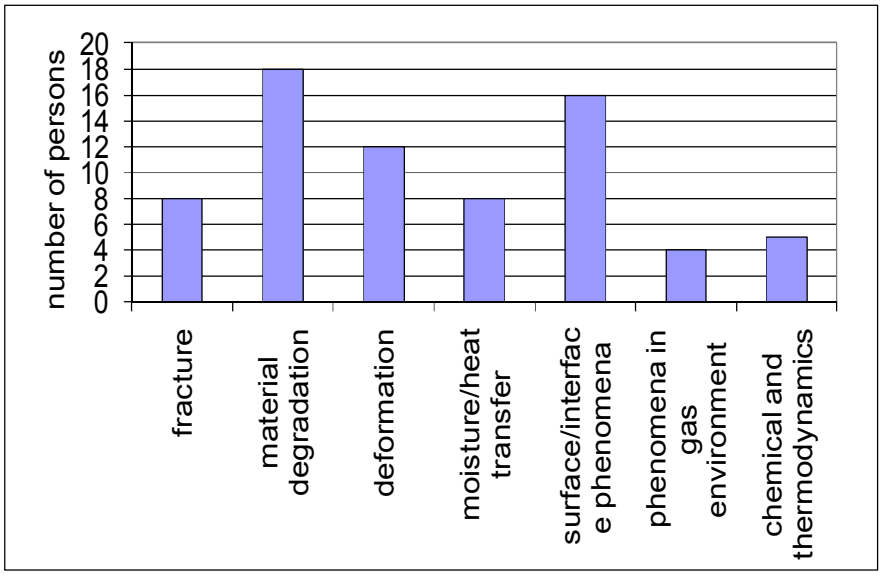

Figure 4. Modelled phenomena.

Several modellers are working with material degradation (corrosion, wear, irradiation embrittlement, pyrolysis, chemical and mechanical erosion), surface or interface phenomena or deformation. Also moisture/heat transfer, damage and fracture are common modelling topics. Chemical reactions and thermodynamics are also fairly common topics. Some people model phenomena occurring in gaseous environment (flame spread and fire extinguishment, sputtering, mixing of materials with plasma). Then there are a few scattered topics modelled by only one or a few modellers interviewed.

Modelling usually contains multi-material combinations. A somewhat surprising result is that most modellers tackle phenomena involving different phases (solid, liquid, gas) and phase changes.

Figure 5 shows the phenomena map in terms of both category and size scale. The most studied fields are material properties and performance in mm to meter scale. Atomic scale study is the lowest in all categories.

2.3.4 Size scale

Figure 6 shows the size scales indicated by the modellers. Even though the models themselves are usually in one scale, the behaviour of the material is usually studied at a large range of size scales.

The survey showed that quite a few people are interested in atomic and molecular scale modelling and molecular dynamics in order to increase understanding of the fundamental phenomena of materials (for examples, fracture and pyrolysis).

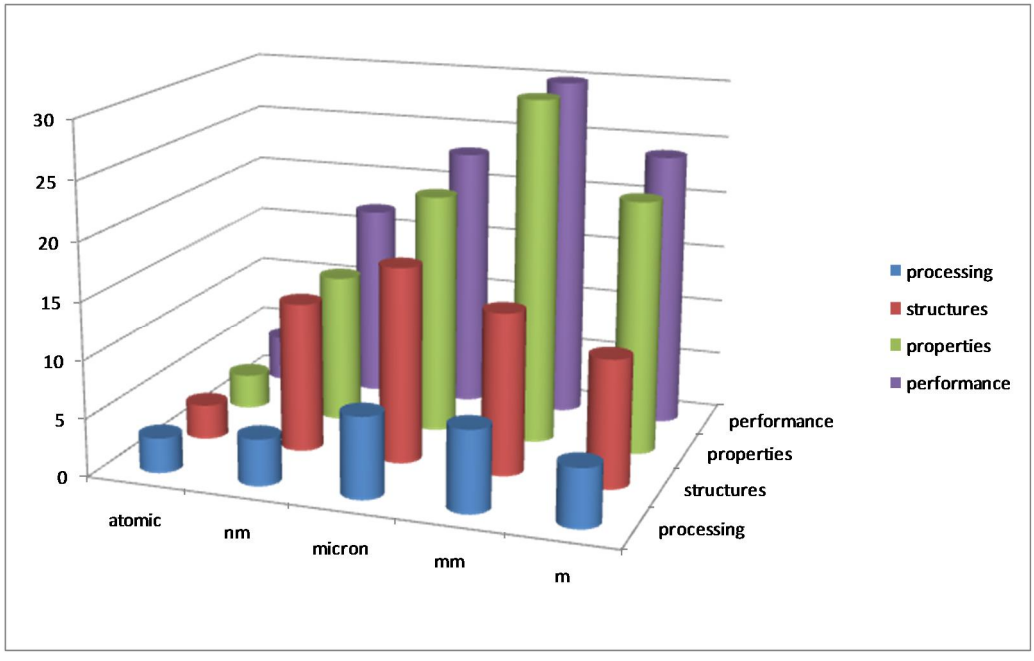

Figure 5. Phenomena map, the vertical axis is the number of cases.

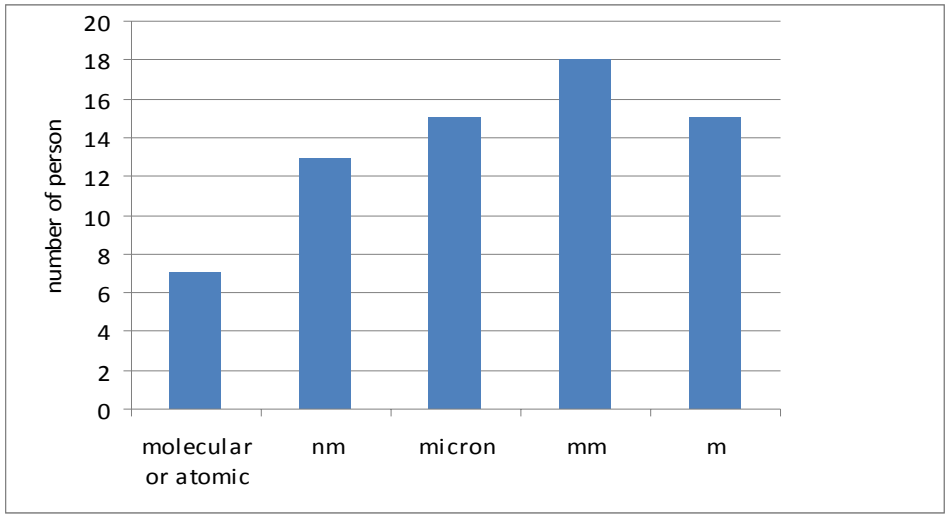

Figure 6. The size scales of the models and research.

2.3.5 Scale transition methods

Figure 7 summarizes how researchers derive material data in one scale and utilize it in another scale. The most common methods for scale transition are homogenization (such as the Representative Volume Element method) utilizing FEM or other software, deduction from small scale experiments or models, and using parameters from small scale experiments as input in larger scale models. Analytical homogenization and statistics are also used. Thermodynamics is a special case – it is rather scale independent.

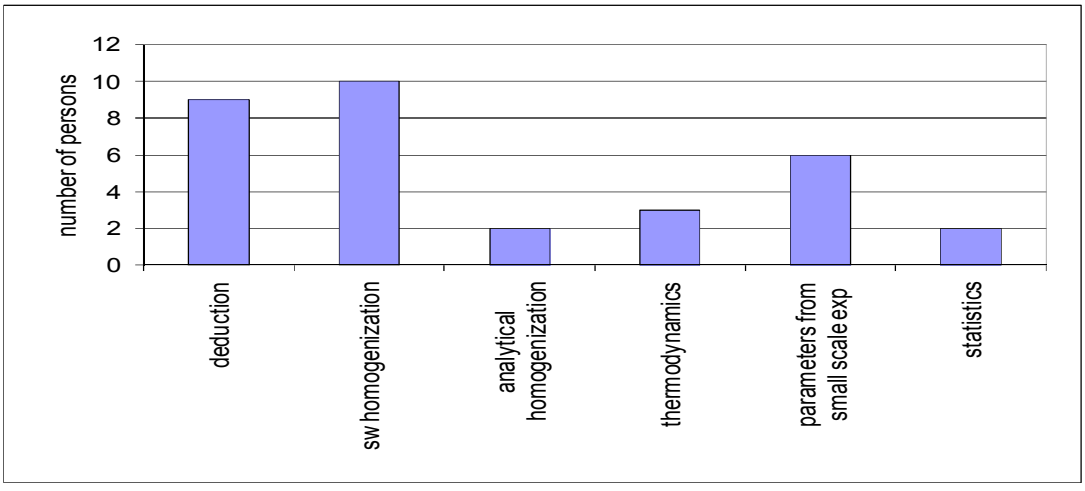

Figure 7. Scale transition methods.

2.4 Tools

Table 1 shows the main commercial software used in VTT. The use is strongest with Matlab, Abaqus and Comsol Multiphysics.

Table 2 shows the open source software usage in VTT. The FDS fire dynamics simulator was created in NIST and it has been actively developed in VTT for many years. Most other specialty programs are used by individual modellers. These include mesh tools (Gmsh), solversolvers (Elmer, openFOAM), post processing tools (Paranoid), modelling languages (Modelica, SCIPY, gcc) and others.

Table 3 shows the software or programs developed inside VTT, including subroutines and scripts for larger programs. There are quite many developments within the last ten years. Many of the VTT developments are subroutines or scripts to some commercial or open source program. The codes are usually developed for the project only. Small software are developed in a few months, while larger ones are taking several years, which may indicate that it has been continued in more than one project.

Table 1. Main commercial modelling software used in VTT.

Program	Type
Abaqus FEA	suite of software applications for finite element analysis and computer-aided engineering
Ansys	engineering simulation software
Chemsheet	EXCEL based multi-phase thermodynamic calculations
Comet Trim	analytical tool that computes the acoustic characteristics of multi-layered, planar materials consisting of structural, elastic-porous and fluid layers
Comsol	finite element analysis, solver and simulation software, especially coupled phenomena, or multiphysics
ExtendSim	simulation program for modelling discrete event
FactSage	integrated database computing system in chemical thermodynamics
Franc3D	work-station based FRacture ANalysis Code for simulating arbitrary non-planar 3D crack growth
Geochemist's Workbench	integrated set of interactive software tools for solving a range of problems in aqueous chemistry
GoldSim	general purpose dynamic, probabilistic simulation software
HSC	thermodynamic chemical reaction and equilibrium software
Materials Studio	software for simulating and modeling materials like polymers, nanotubes, catalysts, metals, ceramics, and so on
Mathematica	computational software program used in scientific, engineering, and mathematical fields and other areas of technical computing
Matlab	numerical computing environment and fourth-generation programming language
Numerrin	mathematical modelling software
Origin	program for interactive scientific graphing and data analysis
Tough2/Toughreact	general-purpose numerical simulator for multiphase fluid and heat flow
Wien2k	code to perform electronic structure calculations of solids using density functional theory (DFT)

Figure 8 shows the man months used for development and usage of the VTT software. In general, it can be seen that the usage time is more than the development time.

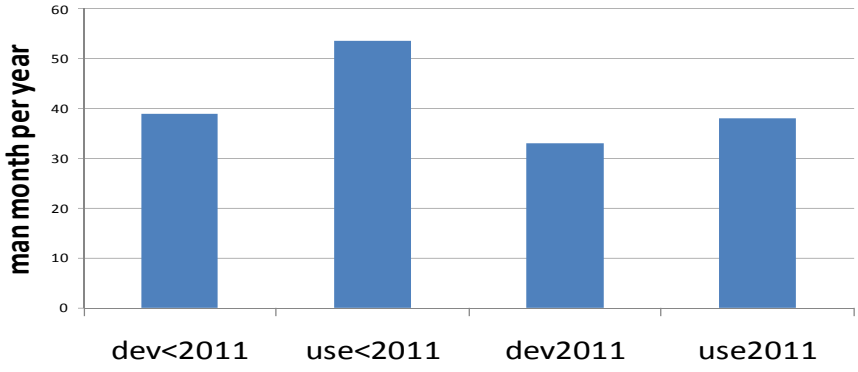

Figure 8. Manmonths for development and usage of the VTT software.

2/3 of the modellers are using personal computer for their work. The rest are using other means, especially Linux clusters. More than 50% of the researchers also do analytical modelling in combination to the numerical work.

Almost all researchers have important collaboration partners outside VTT. The most common partner is Aalto University. The most common domestic collaboration partners are universities. The most common foreign collaboration partners are NIST and Osaka University. More than half of the indicated collaboration partners are foreign. Universities are well represented also in foreign collaboration partners. The contacts seem to be based on researcher – to researcher collaboration. Geographically the collaboration partners are located in Europe, America and Japan.

Table 2. Main open source modelling software used in VTT.

Program	Type
Abinit	suite of programs for materials science, implementing density functional theory, using a plane wave basis set and pseudopotentials, to compute the electronic density and derived properties of materials ranging from molecules to surfaces to solids
Code_Aster	software package for Civil and Structural Engineering finite element analysis and numeric simulation in structural mechanics
dod_tbmd	Tight binding molecular dynamics code
FDS	Fire Dynamics Simulator
Elmer	finite element software for numerical solution of partial differential equations and multiphysical problems

Eq3/6	software package for geochemical modelling of aqueous systems
FEMM	software package for solving electromagnetic problems using FEM
gcc, gdb	compilers and debuggers for GNU system
Gmsh	automatic three-dimensional finite element mesh generator
Lammps	molecular dynamics simulator
Lsmdd	Level Set Method Dislocation Dynamics library provides support for the parallel simulation of dislocation motion and interactions in materials
Micromegas	program for DD (Dislocation Dynamics) simulations
Mika	multigrid-based program package for electronic structure calculations
Modelica	an object-oriented, declarative, multi-domain modelling language for component-oriented modelling of complex systems
NumPy	package for scientific computing with Python
OpenFOAM	toolbox for the development of customized numerical solvers, and pre-/post-processing utilities for the solution of continuum mechanics problems
ParaDiS	FEM dislocation dynamics simulation code
Paranoid	post processing tool
Phreeqc	program for low-temperature aqueous geochemistry calculations
Salome	generic platform for Pre- and Post-Processing for numerical simulation
SciPy	software for mathematics, science, and engineering
Siesta	software implementation for performing electronic structure calculations and ab initio molecular dynamics simulations of molecules and solids
Simantics	software platform for modelling and simulation
Tahoe	research-oriented platform for the development of numerical methods and models for the simulation of complex material behavior
Warp3D	3-D nonlinear finite element analysis of solids for fracture and fatigue processes

Table 3. VTT development software list.

Id	**Software name or type**
1	tesselation and structure generation codes
2	Solvers
3	finite element libraries
4	multiscale codes

5	MD codes
6	Mixed Conduction Code (in ORIGIN)
7	ABAQUS subroutines & scripts
8	ABAQUS subroutines & scripts (Fortran)
9	FDS (Fire Dynamics Simulator)
10	PFS (Probabilistic Fire Simulator)
11	ABAQUS subroutines and scripts
12	Extreme value analysis
13	Ice friction model
14	Icing model
15	THMC in COMSOL Multiphysics
16	ChemSheet (Team)
17	Simulation of degradation
18	Aging management of concrete structures (BridgeLife, RoadLife, MaintenanceManServiceMan
19	FDS / combustion
20	ERO – 3D Monte Carlo code for local impurity transport in plasma (main developers are in FZ Jülich)
21	PARCAS (Molecular dynamics code, University of Helsinki)
22	ChemSheet
23	KilnSimu
24	TubeBank
25	Surfer
26	CheMac
27	solver for electrostatic aided gravure printing
28	ink absorption on porous substrate
29	ABAQUS subroutines
30	Fiber network model (in Fortran)
31	Virtual Web (in Matlab)
32	Drying simulators
33	Simantics – Open SW platform for modelling and simulation
34	Thimes; in-house program for upward flame spread calculations

2.5 Experimental validation of models

Experimental validation is generally a rule for VTT material modellers. In some cases full scale validation is not possible due to large time or size scale, for examples in modelling storage of spent nuclear fuel. In some cases full scale validation is difficult because the full scale measurements would be outdoor experiments in highly non-standard test conditions, for examples in modelling crushing of ice against offshore structures. In some projects – especially customer projects – there is no money allocated for experimental validation. Only a small minority of the researchers rely on experimental data from literature only. Most do experimental validation with experiments made at VTT or by research partners. Sometimes experimental data is taken from some external database. Figure 9 shows the typical sources of experimental data used for model validation. Small scale experiments are the most common type of validation, but medium and large scale experimental validation is also used when possible (Figure 10). In some groups the experiments are the main thing and models are only used for understanding the experimental results.

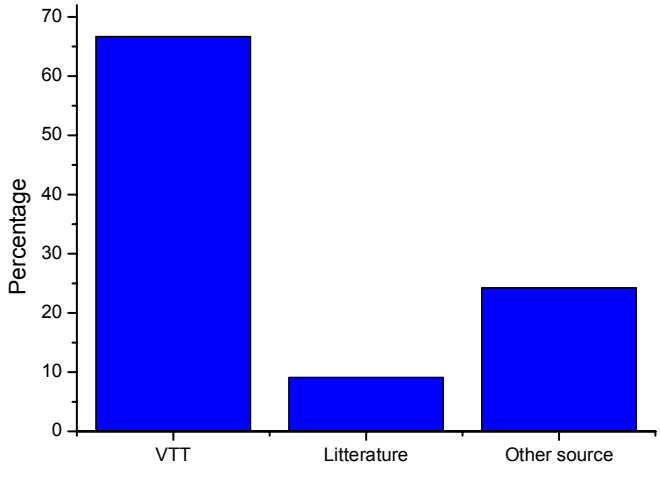

Figure 9. Sources of experimental data used in validation.

Figure 11 shows the problems met in validation. Lack of good quality, well documented experimental data is a common problem. Sometimes the reasons behind the lack of experimental data are financial or organizational, but most often the problem is that the key parameters and material behaviour are difficult to measure. The modelled phenomena are often coupled and rather complicated. In some cases there are experimental values from several decades, but the test conditions

and test setup were not properly documented and the data is thus unreliable. In non-homogeneous materials the test setup strongly affects the results. In natural materials the scatter in material values is large. Even some of the man-made materials are not well standardized and the batches can vary considerably. With small funding it is not possible to make a comprehensive test matrix. In some fields the time or size scales make full scale validation difficult or impossible.

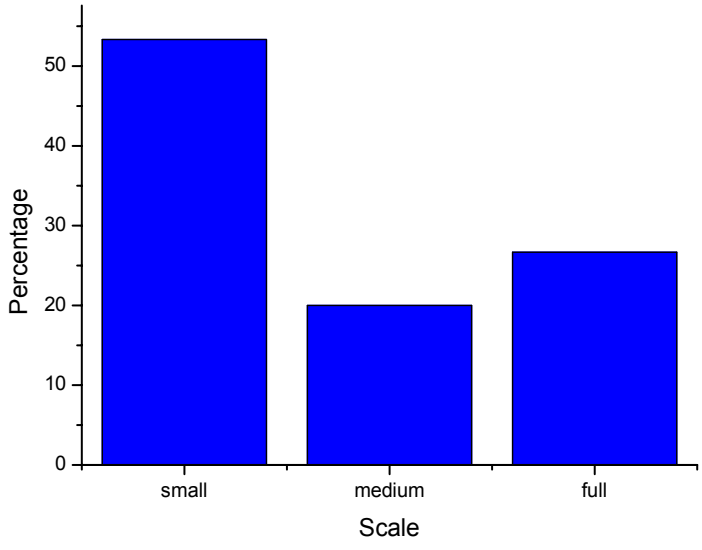

Figure 10. Size scales of experimental validation.

Sometimes the problem lies in correlating the modelled results with experimental ones, especially with models that use simplifications and idealizations not present in reality.

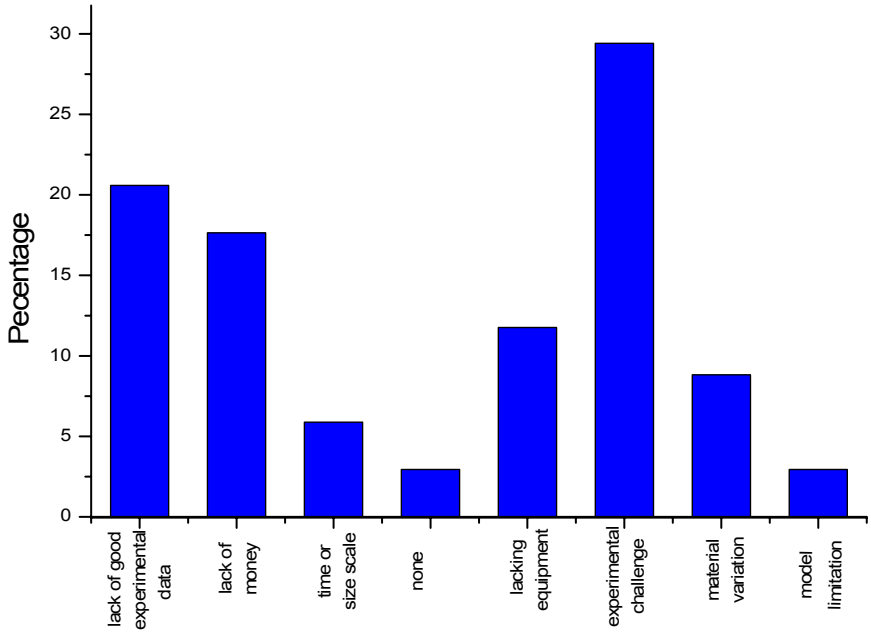

Figure 11. Problems met in validation.

2.6 Discussion

A growing and challenging research field: We can conclude that materials modelling is an important part of the research conducted at VTT and the demand for modelling seems to be still increasing. The materials and phenomena are various and the modelling tasks are usually challenging with several phases, phase changes and several size scales (see Figure 3, Figure 4). Nonlinear and coupled phenomena are also included.

Materials and categories: The largest material group is metals, but coatings, ceramics, biomaterials, polymers, composites, bentonite and ice are also modelled extensively. Material properties and performance were the most common categories. Processing was maybe even surprisingly low.

Phenomena: Material degradation and surface/interface phenomena are the most common to model, but also fracture, moisture/heat transfer and thermodynamics are common modelling tasks.

Size scales and scale transition: Figure 6 shows the size scales indicated by the modellers. Even though the models themselves are usually in one scale, the behaviour of the material is usually studied at a large range of size scales. This calls for development of multiscale modelling, but the software tools for that are

not yet at very high level. The most common methods for utilizing data derived in one scale in another scale are homogenization using some software, deduction, and utilizing material values from small scale experiments in larger scale models. True multiscale modelling is still uncommon. In most fields there is need for improvement of both tools and skills for multiscale modelling.

Software tools: The most often used software tool is Matlab. This could be explained by that it is both a programming language and a calculation toolbox. It can be used for modelling as well as for post processing the results from Abaqus and Comsol. The other two are dedicated state of the art Finite Element or Finite Volume solvers. It should also be noted that although Ansys is rather similar to Abaqus or even better in certain fields, it was much less used in VTT due to modeller's preference or historical reasons.

The VTT developed software tools are beneficial to the projects, although most of them are not yet ready for commercialization. Figure 8 shows that the time spent to develop these programs is less than their usage time, which proves our efficiency and the readiness of the code. On the other hand, the developing and usage time is often related to the time span of the project. A longer or continued project is expected to extend the usage time even longer. Only a few VTT developments have so far been commercialized, for example APROS, ChemSheet and Virtual Web. Most of the other programs could be usable by third party, or they could even be commercialized, but that would mean a lot of extra work: commenting the code, taking away scrap code, documentation, building user friendly interface etc. There is usually no money allocated for this in the project.

There is a slight warning that VTT is spending less time in developing and using our own software tools. This can be seen from Figure 8. The man months we use in software development and usage is dropping compared with the average in the past ten years. However, this could also be due to using more commercial and open source software.

Hardware tools: The most used hardware is PC, Linux clusters are used for heavier calculating jobs. Easy access to powerful clusters and education in parallel computing are wished for. Otherwise the modellers are rather satisfied with the current tools.

Analytical models are not history: VTT modellers do not just rely on numerical tools, the survey results show that analytical methods are still used in many cases. During last twenty years, computing power and numerical methods have greatly improved, complicated engineering problems can now be modelled and solved. More and more analytical modelling has shifted towards numerical analysis. However, analytical modelling is still very essential in the research. It often gives a quick although sometimes rough estimation, means for checking the results of numerical models and reflects modeller's understanding of the system.

Awareness of experimental validation: The importance of experimental validation and working hand to hand with experimentalists is well understood by most modellers at VTT. Some of them indicate that lacking of experimental validation as one of the problems. Both modellers and experimental researchers hope for pro-

jects in which there was money allocated for both models and experiments. This is already a case in many TEKES projects, but less in customer projects.

Problems in validation: The reasons for lack of experimental validation can be difficulty and/or variety of the phenomena and experiments, large size of time scales, lack of time, financial reasons or the validation did not get enough attention in the project planning.

Communication in practice: The co-operation between modellers and experimentalists already works rather well in many fields at VTT, even though information gaps do occur now and then. Often the modelling is done in one team and the experiments in another team. In the beginning there are problems in communication, but when the same people work together in a few projects, they learn to communicate the relevant information. It is seen the responsibility of the experimentalist (the material expert) to indicate the key parameters (and how easy or difficult it is to measure them) and help the modeller to understand the phenomena. On the other hand it is the modeller's responsibility to explain the limitations of the model/program to the experimentalist.

Reference cases and publications: The large amount of published results and the good amount of customer projects show that VTT materials modellers are trusted and valued experts in their field. Some modellers told in the interview that they are among the top in the world in their field of expertise.

2.7 Conclusions

This survey was conducted 2011 in the Multiscale Materials Modelling project to review present activities at VTT related to materials modelling, used techniques, HW and SW tools as well as problems and visions of the modellers. Materials modelling is an important part of the research conducted at VTT and the demand for modelling seems to be still increasing.

The materials and phenomena are various and the modelling tasks usually challenging with several phases, phase changes and several size scales. The largest material group is metals, but coatings, ceramics, biomaterials, polymers, composites, bentonite and ice are also modelled extensively. Material degradation and surface/interface phenomena are the most common to model, but also fracture, moisture/heat transfer and thermodynamics are common modelling tasks. Material properties and performance were the most common categories. Processing was maybe even surprisingly low.

In most fields there is need for improvement of both tools and skills for multiscale modelling. Even though the models themselves are usually in one scale, the behaviour of the material is usually studied at a large range of size scales. This calls for development of multiscale modelling, but the software tools for that are not yet at very high level. The most common methods for utilizing data derived in one scale in another scale are homogenization using some software, deduction, and utilizing material values from small scale experiments in larger scale models. True multiscale modelling is still uncommon.

The most used hardware is PC, Linux clusters are used for heavier calculating jobs. The most used commercial software are Matlab, ABAQUS and COMSOL Multiphysics. FactSage and HSC are used in thermodynamics. Several different open source programs are used. Modellers are rather satisfied with the current tools. VTT researchers also develop subroutines for commercial programs and open source codes.

The importance of experimental validation and working hand to hand with experimentalists is well understood. Validation is done at small, medium and full scale. The full scale validation is less common due to large time, size scale or lack of resources. The researchers on both sides hope for projects in which there was money allocated for both models and experiments. The co-operation between modellers and experimentalists already works rather well in many fields at VTT.

Publication of the modelled results with experimental verification in conferences and journal papers is active.

As one of the biggest problems, the modellers see the complexity and difficulty of the phenomena. In many cases experiments are the main thing and models can only be used in understanding the experimental results, not in predicting anything absolute. Regarding to the level of materials modelling, we are on the level 3 in Figure 1 and our challenge is to reach level 4.

The visions for the future do not have much synergy. Most groups intend to continue on the current path, only a few have plans of enlarging or changing their field. Molecular dynamics modelling is seen as a necessary new area to go into. Thermodynamics is seen as another research gap that should be covered.

2.8 Acknowledgements

The authors wish to thank the VTT Multimodelling team for valuable comments and encouragement in this work. Furthermore the authors acknowledge with gratitude the time and effort given by each researcher who was interviewed and/or answered the questionnaire.

3. Effects of structure, doping, and environment on the tribochemistry of DLC

Judith A. Harrison[1], P. T. Mikulski[1] & J. David Schall[2]

[1]United States Naval Academy
Departments of Chemistry & Physics, 572 Holloway Road, Annapolis, MD 21402, U.S.A

[2]Oakland University
Department of Mechanical Engineering, 2200 N. Squirrel Rd., Rochester, MI 48309, U.S.A

3.1 Introduction

The low friction and good wear resistance of diamondlike carbon (DLC) films make them attractive for many tribological applications. Unfortunately, the friction of DLC is known to be a function of variables, such as structure, hydrogen content, and humidity. In this talk, we will review previous molecular dynamics simulations, and present new data, aimed at elucidating the influence of film structure, doping, and presence of vapour-phase species on the friction and wear of DLC. [1–8]

3.2 Method

Non-hydrogenated and hydrogenated DLC films containing zero (referred to as P_{00}) and twenty (referred to as P_{20}) atomic-percent hydrogen, respectively, were created using a previously described melt and quench technique. [9–11] The same hydrogen-terminated, tetrahedral amorphous carbon surface was used as the counterface for both of these films. The properties of each film have been summarized elsewhere.[11, 12] In what follows, the simulation system comprised of the P_{00} film plus the counterface is referred to as the “non-hydrogenated system” and the P_{20} film plus counterface is referred to as the “hydrogenated system”. Both of these systems are shown in Figure 1. The P_{00} surface is composed of 2.2%,

85.3%, and 12.5% sp-, sp^2-, and sp^3-hybridized carbon. The P_{20} surface is composed of 2.1%, 83.4%, and 14.5% sp-, sp^2-, and sp^3-hybridized carbon.

Interatomic forces needed to conduct molecular dynamics (MD) simulations of sliding were calculated using the reactive empirical bond-order (REBO) potential for hydrocarbons developed by Brenner and coworkers.[13] The many-body nature of the REBO potential allows the bond energy of each atom to depend on the local environment. Therefore, the REBO potential allows for chemical reactions (or tribochemistry), and the accompanying changes in bond-hybridization, to be modelled. During the simulations, the outermost layers of both the surface and counterface are held rigid. Moving inward toward the interface, the next two layers of both the surface and the countersurface are held at 300 K using a Langevin thermostat.[14] All remaining atoms are free to move according to classical dynamics and periodic boundary conditions are applied in the plane that contains the sliding interface.

Molecular dynamics simulations have been used to examine the effects of trapping both hydrogen atoms and H_2 molecules at the sliding interface between the counterface and the DLC surface of interest (Fig. 1). The molecules were placed in between the surfaces and the systems were equilibrated at 300K. The counterface was then moved closer to the lower surface until the desired, constant load was achieved. Two concentrations of atomic hydrogen (0.254 H/Å^2 and 0.508 H/Å^2 in units of parts per unit surface area) ere examined. These concentrations correspond to 200 and 400 total hydrogen atoms added. Sliding is accomplished by moving the rigid layers (outermost) layers of the counterface at a constant velocity of 0.902 Å/ps in the sliding direction.

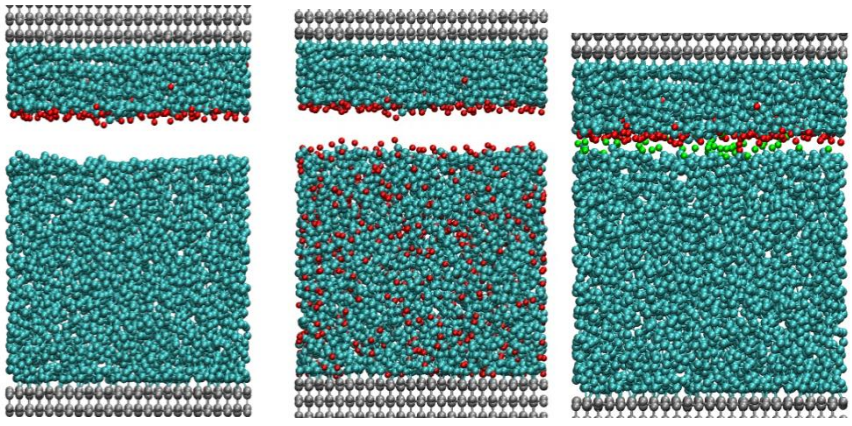

Figure 1. Simulation systems containing the P_{00} (left) and the P_{20} (center) surfaces surface in the absence of interfacial hydrogen and the equilibrated P_{00}-containing system with interfacial atomic hydrogen (right). The counterface (upper surface) is the same in all simulations. Large green, small red, and gray spheres represent carbon atoms, hydrogen atoms, and carbon in the diamond substrate, respectively. (right) The P_{00} system with atomic hydrogen (light green spheres) after equilibration at 0 nN and 300 K. The sliding direction is from left to right.

3.3 Results & discussion

Interesting changes occur in the simulation systems upon equilibration in the presence of interfacial gases. For example, when atomic hydrogen is trapped between the P_{00} surface and the counterface, equilibration results in 95% of these atoms becoming hydrogen molecules, 3.3% of the hydrogen atoms bonding to the P_{00} surface and 1.7% of the hydrogen atoms bonding to the counterface. When hydrogen bonds to the DLC surfaces, the hybridization of the carbon atoms at the interface is altered. Before equilibration in the presence of hydrogen atoms, 18% of the carbon atoms in the 2 Å of the P_{00} surface closest to the sliding interface have sp-hybridization, 76% are sp^2 hybridized, and 7% are sp^3 hybridized. After equilibration in the presence of hydrogen atoms, the unsaturation of the interfacial region of the P_{00} surface is reduced with 11% of the carbon atoms adopting sp hybridization, 80% are sp^2 hybridized, and 9% are sp^3 hybridized. The case of the P_{20} substrate, inclusion of hydrogen through the DLC film results in a slight reduction in the amount of sp and sp2-hybridized carbon in the film, particularly in the interfacial region. As a result, the addition of interfacial hydrogen atoms to the P_{20}-containing system followed by equilibration in the presence of atomic hydrogen, does not alter the top 2 Å of the film and all the atomic hydrogen forms gaseous H_2.

Sliding simulations were performed for 200 ps (or six complete passes over the film) at constant load. The instantaneous friction forces on the rigid layer were saved every 0.1 ps of sliding. For the P_{00}-containing system, the smoothed, instantaneous friction forces are plotted as a function of time in the right hand side of

Figure 2. In the absence of atomic hydrogen (green line), interfacial chemical bonds form and are break between the P_{00} film and the countersurface during sliding. (This type of bonding was previously referred to as interfilm bonding.[15]) Once carbon-carbon bonds form across the sliding interface, continued sliding strains the bonds resulting in an increase in friction, which corresponds to the maxima in the friction versus distance (Fig. 2, green line). Continued sliding of the counterface, increases the stress on the interfacial carbon-carbon bonds enough to rupture of these bonds, which is associated with a concomitant decrease in friction. The structure of the interfacial region of the DLC films is continually changing as a result of the making and breaking of interfacial bonds during sliding.[11] These changes in structure can also be monitored by tracking the changes in the distribution of bond angles and the changes in carbon-atom coordination number. Finally, when the strain-energy is released by the rupture of the carbon-carbon bonds during sliding and the instantaneous friction decreases, the temperature of the interfacial region increases.[11] This has been identified as an important mode of energy dissipation in films.

It is apparent from examination of the friction versus load data in Figure 2 that the inclusion of hydrogen within the DLC film reduces friction at all loads, even in the absence of interfacial hydrogen. The number of interfacial bonds formed during sliding, and thus the friction, can also be reduced by the addition of atomic hydrogen to the interfacial region prior to sliding. Friction versus sliding distance of the P_{00}-containing system is shown for two different starting concentrations of interfacial hydrogen atoms. It is clear from the absence of discontinuities in the friction versus time data for the 0.508 H/Å^2 coverage that the formation of interfacial, chemical bonds between the counterface and the P_{00} film have almost completely been eliminated.

In general, these simulations demonstrate that reducing unsaturated carbon atoms at the sliding interface of self-mated DLC contacts reduces the number of adhesive interactions, alters the nature of the transfer film formed, and reduces friction compared to non-hydrogenated systems. These, and related, simulation results will be discussed in this talk and placed in the broader context of what is know about the friction of DLC films.

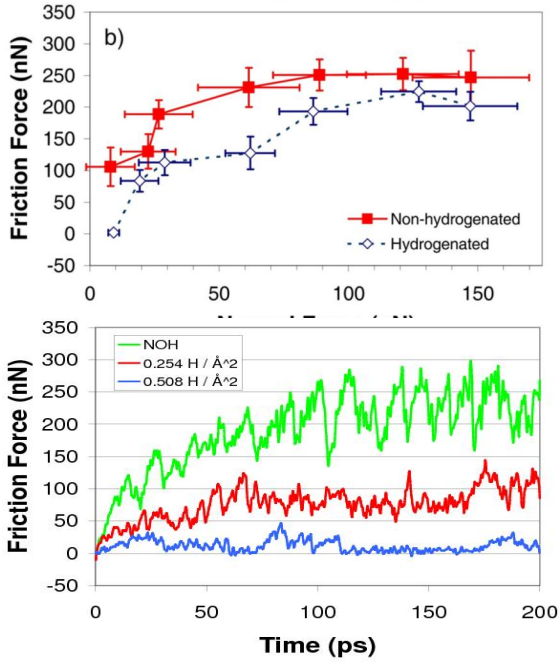

Figure 2. (above) Average friction force as a function of average normal load for the P_{00}-containing system (red squares) and the P_{20}-containing system (blue diamonds).[11] (below) Friction as a function of time at an average (constant) load of 60 nN for the P_{00}-containing system. The green line is the friction in the absence of interfacial atomic hydrogen. The red and the blue lines correspond to initial surface coverages of 0.254 and 0.508 H/Å^2, respectively.

3.4 References

1. Erdemir, A., The role of hydrogen in tribological properties of diamond-like carbon films. Surf. Coat. & Technol. 2001, 146, 292–297.

2. Erdemir, A.; Donnet, C., Tribology of Diamond, Diamond-Like Carbon, and Related Films. In Modern Tribology Handbook, Bhushan, B., Ed. CRC Press LLC: Boca Raton, FL, 2001; Vol. 2, 871–908.

3. Erdemir, A.; Donnet, C., Tribology of diamond-like carbon films: recent progress and future prospects. Journal of Physics D-Applied Physics 2006, 39, (18), R311-R327.

4. Kim, H. I.; Lince, J. R.; Eryilmaz, O. L.; Erdemir, A., Environmental effects on the friction of hydrogenated DLC films Tribol. Lett. 2006, 21, 53–58.

5. Ronkainen, H.; Koskinen, J.; Varjus, S.; Holmberg, K., Load-carrying capacity evaluation of coating/substrate systems for hydrogen-free and hydrogenated diamond-like carbon films. Tribology Letters 1999, 6, (2), 63–73.

6. Ronkainen, H.; Varjus, S.; Holmberg, K., Tribological performance of different DLC coatings in water-lubricated conditions. Wear 2001, 249, (3–4), 267–271.

7. Ronkainen, H.; Varjus, S.; Koskinen, J.; Holmberg, K., Differentiating the tribological performance of hydrogenated and hydrogen-free DLC coatings. Wear 2001, 249, (3–4), 260–266.

8. Konicek, A. R.; Grierson, D. S.; Sumant, A. V.; Friedmann, T. A.; Sullivan, J. P.; Gilbert, P.; Sawyer, W. G.; Carpick, R. W., Influence of surface passivation on the friction and wear behavior of ultrananocrystalline diamond and tetrahedral amorphous carbon thin films. Physical Review B 2012, 85, (15).

9. Gao, G.-T., Mikulski, P. T., Chateauneuf, G. M., and Harrison, J. A., The Effects of Film Structure and Surface Hydrogen on the Properties of Amorphous Carbon Films. J. Phys. Chem. B 2003, 107, 11082–11090.

10. Gao, G. T., Mikulski, P. T., and Harrison, J. A., Molecular-Scale Tribology of Amorphous Carbon Coatings: Effects of Film Thickness, Adhesion, and Long-Range Interactions. J. Am. Chem. Soc 2002, 124, 7202–7209.

11. Schall, J. D.; Gao, G. T.; Harrison, J. A., Effects of Adhesion and Transfer Film Formation on the Tribology of Self-Mated DLC Contacts. Journal of Physical Chemistry C 2010, 114, (12), 5321–5330.

12. Schall, J. D.; Mikulski, P. T.; Chateaueuf, G. M.; Gao, G. T.; Harrison, J. A., Molecular Dynamics Simulations of Tribology. In Superlubricity, Erdemir, A. a. M., J.J., Ed. Elseveir: Amsterdanm, The Netherlands, 2007; Vol. Chapter 5, 79–102.

13. Brenner, D. W.; Shenderova, O. A.; Harrison, J. A.; Stuart, S. J.; Ni, B.; Sinnott, S. B., Second Generation Reactive Empirical Bond Order

(REBO) Potential Energy Expression for Hydrocarbons. J. Phys. C. 2002, 14, 783–802.

14. Adelman, S. A.; Doll, J. D., Generalized Langevin Equation Approach for Atom/Solid-Surface Scattering: General Formulation of Classical Scattering off Harmonic Solids. J. Chem. Phys. 1976, 64, 2375–2388.

15. Gao, G. T.; Mikulski, P. T.; Chateauneuf, G. M.; Harrison, J. A., The Effects of Film Structure and Surface Hydrogen on the Properties of Amorphous Carbon Films. J. Phys. Chem. B 2003, 107, 11082–11090.

4. Introduction to the IMAGO project

Maria Oksa

VTT Technical Research Centre of Finland
Metallimiehenkuja 8, P.O. Box 1000, FI-02044 Espoo

4.1 Introduction to the IMAGO project

Modelling assisted material design is an important development target at VTT. At VTT, frontier projects are used to develop competence and know-how development. Frontier projects are self-funded instruments to increase top skills in selected areas. IMAGO – *Integrated material modelling for demanding applications* is a frontier project, which combines materials science and computer modelling. The main focus of the project is to develop and validate material modelling tools, which can simulate and predict material behaviour in demanding environments. The modelling tools will integrate physical and chemical material transformation models in multiscale, from nano to macro size and different time scales. These modelling tools being developed in IMAGO project belong to an overall modelling concept **VTT ProperTune™**. VTT ProperTune™ represents a systematic approach for controlled performance by material modelling. It enables understanding and controlling the relationship between processing, structure, properties and performance in material development. Together with multiscale modelling tools and deep understanding of materials, processes, characterization and performance, it is possible to perform modelling assisted material design, and avoid excess experimental work and hence generate cost and time savings. The IMAGO project focuses on three different material cases, which aim for creation of tools for tailored material and component design, and targeting to energy savings, development of new products, and lifetime control.

4.2 Material modelling development by focused cases in IMAGO project

The three cases in the IMAGO project are diamond-like carbon coatings, and the effect of the coating structure to coating properties, high temperature corrosion and erosion protection properties of thermal spray coatings, and effect of bio fibre structure into processing of the material. A more detailed description of the cases is presented in the following presentations:

- Modelling of friction and structural transformations in diamond like carbon coatings by Helena Ronkainen
- Molecular dynamics simulations of mass transport in chromium oxide scales by Jukka Vaari, and
- μFEM modelling of wood cell deformation under pulping-type dynamic loads by Stefania Fortino.

4.2.1 Optimized structure of diamond-like carbon coatings (DLC) for low friction and wear by material modelling

Diamond-like carbon (DLC) coatings have excellent properties, such as high mechanical strength, high hardness, low friction and good wear resistance. They offer beneficial properties to applications like slide bearings, valve rockers, gears, other sliding components, cutting tools, flat panel displays and surgical tools. DLC coatings are amorphous and contain mixture of sp3 and sp2 carbon bonds and generally significant quantities of hydrogen due to the deposition process (e.g. CVD – chemical vapour deposition, and PVD – physical vapour deposition). The effect of the structure to the coating properties, and thermal and aging effects on friction and wear are under study in the IMAGO project. The novel modelling approach combines several multiscale components from atomistic scale to macro scale by molecular dynamics (MD), finite element modelling (FEM), Monte Carlo simulations (MC) and thermodynamical calculations (CFE – constraint free energy). The models are being validated by thorough analysis of the different DLC coating structures and careful testing of different coating properties. Co-operation with Argonne National Laboratory, USA, and Universities of Sheffield, UK; and Jyväskylä is active. An example of atomistic modelling is presented in Figure 1 simulating nanoindentation measurement on DLC coating with a diamond tip.

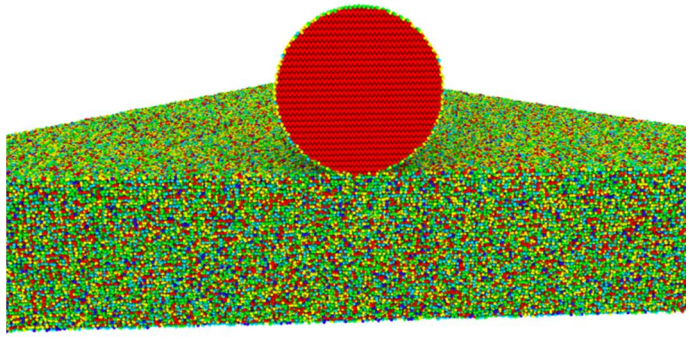

Figure 1. Nanoindentation (~15 nm tip size) of an a-C:H (25 at% H) DLC coating with a diamond tip. Colouring based on atomic coordination, model cut in half diagonally.

4.2.2 Increased lifetime of components by optimized high temperature protective thermal spray coatings through material modelling

Thermal spray coatings for high temperature applications are typically metallic, cermet or ceramic coatings sprayed with HVOF (high velocity oxy-fuel) or plasma methods, using high temperature and high velocity to form dense lamellar structures with good corrosion and wear properties. High temperature corrosion and erosion resistant coatings can be used for example to protect economical low alloyed substrate material in heat exchanger surfaces of power plant boilers. The material modelling in the IMAGO project combines atomistic simulation by MD to calculate diffusion coefficients, which can be used in thermodynamic calculations to estimate the corrosion mechanics, and FEM to simulate the effect of erosion. The development and validation of the models are performed by using data from literature and concurrent experimental work. The different levels in the modelling are presented in Figure 2.

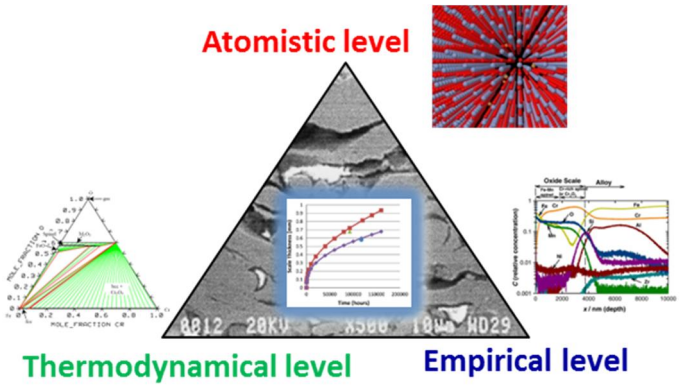

Figure 2. Three different levels of integrated modelling for high temperature corrosion are atomistic, thermodynamical and empirical.

4.2.3 Energy savings in bio fibre processing by material modelling

Use and processing of bio fibres, e.g. wood, is an important industrial sector. Bio fibre refining is vastly energy consuming process. μ-FEM modelling is used for development of elastic and inelastic models of bio fibre deformation, to understand the effect bio fibre structure on processing and to gain energy savings, see Figure 3. Experiments on wood to understand the mechanisms of crack propagation and disintegration starting from the external surface are performed to validate the models. Collaboration on microscale modelling and experiments is being conducted with University of Uppsala, Sweden.

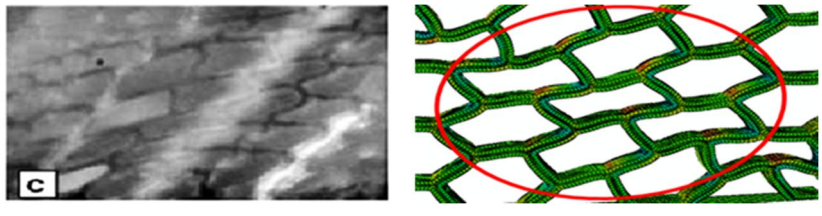

Figure 3. Elastic model of wood cell deformation. On left a SEM figure of wood cell under load (by De Magistris & Salmén 2006), and on right modelled wood cell deformation under pulping-type load.

4.3 Benefits from the IMAGO materials modelling tools

The **VTT ProperTune™** concept enables deep understanding of the relationship in the process-structure-properties-performance chain and hence more effective

material design. The material modelling tools being developed in the IMAGO project can estimate wear, aging and high temperature behaviour of DLC coatings, and help tailoring of the coating structure for best performance in selected applications and conditions. These tools enable selecting optimal materials to increase lifetime by protective thermal spray coatings, decreasing maintenance work and extending replacement cycle of failured components, providing cost savings in energy and process sector. Furthermore, the use of material modelling tools can produce energy and cost savings by more efficient process development for biofibre processing and enable to create new bio based products. Expected impact and benefits of the materials modelling tools in the VTT ProperTune™ concept are more effective material and component design targeting for energy, time and cost savings.

5. Modelling of friction and structural transformations in diamond-like carbon coatings

Helena Ronkainen, Anssi Laukkanen & Kenneth Holmberg

VTT Technical Research Centre of Finland
Metallimiehenkuja 8, P.O. Box 1000, FI-02044 Espoo

5.1 Introduction

Diamond and diamond-like carbon (DLC) based coatings have attracted a rapidly increasing number of researchers since the middle of 1980's and these films are today the most intensively researched tribological coatings [Donnet & Erdemir 2008; Holmberg & Matthews 2009]. The commercial interest in diamond and diamond-like coatings is considerable, not only because of their great potential in tribological applications but also because of their potential as new and more efficient semiconductor and optical thin film materials.

Diamond-like carbon coatings are extensively used in the computer industry as wear protective layer in the multilayer system deposited on practically all computer hard disks. This means that only for this purpose there are one million DLC coatings deposited every day. There is a large variety of other commercial applications where the excellent low friction and good wear resistant properties of DLC films are beneficial such as: valve rockers, gears, injection pumps, tappets, other automotive sliding components, cutting tools, mechanical seals, textile industry parts, optical windows, flat panel displays, photomultiplier and microwave power tubes, acoustic wave filters, sensors, heat spreaders, razor blades, surgical tools and biological implants [Hauert 2004; Erdemir and Donnet 2005].

The purpose of this paper is to present the state-of-art understanding of the structures of DLC coatings and an integrated computational modelling and simulation approach combining macro-to-microscale Finite Element Method (FEM) modelling and Constrain Free Energy (CFE) modelling with micro-to-nano scale Monte

Carlo (MC) statistical modelling and nano scale Molecular Dynamic Simulations (MDS). Simulations of macro-to-micro scale FEM modelled hydrogenated and hydrogen free DLC coatings and nano scale MDS modelled hydrogenated DLC coatings are demonstrated and reported.

5.2 DLC coating structure

Diamond-like carbon (DLC) is the name commonly used for hard carbon coatings which have similar mechanical, optical, electrical and chemical properties to natural diamond, but which do not have a dominant crystalline lattice structure. They are amorphous and consist of a mixture of sp3 and sp2 carbon structures with sp2-bonded graphite-like clusters embedded in an amorphous sp3-bonded carbon matrix. Generally they contain significant quantities of hydrogen originating from the use of hydrogen for controlling the initial nucleation and subsequent growth in the deposition process.

Several CVD and PVD deposition techniques such as plasma-enhanced CVD, sputtering, ion plating, laser ablation etc., have been successfully used for depositing DLC films. The substrate temperature during deposition is mostly below 200 ºC. The adhesion to the substrate has been improved by depositing an interlayer some nanometres thick, of Si or Ti, between the DLC coating and the substrate. DLC coatings are typically used in the thickness range of 0.01 to 2 µm but they have been prepared with thicknesses down to only a few nanometres and as nanosmooth coatings with intrinsic roughness less than 0.1 nm [Grill 1997; Bhushan 2008].

The CVD and PVD deposition techniques offer good possibilities to tailor DLC coatings with various structures corresponding to the required properties. The main categories of DLC coatings and their abbreviations are [VDI-Richtlinien 2005]:

- a-C : hydrogen-free amorphous carbon coating
- ta-C : tetrahedral hydrogen-free amorphous carbon coating
- a-C:Me : metal-containg hydrogen-free amorphous carbon coating (Me = W, Ti ....)
- a-C:H : hydrogenated amorphous carbon coating
- ta-C:H : tetrahedral hydrogenated amorphous carbon coating
- a-C:H:Me : metal-containing hydrogenated amorphous carbon coating (Me = W, Ti ...) and
- a-C:H:X : modified hydrogenated amorphous carbon coating (X = Si, O, N, F, B ...).

Since small quantities of hydrogen, e.g. from residual gases, can still be incorporated in the films even when there is no use of hydrogen gas in the deposition process, a hydrogen limit of about 3 at. % is quoted [VDI-Richtlinien 2005] as the transition between hydrogen-free and hydrogenated carbon coatings.

The most important structural parameters are the sp3/sp2-ratio and the hydrogen content in the coating. The balance between them and the regions of the various DLC coatings is illustrated in the ternary phase diagram in Figure 1a. At higher temperatures a recrystallisation of the carbon structure to graphite takes place and this transition is depending on the sp3/sp2 ratio.

Molecular dynamic simulations have shown that the three dimensional structure, not just the sp3/sp2-ratio, is important in determining the mechanical properties of the coatings [Gao et al. 2003]. Particular orientations of sp2 ring-like structures create coatings with both high sp2 content and large elastic constants. Coatings with graphite-like top layers parallel to the substrates have lower elastic constants than coatings with large amounts of sp3-hybridised carbon. The layered structure of the hydrogen-free coatings results in a mechanical behaviour that influences the friction to load relationship. The atomic-scale structure of the coating at the interface has turned out to be of critical importance in determining the load at which tribochemical reactions and wear between the coating and the counterface is induced. The coatings that are highly hydrogenated to provide enough hydrogen for all free dangling bonds to avoid the possibility that some strong covalent bonds are formed between the surfaces. Some unbonded free hydrogen can serve as a reservoir and replenish or replace those hydrogen atoms that may have been lost due to thermal heating and mechanical grinding during sliding. A molecular dynamic simulation of a highly hydrogenated a-C:H coating structure including bonded, atomic and molecular hydrogen within the coating is shown in Figure 1b.

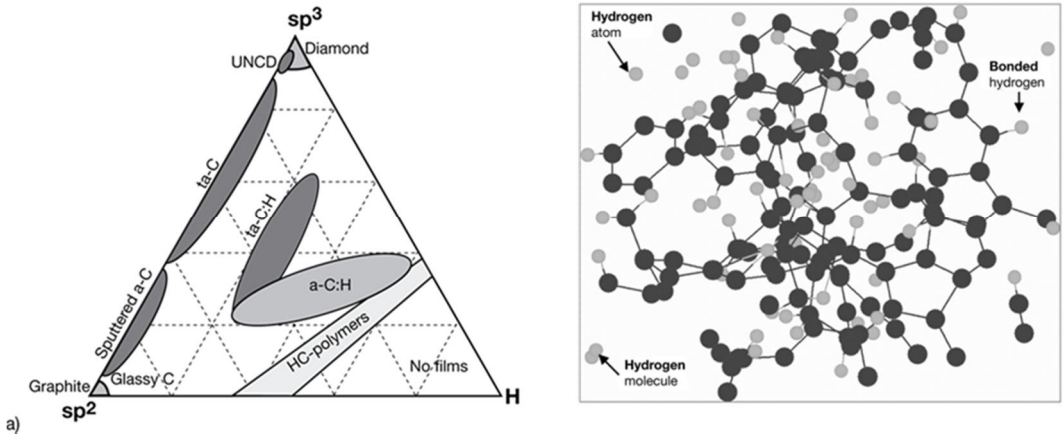

(a) (b)

Figure 1. (a) Ternary phase diagram for DLC coatings showing the balance of the sp3/sp2-ratio and the hydrogen content in the coating [after Ferrari and Robertson 2000]. UNCD refers to ultrananocrystalline diamond and HC to hydrocarbon. (b) Tight-binding molecular dynamic simulation of highly hydrogenated DLC coatings, showing bonded, atomic and molecular hydrogen within the structure [from Erdemir 2004, with permission].

5.3 Tribological mechanisms of DLC

Diamond-like carbon coatings have excellent tribological properties, very similar to the diamond coatings; they are chemically inert and have excellent biocompatibility. However, because of their amorphous structure they are less brittle than diamond coatings and due to their lower deposition temperature, down to room and even sub-zero temperatures, they can be deposited on a large variety of materials, including all kinds of metals and ceramics, with good adhesion.

The coefficient of friction for DLC is generally in the range of 0.02 to 0.4 and the wear rate 0.0001 to 1 • 10-6 mm3/N•m in normal air. For the hydrogenated DLC the coefficient of friction in a vacuum or inert environment is in the range of 0.001 to 0.02 and the wear rate may be as low as 0.00001 • 10-6 mm3/N•m [Robertson 1992; Holmberg and Matthews 1994; Grill 1997; Gangopadhyay 1998; Bhushan 1999; Nastasi et al. 1999; Ronkainen 2001; Erdemir 2002; Singer et al. 2003; Klaffke et al. 2004; Hauert 2004; Donnet and Erdemir 2008]. On the other hand the hydrogen-free DLC films typically had high friction performance in dry and inert environments [Voevodin and Donley 1996, Ronkainen et al. 1999, Andersson et al. 2003, Meunier et al. 2005].

It was already in the 90´s speculated that the very low coefficient of friction of diamond-like carbon coatings in sliding contacts is due to graphitisation and the formation of a thin graphitic layer on top of the hard. Later number of studies have pointed to the appearance of graphite in the wear tracks. They have also shown another important contact mechanism that influences friction and wear – the formation of a carbon-rich transfer layer on the counter surface [Hirvonen et al. 1990; Ronkainen et al. 1993; Grill 1997; Voevodin and Zabinski 2000; Ronkainen 2001; Sanchez-Lopez et al. 2003; Erdemir and Donnet 2005; Kano et al. 2005; Scharf and Singer 2003]. This transfer layer covers more or less completely the counter surface giving it a smooth load carrying platform ideal for low shear in combination with the graphitised top layer of the DLC coating. Transfer layers consisting of carbon, oxygen, chromium, aluminium and iron have been observed. The result is that the friction occurs between two surfaces with amorphous carbon top layers, which have a structural chemistry quite different from the original DLC coating, but similar to that of crystalline graphite. Recently tehere have also been carried out in situ TEM and EELS (electron energy loss spectra) analysis showing a mechanically-induced increase in sp^2 bond content in the tribolayers formed on a-C:H nearly frictionless carbon coatings in sliding. The study established a nanoscale sliding interface within the TEM and performed real-time imaging and spectroscopy of the moving contact and offered strong evidence that the formation of a graphitic layer is the frictional controlling mechanism.

The hydrogen content in a diamond-like carbon coating has a most significant influence on its hardness, modulus of elasticity, density and the sp3/sp2 ratio [Dunlop et al. 1991]. The presence of hydrogen is also important for the development of favourable friction conditions in diamond and DLC coatings according to the dangling bond orbital and graphitisation mechanisms described earlier. The

decrease in microhardness for a variety of DLC coatings with increasing hydrogen content in the coating has been shown [Raveh et al. 1993; Gupta et al. 2004]. The influence of hydrogen content in the coating as well as the presence of hydrogen in the surrounding environment has been shown by several studies [Ronkainen et al. 1993; Andersson et al. 2003; Sanchez-Lopez et al. 2003; Fontaine et al. 2004; Erdemir and Donnet 2005; Li et al. 2007; Ronkainen and Holmberg 2008]. For higher hydrogen content in the coating, the surface is covered by hydrogen atoms, leading to weak van der Waals bonds between the sliding surfaces. For lower hydrogen content, on the other hand, there are not enough hydrogen atoms to shield the strong interactions between the free orbitals of carbon bonds.

In non-oxidising controlled environments like vacuum, argon or dry nitrogen the tribological behaviour of diamond-like carbon coatings is often similar to that of bulk diamond. However, water vapour influences the DLC coating and in humid air the coating behaves more like bulk graphite [Miyoshi 1990; Erdemir et al. 1991; Ronkainen and Holmberg 2008]. It is well documented that graphite requires moisture or other vapours to achieve low friction and low wear. The adsorbed vapour covers the edge sites, thereby lowering the surface energy and reducing the adhesion to other surfaces [Spear 1989].

The very low coefficient of friction, often below 0.05, when a steel slider slides over a hydrogenated DLC surface in dry air gradually increases with increasing humidity and reaches values in the range of 0.15 to 0.3 at relative humidities close to 100% [Enke et al. 1980; Memming et al. 1986; Franks et al. 1990]. Ronkainen and Holmberg (2008) have reviewed the environmental effects on the tribological performance of DLC coatings and they show the different influences of humidity on different categories of DLC coatings and the mechanisms controlling their tribological performance as presented in Figure 2.

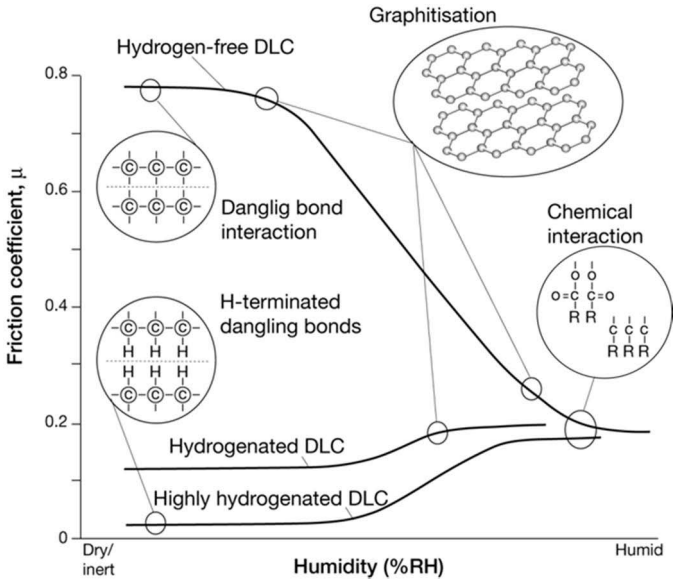

Figure 2. Schematic presentation of friction performance of DLC coatings as a function of humidity and the related mechanisms controlling their tribological performance (from Ronkainen and Holmberg, 2008).

5.4 Integrated modelling of DLC films at VTT

The tribological friction and wear mechanisms in contacts with DLC coated surfaces may be very different depending on the geometrical and topographical scales investigated [Holmberg et al. 2007]. Some phenomena are best understood on nano scale while other may be better understood on micro scale. From an industrial application point of view is it important to manage to scale up and consolidate these mechanisms to macro scale conditions typically observed and measured in practical applications.

To achieve this VTT has developed the integrated computational modelling and simulation approach, shown in Figure 3. The basic physical mechanisms that appear on nano sacle are modelled with Molecular Dynamic Simulation (MDS) and combined with their statistical features by Monte-Carlo (MC) methods. The thermochemical features are introduced by Constrain Free Energy (CFE) modeling and this information is consolidated to global tribological behaviour on macro scale by Finite Element Method (FEM). It is necessary to carry out a number of separate validation exercises on different scale levels to be sure that the models are reflecting the material behaviour of real materials in real contacts. Nano scale models are validated by nano indentation, Atomic Force Microscopy (AFM) and in-situ Scanning Electron Microscopy (SEM) scratch testing. Scratch testing and Raman surface analysis are carried out on micro scale, residual stresses meas-

ured on macro scale and the final validation on macro scale is done by pin-on-disc tribometer friction and wear measurements.

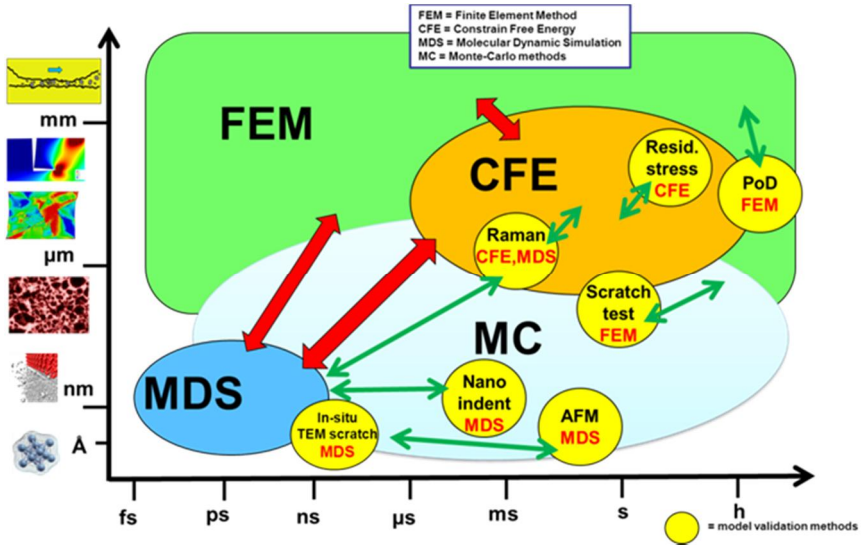

Figure 3. Integrated multiscale material modelling with length and time scale ranges of the four modelling techniques (FEM, CFE, MC and MDS) and used empirical validation techniques, shown in yellow circles.

5.4.1 FE modelling of a-C:H and ta-C

Meso and macroscale modelling is commonly carried out using the finite element method, since it provides a direct link to means applied to perform component analyses. The best all around method for determination of mechanical performance of coatings is the scratch test. A typical finite element model of a scratch test of a DLC coating is presented in Figure 4. Symmetry of the setup is exploited and the relevant coating, interface and substrate layers are included along with the diamond tip usually with a radius ranging from some tens of micrometers to 200 µm. In Figure 5 results are presented for a 0.6 µm thick a-C:H coating and 0.3 µm ta-C coating. The results for both a-C:H and ta-C demonstrate typical behavior as far as the principal stress distribution is concerned, the peak values being located at the edge of the scratch test groove, which along with the scratch bottom is one of the most common locale for crack field initiation.

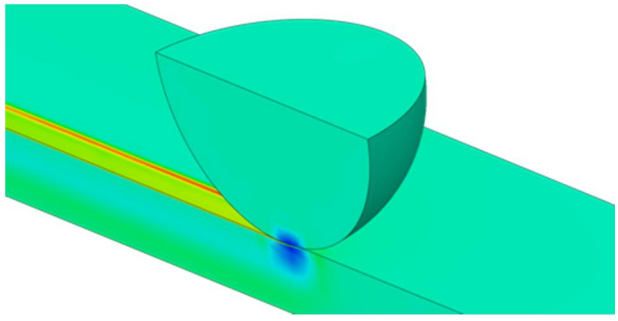

Figure 4. Finite element modelling of DLC scratch testing.

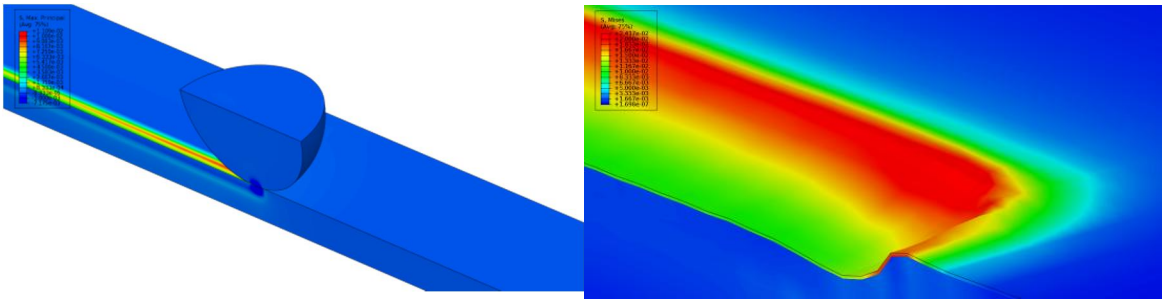

Figure 5. Contours of first principal stress in 0.6 µm thick a-C:H DLC coating (left) and equivalent von Mises stress in 0.3 µm thick ta-C DLC coating (right).

The FE modelling can provide more thorough understanding on the performance of different DLC coating types in tribological contacts. By studying the stress and strain performance of DLC films under load it is possible to understand the different properties and aspects influencing the coating performance. For expample the a-C:H and ta-C coatings with different coating thicknesses were evaluated in pin-on-disc tests with increasing normal load. The test results showed delamination of the 0.3 µm thick ta-C coating with a lower normal load compared to the 0.6 µm thick a-C:H coating as described in Figure 6. The modelling results of the coatings clearly explaned the coating performance by generation of higher stresses in the ta-C coating when subjected to high contact loads. The modelling results also showed that the coating thickness is playing an important role in coating performance [Ronkainen et al. 2012].

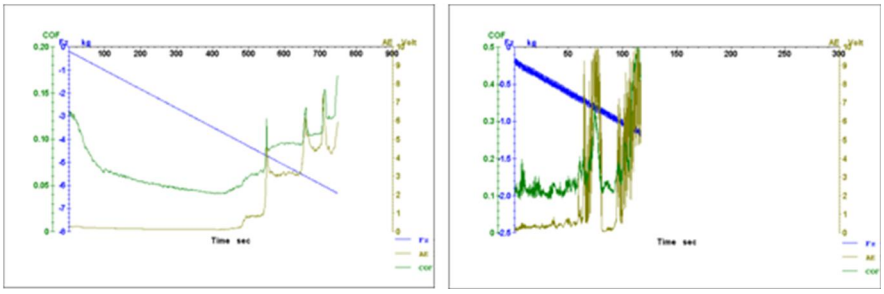

Figure 6. The friction performance of 0.6 µm thick a-C:H DLC coating (left) and 0.3 µm thick ta-C DLC coating (right) with increasing normal load in pin-on-disc testing.

5.4.2 Molecular dynamic simulation of a-C:H

Molecular dynamics (MD) analysis can take a direct stance on the mechanisms of friction, material damage and wear arising from nanoscale upwards [Harrison et al. 1992; 1995; 1998]. Molecular dynamics analyses have been carried out using various force fields, in the following results utilizing the AIREBO potential are reported [Stuart et al. 2000]. The amorphous DLC structures are derived using a liquid quench method, where a randomized ordered cubic lattice of C and H in the respective fractions of a given density is allowed to spontaneously melt. After melting and reaching temperatures of approximately 8000K the system is thermostatted using velocity rescaling and stabilized. After a stabilization period cooling to 300K is conducted using several temperature gradients and again velocity rescaling, followed by a stabilization period of the final structure. What results is an amorphous C-H structure to be utilized as a starting structure in further analyses. One such demonstration is given in Figure 7 presenting the distribution of the normal stress component in the direction of the indentation, providing a glimpse how the stress distribution differs in the atomic scale from that of the continuum, e.g. when comparing to Figure 4. One of the main goals in MD studies of DLC is identification of the mechanisms responsible for its performance with respect to friction, i.e. the reasoning underlying the low coefficients of friction and on the other hand limitations in its range of application. Results to this effect are presented in Figure 8, where the coordination number of a system is plotted during scratch testing of a 25at% H a-C:H structure. One of the long standing theories for friction behavior of DLC surfaces under contact is surface stress state induced phase transformation to graphitization, which forms a low friction surface layer. Reasoning towards such a conclusion is given in Figure 6 by acknowledging the formation of a shear layer, i.e. orientation of the surface atomic structure from a sp3 dominated atomic coordination to graphite like sp2, and to some extent even further, sp1 bonding. This arises solely from the mechanical interaction between the two surfaces at ambient conditions.

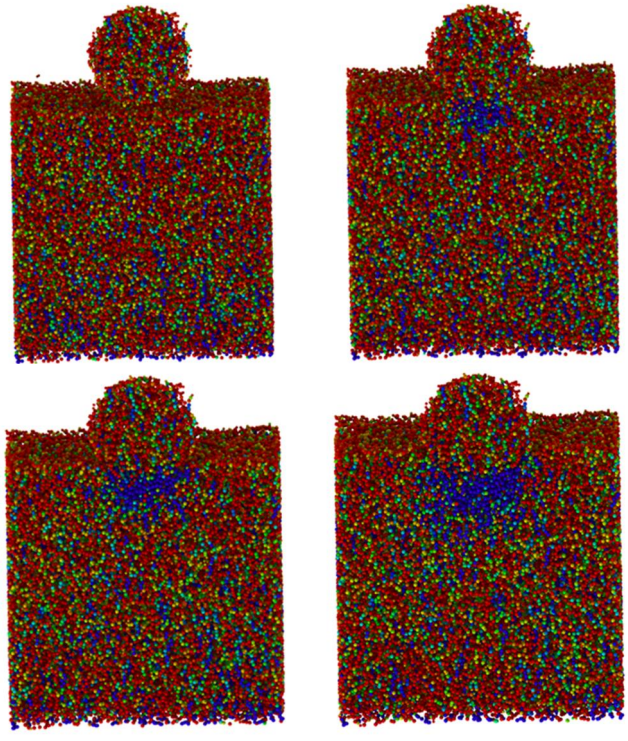

Figure 7. MD results for in-plane compressive stress during indentation of 25at% H a-C:H DLC surface with a-C:H DLC tip.

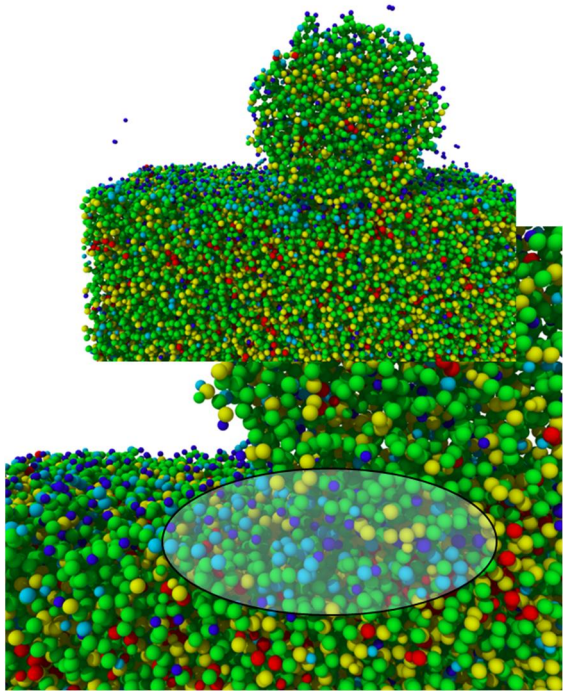

Figure 8. MD coordination plot during scratch testing of 25at% H a-C:H DLC surface with a-C:H DLC tip.

5.5 Conclusions and future aspects

The modelling provides an excellent tool to understand the coating performance and to design coatings with optimal structures and properties. Modelling aided design can also be used to greate design rules for coatings and coated component for real applications.

The integrated computational modelling and simulation approach adobled at VTT combine the MDS modelling of basic physical mechanisms on nano sacle, MC modelling with statistical features, CFE modeling for the thermochemical features, and finally consolidate the information to global tribological behaviour on macro scale by FEM. With this approach the aging and thermal effects of DLC coatings will be studied and the modelling will be verified by testing.

5.6 References

Andersson, J., Erck, R.A. and Erdemir, A. 2003. Frictional behavior of diamondlike carbon films in vacuum and under varying water vapor pressure. Surface and Coatings Technology, Vol, 163-164, pp. 535–540

Bhushan, B. 1999. Chemical, mechanical and tribological characterization of ultrathin and hard amorphous carbon coatings as thin as 3.5 nm: recent developments. Diamond and Related Materials, Vol. 8, pp. 1985–2015.

Bhushan, B. 2008. Nanotribology of ultrathin and hard amorphous carbon films. In: Tribology of diamond-like carbon films. Donnet, C. and Erdemir, A. (Eds.). Springer, New York, USA. Pp. 510–570.

Donnet, C. and Erdemir, A. (Eds.). 2008. Tribology of diamond-like carbon films – Fundamentals and applications. Springer, New York, USA. 664 p.

Dunlop, E., Haupt, J., Schmidt, K. and Gissler, W. 1991. Hardness and Young's modulus of diamond-like carbon films prepared by ion beam methods. In: Proceedings 2nd European Conference on Diamond, Diamond-like and Related Coatings, Nice, France, 2-6.9.1991. Pp. 644–649.

Enke, K., Dimigen, H. and Hübsch, H. 1980. Frictional properties of diamondlike carbon layers. Applied Physics Letters, Vol. 36, pp. 291–292.

Erdemir, A., Switala, M., Wei, R. and Wilbur, P. 1991. A tribological investigation of the graphite-to-diamond-like behaviour of amorphous carbon films ion beam deposited on ceramic substrates. Surface and Coatings Technology, Vol. 50, pp. 17–23.

Erdemir, A. 2002. Friction and wear of diamond and diamond-like carbon films. Proceedings of the Institution of Mechanical Engineers, Part J: Journal of Engineering Tribology, Vol. 216, pp. 387–400.

Erdemir, A. 2004. Genesis of superlow friction and wear in diamondlike carbon films. Tribology International, Vol. 37, pp. 1005–1012.

Erdemir, A. and Donnet, C. 2005. Tribology of Diamond and Diamond-Like Carbon Films: An Overview. In: Wear – Materials, Mechanisms and Practice. Stachowiak, G.W. (Ed.). Tribology in Practice Series, John Wiley and Sons, Chichester, UK. Pp. 191–222.

Ferrari, A.C. and Robertson, J. 2000. Interpretation of Raman spectra of disordered and amorphous carbon. Physical Review B, Vol. 61, No. 20, pp. 14095–14107.

Fontaine, J., Belin, M., Le Mogne, T. and Grill, A. 2004. How to restore superlow friction of DLC : the healing effect of hydrogen gas. Tribology International, Vol. 37, pp. 869–877.

Franks, J., Enke, K. and Richardt, A. 1990. Diamond-like carbon – properties and applications. Metals and Materials, November, 1990, pp. 695–700.

Gangopadhyay, A. 1998. Mechanical and tribological properties of amorphous carbon films. Tribology Letters, Vol. 5, pp. 25–39.

Gao, G.T., Mikulski, P.T., Chateauneuf, G.M. and Harrison, J.A. 2003. The effects of film structure and surface hydrogen on the properties of amorphous carbon films. Journal of Physysical Chemistry B, Vol. 10, No. 40, pp. 11082–11090.

Grill, A. 1997. Tribology of diamondlike carbon and related materials: an updated review. Surface and Coatings Technology, Vol. 94–95, pp. 507–513.

Gupta, P., Singh, V. and Meletis, E.I. 2004. Tribological behavior of plasma-enhanced CVD a-C:H films. Part I: effect of processing parameters. Tribology International, Vol. 37, pp. 1019–1029

Harrison, J.A., White, C.T., Colton, R.J., Brenner, D.W. 1992. Molecular-dynamic simulations of atomic-scale friction of diamond surfaces. The American Physical Society, Physical Review B, Vol. 46, 15. pp. 9700-9708.

Harrison, J., White, J., Colton, R., Brenner D. 1995. Investigation of the atomic-scale friction and energy dissipation in diamond using molecular dynamics. Thin Solid Films, Vol. 260, pp. 205-211.

Harrison, J., Stuart, S., Perry, M. 1998. The tribology of hydrocarbon surfaces investigated using molecular dynamics. In: Tribology Issues and Opportunities in MEMS. Bhushan, B. (ed.), Kluwer Academic Publishers, The Netherland, pp. 285-299.

Hauert, R. 2004. An overview on the tribological behavior of diamond-like carbon in technical and medical applications. Tribology International, Vol. 37, pp. 991–1003.

Hirvonen, J.-P., Koskinen, J., Anttila, A., Lappalainen, R., Toivanen, R.O., Arminen, E. and Trkula, M. 1990. Characterization and unlubricated sliding of ion-beam-deposited hydroge-free diamond-like carbon films. Wear, Vol. 141, pp. 45–58.

Holmberg, K. and Matthews, A. 1994. Coatings Tribology – Properties, Techniques and Applications in Surface Engineering. Tribology Series 28, Elsevier, Amsterdam. 442 p.

Holmberg, K. and Matthwes, A. 2009. Coatings Tribology – Properties, Mechanisms, Techniques and Applications in Surface Engineering, Tribology and Interface Engineering Series No. 56. Elsevier, Amsterdam.

Holmberg, K., Ronkainen, H., Laukkanen, A. and Wallin, K. 2007. Friction and wear of coated surfaces – scales, modelling and simulation of tribomechanisms. Surface and Coatings Technology 202, pp. 1034–1049.

Klaffke, D., Brand, J., Brand, C., Wittorf, R. and Hartelt, M. 2004. Tribologische characterisierung metalldotierter DLC-schichten. Tribologie und Schmierungstechnik, Vol. 51, No. 4, pp. 15–19.

Kano, M., Yasuda, Y., Okamoto, Y., Mabuchi, Y., Hamada, T., Ueno, T., Ye, J., Konishi, S., Takeshima, S., Martin, J.M., De Barros Bouchet, M.I. and Le Mogne, T. 2005. Ultralow friction of DLC in presence of glycerol monooleate (GMO). Tribology Letters, Vol. 18, No. 2, pp. 245–251.

Li, H., Xu, T., Wang, C., Chen, J., Zhou, H. and Liu, H. 2007. Tribochemical effects on the friction and wear behaviors of a-C:H and a-C films in different environment. Tribology International, Vol. 40, pp. 132–138.

Memming, R., Tolle, H.J. and Wierenga, P.E. 1986. Properties of polymeric layers of hydrogenated amorphous carbon produced by a plasma-activated chemical vapour deposition process, II: Tribological and mechanical properties. Thin Solid Films, Vol. 143, pp. 31–41.

Meunier, C., Alers, P., Marot, L., Stauffer, J., Randall, N. and Mikhailov, S. 2005. Friction properties of ta-C and a-C :H coatings under high vacuum. Surface and Coatings Technology, Vol. 200, pp. 1976–1981.

Miyoshi, K. 1990. Studies of mechanochemical interactions in the tribological behavior of materials. Surface and Coatings Technology, Vol. 43/44, pp.799–812.

Nastasi, M., Kodali, P., Walter, K.C., Embury, J.D., Raj, R. and Nakamura, Y. 1999. Fracture toughness of diamondlike carbon coatings. Journal of Material Research, Vol. 14, No. 5, pp. 2173–2180.

Raveh, A., Martinu, L., Hawthorne, H.M. and Wertheimer, M.R. 1993. Mechanical and tribological properties of dual-trequency plasma-deposited diamond-like carbon. Surface and Coatings Technology, Vol. 58, pp. 45–55.

Robertson, J. 1992. Properties of diamond-like carbon. Surface and Coatings Technology, Vol. 50, pp. 185–203.

Ronkainen, H., Koskinen, J., Likonen, J., Varjus, S. and Vihersalo, J. 1993. Characterization of wear surfaces in dry sliding of steel and alumina on hydrogented and hydrogen free carbon films. Diamond Films '93 Conference Albufeira, Portugal, 20.–24.9.1993. 30 p.

Ronkainen, H., Koskinen, J., Varjus, S. and Holmberg, K. 1999. Load-carrying capacity evaluation of coating/substrate systems for hydrogen-free and hydrogenated diamond-like carbon films. Tribology Letters, Vol. 6 No. 2, pp. 63–73.

Ronkainen, H. 2001. Tribological properties of hydrogenated and hydrogen-free diamond-like carbon coatings. Espoo, VTT Manufacturing Technology, VTT Publications 434. 52 p. + app. 91 p.
http://www.vtt.fi/inf/pdf/publications/2001/P434.pdf

Ronkainen, H. and Holmberg, K. 2008. Environmental and thermal effects on the tribological performance of DLC coatings. In: Tribology of diamond-like carbon films. Fundamentals and applications. Donnet, C. and Erdemir, A. (Eds.). Springer, New York, USA. Pp. 155-200.

Ronkainen, H., Holmberg, K., Laukkanen, A., Andersson, T., Kano, M., Horiuchi, T., Wakabayashi, T., Suzuki, T., Kumagai, M., Taki, M. 2012. The effect of coating characteristics on the coating performance of a-C:H and ta-C films. In: Proceeding of Nordic Tribology Congress, NordTrib 2012. Trondheim, Norway. 6 p.

Sanchez-Lopez, J.C., Erdemir, A., Donnet, C. and Rojas, T.C. 2003 Friction-induced structural transformations of diamondlike carbon coatings under various atmospheres, Surface and Coatings Technology, Vol. 163–164, pp. 444–450

Scharf, T.W. and Singer, I.L. 2003. Monitoring transfer films and friction instabilities with in situ Raman tribometry. Tribology Letters, Vol. 14, No. 1, pp. 3–8.

Singer, I.L., Dvorak, S.D., Wahl, K.J. and Scharf, T.W. 2003. Role of third bodies in friction and wear of protective coatings. Journal of Vacuum Science and Technology A, 21 (5), pp. S232–S240.

Spear, K.E. 1989. Diamond – ceramic coating of the future. Journal of American Ceramic Society, Vol. 72, No. 2, pp. 171–191.

Stuart, S., Tutein, A. and Harrison, J. 2000. Journal of Chemical Physics, 2000.

VDI-Richtlinien: 2005. Carbon films – Basic knowledge, film types and properties. VDI 2840, November 2005, 44 p.

Voevodin, A.A., Donley, M.S. 1996. Surface and Coatings Technology 82:199-213.

Voevodin, A.A. and Zabinski, J.S. 2000. Supertough wear-resistant coatings with ‘chameleon’ surface adaption. Thin Solid Films, Vol. 370, pp. 223–231.

6. Molecular dynamics simulations of mass transport in chromium oxide scales

Jukka Vaari

VTT Technical Research Centre of Finland
Kemistintie 3, P.O. Box 1000, FI-02044 Espoo

6.1 Abstract

Mass transport in bulk α-Cr_2O_3 has been studied by means of classical molecular dynamics (MD) simulations. Point defects were assumed to be responsible for ionic diffusion. The focus of this study were vacancies both in the cation and anion lattice (Schottky defects). Two parametrizations of the Buckingham potential were used to describe the interactions between ions. Defect concentrations between 8e-5 and 8e-4 were studied in the temperature range 1300 K – 2000 K. Diffusion coefficients were calculated from mean square displacements. Activation energies for migration were determined from Arrhenius plots. The results were compared to literature values for diffusion coefficients and parabolic growth constants.

6.2 Introduction

Mass transport properties of chromium(III) oxide have been the subject of much interest both experimentally and theoretically. These studies have revealed that not only does Cr_2O_3 exhibit a complex defect chemistry, but that the method by which the Cr_2O_3 samples are manufactured will greatly affect the defect chemistry.

An ideal α-Cr_2O_3 (corundum) single crystal has no grain boundaries and no impurities, and the only mechanism for bulk mass transport would be through intrinsic defects present at finite temperatures. The energy required to generate these defects can be readily computed, and Atkinson et al. [Atkinson et al. 2003] report values of 5.59 eV, 5.34 eV, and 7.80 eV for intrinsic Schottky, anion Frenkel and

cation Frenkel defects, respectively. Clearly, these energies are large compared to k_BT at temperatures of practical interest, so one would expect mass transport in such crystals to be extremely slow due to a low concentration of point defects.

The defect chemistry of Cr_2O_3 is complicated by impurities present in the bulk material. Since intrinsic defect concentrations in Cr_2O_3 are small, small impurity concentrations, down to the ppm level, may have significant effects on the defect chemistry. Impurities are unavoidable in practical materials, but they may also be introduced during experimental measurements. For example, Holt and Kofstad [Holt and Kofstad 1994] report elevated levels of Mg and Al impurities in their Cr_2O_3 samples due to extended exposure to the materials in the conductivity measuring instruments.

According to Atkinson et al. [Atkinson et al. 2003], small divalent substitutional cations (such as Mg) in a Cr_2O_3 lattice have solution energies of the order of 2 eV, significantly less than the energies of intrinsic defect formation. This implies that real Cr_2O_3 samples should be regarded as doped semiconductors with the charge carrier concentration dictated by the impurity concentration. The nature of the charge carrier depends on the dopant, and can be modeled by writing equations describing the mass (and charge) balance of the possible defect reactions. Accordingly, Atkinson et al. [Atkinson et al. 2003] argue that doping a Cr_2O_3 crystal with a divalent cation will drive up the concentration of oxygen vacancies. However, since both Schottky and anion Frenkel defects involve oxygen vacancies, it is not possible to make definite conclusions on the type of defect introduced.

Experimental work on the nature of ion transport in Cr_2O_3 remains somewhat inconclusive. For example, Su and Simkovich [Su and Simkovich 1987] present a comprehensive analysis on the point defect structure of Cr_2O_3 fully starting out from the assumption that the point defects are in the cation lattice. Young et al. [Young et al. 1987] acknowledge the possiblity of defects in the oxygen lattice to explain the observed p-type conductivity in their Cr_2O_3 samples, but go on to conclude that Cr lattice defects are a more plausible explanation. Holt and Kofstad [Holt and Kofstad 1997], in a study of Mg-doped Cr_2O_3, discuss the possibility of defects in the oxygen lattice, especially at low oxygen partial pressures.

One complication regarding the experiments is the method of sample preparation. The Cr_2O_3 scales of Tsai et al. [Tsai et al. 1996] were prepared by oxidizing a $Ni_{70}Cr_{30}$ alloy, and those of Young et al. [Young et al. 1987] by first die pressing Cr_2O_3 powder particles together, followed by high-temperature sintering at low-oxygen atmosphere. Lillerud et al. [Lillerud et al. 1980] employed thermal etching in high vacuum, Salomonsen et al. [Salomonsen et al. 1989] used electron-gun-evaporation of Cr on a Si substrate followed by oxidation. The variety of procedures raises issues about the comparison of results in view of the differing morphology of the samples prepared by different methods. This is important especially regarding diffusion along grain boundaries, as it may be much faster than bulk diffusion. Tsai et al. [Tsai et al. 1996] report bulk diffusion coefficients of the order of 10^{-18} to 10^{-16} cm^2/s at 800–900 °C, with corresponding grain boundary diffusion coefficients of the order of 10^{-13} to 10^{-12} cm^2/s. The apparent macroscopic diffusion coefficient, as reflected by the parabolic growth constant, is a weighted average of

bulk and grain boundary diffusion coefficients, where the weighting depends on the details of the grain boundary morphology. It should also be noted that the low bulk diffusion coefficients for Cr_2O_3 also imply long equilibriation times after a possible high-temperature treatment of a sample which in practice means that defects introduced during the sample preparation process are effectively frozen in.

In this work, molecular dynamics simulations have been used in order to gain insight into the relationship between the defect structure and mass transport properties of Cr_2O_3. The basic assumption in this work is that point defects are responsible for the ion transport. No attempt is made to predict the defect structure either qualitatively or quantitatively. Instead, a range of Schottky defect concentrations are considered. Diffusion coefficients are determined from the mean square displacement of ions. The Cr_2O_3 crystal is treated as a regular single crystal with Schottky defects introduced randomly throughout the crystal. The approach is thus similar to the one taken by Beverskog et al. [Beverskog et al. 2002] where the kinetic and transport parameters for oxide layer growth are obtained solely based on defect concentration, not regarding the type of defect. Therefore, the role of grain boundaries, dislocation defects, etc. in the transport process are not explicitly modeled. The defect concentrations have been chosen sufficiently low that individual point defects are not expected interact with each other, but high enough (in combination with a temperature range) that diffusion coefficients can be observed with reasonable accuracy given the limitations of the computational resources.

6.3 Computational details

The atomic interactions in this work were described by a Buckingham potential in combination with a Coulomb term:

$$V_{ij}(r_{ij}) = A_{ij}\exp\left(-\frac{r_{ij}}{\rho_{ij}}\right) - \frac{C_{ij}}{r_{ij}^6} + \frac{q_i q_j}{r_{ij}}$$

Two sets of parameters applicable to α-Cr_2O_3 were used in this work, as shown in Table 1. Pairwise interactions were explicitly calculated up to a distance of 15 Å. Long-range Coulombic interactions were computed by the Ewald method. Polarization effects were not accounted for. Only Coulombic interaction was assumed between chromium ions due to the small radius of these ions. Ions were assumed to adopt their formal charges.

A supercell of 20 x 20 x 10 hexagonal unit cells with periodic boundary conditions was used in the simulations for a total of 120000 atoms. Schottky defects were generated by randomly deleting atoms from both cation and anion lattices to maintain charge neutrality. The integration of Newton's equations was performed by the Verlet algorithm. A timestep of 1.0 fs was used. All simulations were conducted in the NPT ensemble. Simulations were typically run up to 400 ps of real time.

The diffusion of ions was measured by recording the Mean Square Displacement (MSD) for ion type i as a function of time, and computing the diffusion constant from the slope of the MSD(t) curve according to

$$\left\langle r_i^2(t)\right\rangle = \frac{1}{N}\sum_N \left[r_i(t) - r_i(0)\right]^2 = 6Dt$$

To obtain the slope, a line was fitted to the MSD(t) curve between 200 and 400 ps.

The MD simulations were performed using LAMMPS software [Plimpton 1995].

Table 1. Buckingham potential parametrizations used in this work.

	Parameter set 1 [Lewis and Catlow 1985, Catlow 1977]			Parameter set 2 [Minervini et al. 1999]		
	A (eV)	r (Å)	C (eV·Å^6)	A (eV)	r (Å)	C (eV·Å^6)
Cr^{3+}–O^{2-}	1734.1	0.301	0	1204.18	0.3165	0
O^{2-}–O^{2-}	22764	0.149	27.88	9547.96	0.2192	32
Cr^{3+}–Cr^{3+}	Only Coulombic			Only Coulombic		

6.4 Results

Simulations were performed for defect fractions of $8.3\cdot10^{-5}$, $2.0\cdot10^{-4}$, $\cdot4.2\cdot10^{-4}$, and $8.3\cdot10^{-4}$ and for temperatures from 1300 K to 2000 K at 100 K intervals. The defects were created at 300 K, followed by a 10 ps heating time from 300 K to the target temperature. Figure 1 presents typical MSD(t) curves from the simulations. The time zero in the figure has been set to the point in time when the simulation has reached the target temperature. This explains the initial non-zero MSD values which are slightly different for the two parameter sets. The data contains considerable noise due to the low defect fraction, limiting the accuracy of determining the slope of the MSD(t) curve especially at lower temperatures. The main difference between the parameter sets is that for set 1, oxygen appears to be the mobile ion, while chromium shows essentially no diffusion. For set 2, both ions are mobile.

It can be observed from Figure 1 that for parameter set 2, the initial 10 ps heating period is not sufficient to equilibriate the system. The shape of the MSD curves is curved up to about 200 ps, after which a linear trend continues. This is the reason for determining diffusion coefficients from the MSD data between 200 and 400 ps.

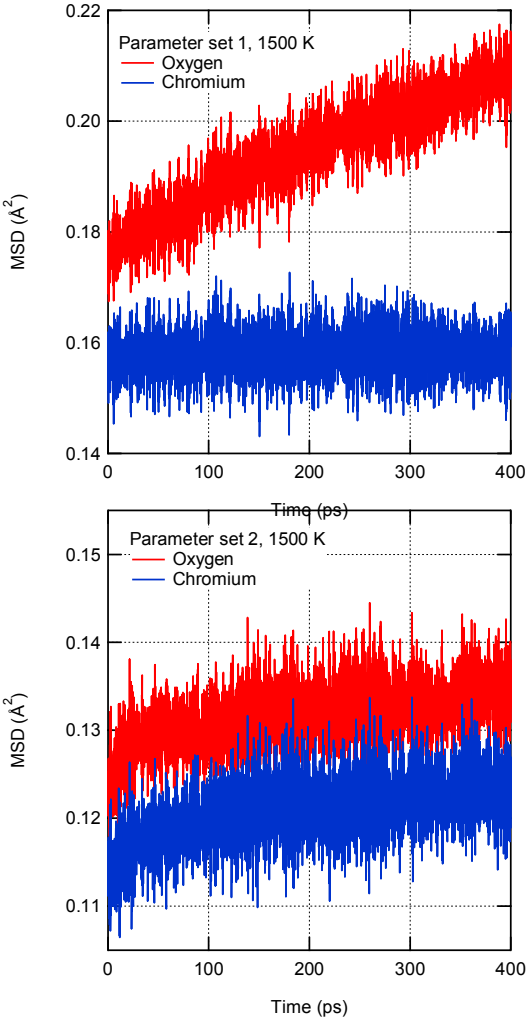

Figure 1. Mean square displacement of oxygen and chromium ions for a Schottky defect fraction of $8.3 \cdot 10^{-4}$ at a temperature of 1500 K. Above: Parameter set 1. Below: Parameter set 2.

The diffusion coefficients determined from the simulations for parameter set 1 are presented in the left part of Figure 2 for O diffusion in α-Cr_2O_3 at a Schottky defect fraction of $8.3 \cdot 10^{-4}$. There is scatter in the data, and especially the diffusion coefficient determined at 1700 K seems to be an outlier. However, when presented in the form of an Arrhenius plot (lower part of Figure 2), the data can be reasonably fitted with a line, yielding an activation energy of 0.85 eV for O migration. Chromi-

um data is not presented, as the MSD curves for chromium showed no slope that could have been determined reliably.

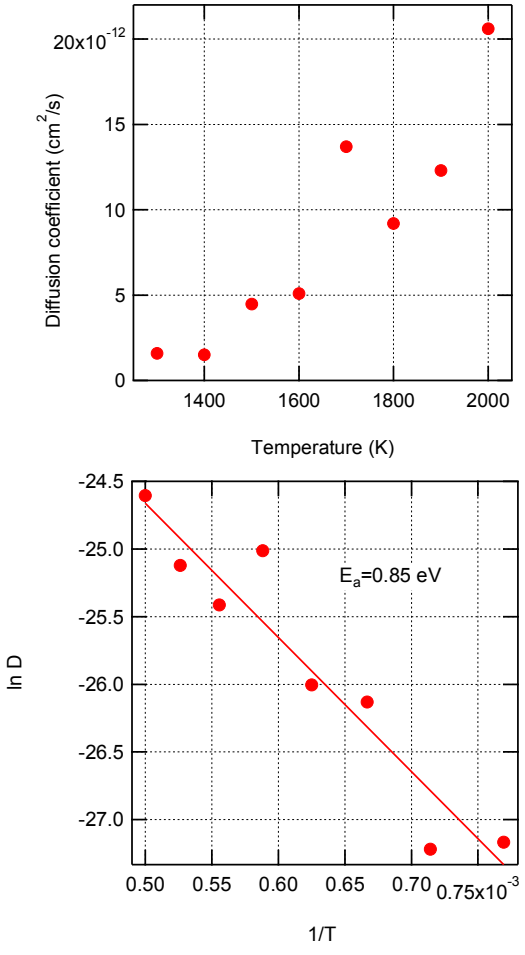

Figure 2. Diffusion coefficients and Arrhenius plot for O diffusion in α-Cr_2O_3 for parameter set 1 at a Schottky defect fraction of $8.3 \cdot 10^{-4}$.

The diffusion coefficients determined from the simulations for parameter set 2 are presented in the left part of Figure 3 for O diffusion in α-Cr_2O_3 at a Schottky defect fraction of $8.3 \cdot 10^{-4}$. It can be noted that the diffusion coefficients are roughly half of those obtained for parameter set 1. The Arrhenius plot for the data (lower part of Figure 3) gives an activation energy of 1.1 eV for O migration.

In order to understand the scatter in the data, five simulations at 1600 K and two simulations at 1700 K were conducted. The initial velocity vectors for the atoms, as well as the defect configurations were different for each run. The range of

the data points for these runs gives an indication of the sensitivity of the approach to the initial configuration, and explains the scatter observed in the data of Figure 3. Although a similar sensitivity study was not conducted for parameter set 1, it is expected that the result would have not differed too much.

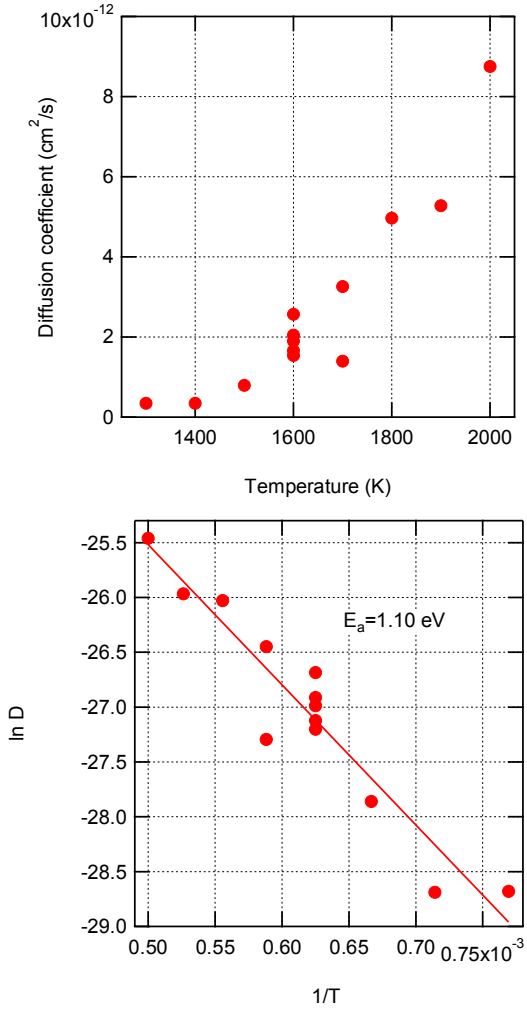

Figure 3. Diffusion coefficients and Arrhenius plot for O diffusion in α-Cr_2O_3 for parameter set 2 at a Schottky defect fraction of $8.3 \cdot 10^{-4}$.

The diffusion coefficients determined from the simulations for parameter set 2 are presented in the left part of Figure 4 for Cr diffusion in α-Cr_2O_3 at a Schottky defect fraction of $8.3 \cdot 10^{-4}$. In this case, the scatter in the data is considerable, and the five simulations conducted at 1600 K suggest a large error bar for an individual data

point. The diffusion coefficients are roughly half of those obtained for O diffusion. The Arrhenius plot for the data (lower part of Figure 4) gives an activation energy of 0.37 eV for Cr migration, but there is significant uncertainty involved with this number.

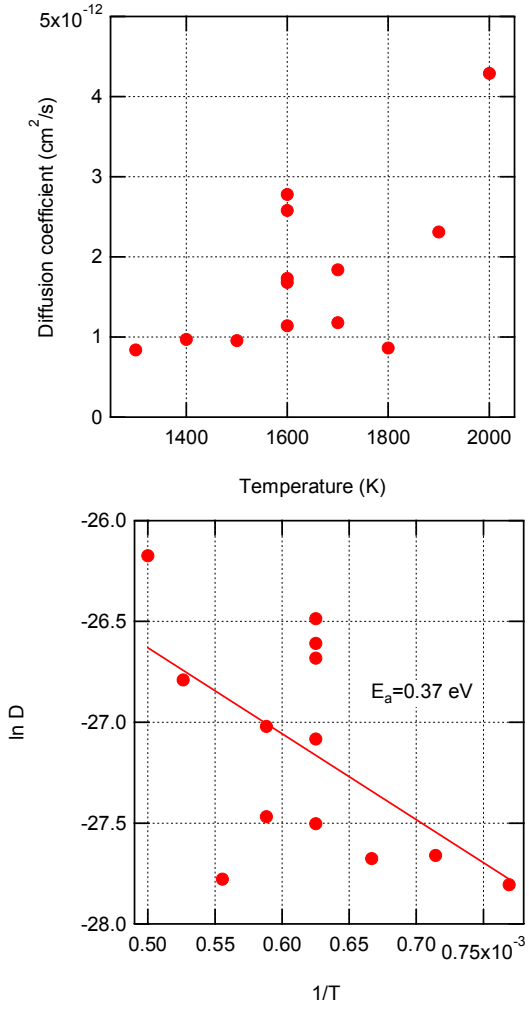

Figure 4. Diffusion coefficients and Arrhenius plot for Cr diffusion in α-Cr_2O_3 for parameter set 2 at a Schottky defect fraction of $8.3 \cdot 10^{-4}$.

Direct comparison of the diffusion coefficients to literature values is not possible due to the high temperatures used in the simulations. For example, Tsai et al. [Tsai et al. 1996] determined the Cr and O diffusion constants at 1073 K and 1173 K, and Liu et al. [Liu et al. 1998] used a temperature range from 573 K to 1173 K.

However, if it is assumed that the physical migration mechanism remains the same regardless of temperature, the activation energies from the Arrhenius plots may be used to extrapolate results to lower temperatures by writing the diffusion coefficient in the form

$$D = D_0 \exp\left(-\frac{E_M}{kT}\right)$$

It is important to understand that the above expression strictly relates to migration, which is the reason for the activation energy having a subscript 'M'. The true diffusion constant depends on the defect fraction, which in principle adds the activation energy for defect formation to the equation. As already mentioned in the introduction, the defect fraction in α-Cr_2O_3 is dependent on the impurity levels in the material, and the details of the manufacturing process of the samples, especially the high temperature treatments. It is not the purpose of this paper to try and predict defect fractions in Cr_2O_3 scales. The approach is to assume various point defect fractions and to see whether they are realistic in the first place, and secondly whether they yield diffusion coefficients that are in line with experiments. Thus, it is assumed that the diffusion coefficients in this work are of the form [Murphy 2009]

$$D = D_0 \exp\left(-\frac{E_M}{kT}\right) = \frac{n}{N} d_i = \frac{n}{N} d_{i,0} \frac{1}{6} fza^2 \nu_0 \exp\left(-\frac{E_M}{kT}\right)$$

where n is the number of defects, N is the total number of lattice sites, and d_i is the diffusion coefficient associated with defect type i. The last form of the expression tells that d_i depends on the vibrational frequency of the diffusing atom ν_0 (the number of attempts per time unit to cross the activation barrier E_M), the jump distance a, the number of equivalent pathways z the diffusing mechanism can follow, and a correlation factor f which relates diffusion of actual atoms to the diffusion of the defect (often between 0.4 and 1).

The dependence of the oxygen diffusion coefficient on the defect fraction, as found in the simulations of this work, is presented in Figure 5. It can be observed that the dependence seems to be close to linear between for the three lower defect fractions studied, but a deviation from linearity occurs when going to the highest defect fraction especially for temperatures between 1300 K and 1700 K. Given the expression for the diffusion coefficient above, this may suggest that at a defect fraction of $8.3 \cdot 10^{-4}$ the defects can no longer be regarded as completely isolated from each other. In particular, the possibility of two defects being initially close to each other increases, which gives more freedom for the lattice to deform and allow atoms to diffuse. In addition Atkinson et al. [Atkinson et al. 2003] point out the possibility of the formation of stabile defect clusters, although it is not immediately clear how this should affect the overall diffusion constant.

To compare defect fractions to experiments, we refer to the work of Young et al. [Young et al. 1987] who employed a Seebeck measuring system. In this case,

the measured thermoelectric power (ε) relates to the concentration of charge carriers (n) through

$$\varepsilon = \frac{k}{e} \ln\left(\frac{N}{n}\right)$$

where k is the Bolzmann constant and N is the density of states, which is taken equal to the number of cation sites. For p-type Cr_2O_3 at temperatures below 1300 K Young et al. find a thermoelectic power of 750 μV/K corresponding to an electron hole concentration of $2 \cdot 10^{-4}$ per cation site. Young et al. then assume that chromium vacancies are present in the p-type material, and since one vacancy in a triply charged lattice corresponds to three holes, a defect fraction of $6.7 \cdot 10^{-5}$ comes out of the analysis, close to the lower range of defect fractions used in this work.

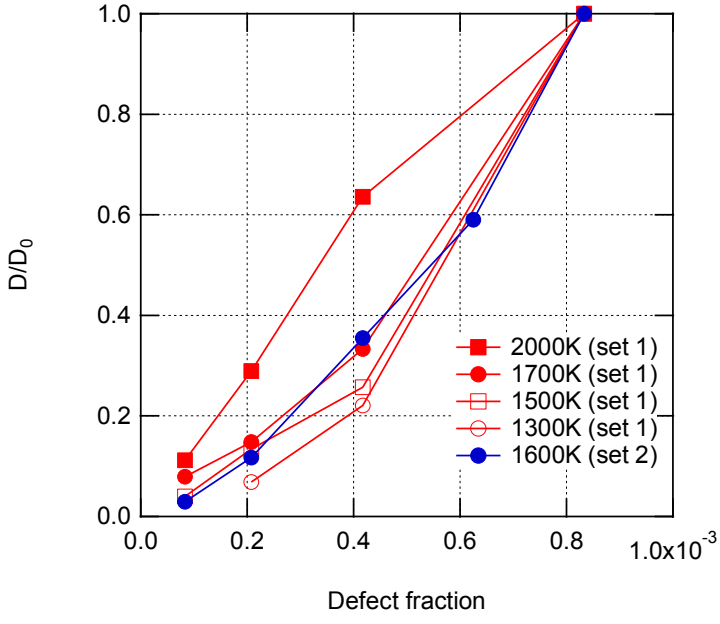

Figure 5. Normalized oxygen diffusion coefficients as a function of Schottky defect fraction.

The activation energies for electronic and ionic diffusion were measured by Liu et al. [Liu et al. 1998] using asymmetry polarization technique. Whereas pure electronic conductivity was observed above 700 °C, mixed electronic and ionic conductivity was observed below 700 °C. The activation energies for electronic and ionic conductivities were 0.6 eV and 0.3 eV, respectively. The analysis by Liu et al. assumes that chromium interstitials dominate the ionic conduction. Interestingly,

the activation energy of 0.3 eV for ionic conduction is close to the activation energy of 0.37 eV found in Figure 4 for Cr diffusion. Betova et al. [Betova et al. 2007] determined kinetic and transport parameters for the 'inner' (compact oxide) layer on AISI 316 L(NG) stainless steel in temperature range of 150–300 °C using the mixed-conduction model [Beverskog et al. 2002], and found an activation energy of 0.45 eV for chromium diffusion.

For oxygen, Horita et al. [Horita et al. 2008] used an isotope tracer technique to study oxygen diffusion in the oxide scales formed on Fe-Cr -based ferritic stainless steels. They found an activation energy of 1.4 eV for oxygen diffusion which is close to the value of 1.1 eV found in Figure 3 for parameter set 2.

Whereas the above comparisons were favourable with respect to the MD results, it must be noted that different interpretations exist. For example, Salomonsen et al. [Salomonsen et al. 1989] find a parabolic growth constant to have an activation energy of 1.2 eV but they claim, based on implanted Xe marker studies, that the mobile species is Cr rather than O.

We may now attempt to extrapolate the diffusion coefficients from MD simulations to lower temperatures based on the approximation that the diffusion coefficient is linearly dependent on the defect fraction. Figure 6 shows the linear fits to the Arrhenius plots of Figures 3 and 4 together with the experimental data from Tsai et al. [Tsai et al. 1996]. The experimental data distinguishes between bulk and grain boundary diffusion coefficients, and it also includes an apparent diffusion coefficient which is a suitably weighted average over the bulk and grain boundary values.

It is seen that extrapolation of the MD data (for a defect fraction of $8.3 \cdot 10^{-4}$) passes close to the experimental grain boundary diffusion coefficients. Decreasing the defect fraction to $2.5 \cdot 10^{-6}$ makes the MD data pass close to the apparent diffusion coefficient data. This defect fraction is of the same order of magnitude as determined experimentally by Young et al. [Young et al. 1987]. In order to make the MD data pass close to the bulk diffusion data, the defect fraction needs to be decreased by roughly four orders of magnitude which seems not credible given the data in [Young et al. 1987]. Regarding the accuracy of the experimental data, Tsai et al. note that the experimental diffusion coefficients presented by various authors (see Figures 8 and 9 in [Tsai et al. 1996]) vary by orders of magnitude, reflecting the difficulties in obtaining consistent experimental data.

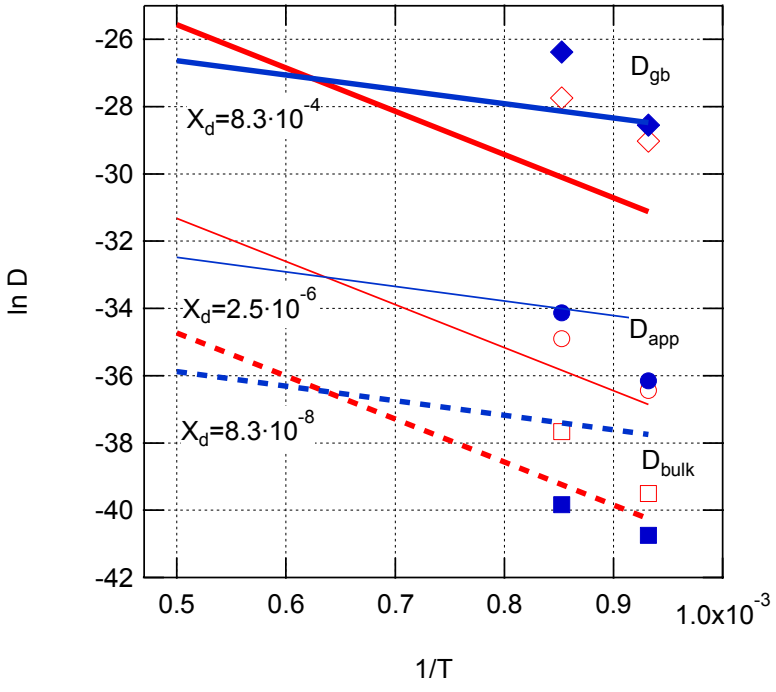

Figure 6. Extrapolation of MD diffusion coefficients to lower temperatures and defect fractions for parameter set 2. Thick solid lines are the extended linear Arrhenius fits to Cr (blue) and O (red) data of Figures 3 and 4. Thin solid lines are calculated for a defect fraction of $2.5 \cdot 10^{-6}$, and the dotted lines for a defect fraction of $8.3 \cdot 10^{-8}$. The markers are the experimental data by Tsai et al. [Tsai et al. 1996] for Cr (blue) and O (red) bulk diffusion (squares), grain boundary diffusion (diamonds) and apparent (spheres) diffusion coefficients.

Finally we note that according to the MD data of Figure 6, temperature has an effect on the relative mobility of oxygen and chromium. At high temperatures (above 1600 K), oxygen is more mobile, whereas at lower temperatures chromium is the more mobile ion. It can be noted that the apparent and grain boundary diffusion data of Tsai et al. [Tsai et al. 1996] is in agreement with this observation. The mobility of chromium is often associated with interstitial Cr ions, but the results of this study suggest that the mobility can be explained by lattice diffusion. The potential used to make the simulations is clearly important, as parameter set 1 resulted in no mobility for chromium. Therefore, we believe that parameter set 2 is better suited to describe mass transport in Cr_2O_3.

6.5 Conclusions

Classical molecular dynamics simulations were used to gain insight into the relationship between the defect structure and mass transport properties of Cr_2O_3. The basic assumption was that Schottky defects are responsible for the ion transport.

The results turned out to be sensitive to the Buckingham potential parametrization used. One parameter set resulted in oxygen only being the mobile species, while for the other parameter set, both chromium and oxygen were mobile. The latter parametrization was considered to be more credible, as many experimental studies have suggested that chromium is mobile. However, whereas literature often attributes chromium mobility to interstitial diffusion, the results from this study suggest that lattice diffusion may be responsible for mass transport.

For the defect concentrations involved in this study, diffusion constants could be reilably determined from the mean square displacement data only at temperatures of 1300 K and above. Extrapolation of the diffusion coefficients to lower temperatures was done through an Arrhenius plot. For parameter set 2, the activation energies for oxygen and chromium migration were 1.1 eV and 0.37 eV, respectively.

The diffusion constants were approximately linearly proportional to the defect concentration. However, the highest studied defect concentration ($8.3 \cdot 10^{-4}$) showed a deviation from linearity, suggesting that the point defects were no longer isolated.

Experimental studies from literature suggested charge carrier concentrations of the order of 10^{-5}. The diffusion constants in this work were mostly obtained using a defect concentration that was a magnitude higher. Extrapolation of the simulated diffusion coefficients to a lower defect fraction ($2.5 \cdot 10^{-6}$) and temperature (800–900 °C) showed agreement with experimental apparent diffusion coefficients (of the order of 10^{-15} cm^2/s).

6.6 References

Atkinson, K.J.W, Grimes, R.W., Levy, M.R., Coull, Z.L. and English, T. 2003. Accommodation of impurities in α-Al_2O_3, α -Cr_2O_3 and α-Fe_2O_3. Journal of the European Ceramic Society vol. 23 pp. 3059–3070.

Betova, I., Bojinov, M., Kinnunen, P. and Saario, T. 2007. Mixed Conduction Model for Oxide films – quantitative procedure for determination of kinetic parameters for individual species. VTT Research Report No VTT-R-04098-07.

Beverskog, B., Bojinov, M., Englund, A., Kinnunen, P., Laitinen, T., Mäkelä, K., Saario, T. and Sirkiä, P. 2002. A mixed-conduction model for oxide films on Fe, Cr and Fe-Cr alloys in high-temperature aqueous electrolytes.

Part 1. Comparison of the electrochemical behaviour at room temperature and at 200 °C. Corrosion Science vol. 44 pp. 1901–1921.

Catlow, C.R.A. 1977. Point Defect and Electronic properties of Uranium Dioxide. Proceedings of the Royal Society A vol. 353 pp. 533–561.

Holt, A. and Kofstad, P. 1994. Electrical conductivity and defect structure of Cr_2O_3. Part 1. High temperatures (> ~1000 °C). Solid State Ionics vol. 69 pp. 127–136.

Holt, A. and Kofstad, P. 1997. Electrical conductivity and defect structure of Mg-doped Cr_2O_3. Solid State Ionics vol. 100 pp. 201–209.

Horita, T. et al. 2008. Evaluation of Laves-phase forming Fe–Cr alloy for SOFC interconnects in reducing atmosphere. Journal of Power Sources vol. 176 pp. 54–61.

Lewis, G.V. and Catlow, C.R.A. 1985. Potential models for ionic oxides. Journal of Physics C: Solid State Physics vol. 18 pp. 1149–1161.

Lillerud, K.P. and Kofstad, P. 1980. On High Temperature Oxidation of Chromium. Part 1. Oxidation of Annealed, Thermally Etched Chromium at 800°–1100°C. Journal of the Electrochemical Society: Solid-State Science and Technology vol. 127 pp. 2397–2409.

Liu, H., Stack, M.M. and Lyon, S.B. 1998. Reactive element effects on the ionic transport processes in Cr_2O_3 scales. Solid State Ionics vol. 109 pp. 247–257.

Minervini, L., Zacate, M.O. and Grimes, R.W. 1999. Defect cluster formation in M_2O_3-doped CeO_2. Solid State Ionics vol. 116 pp. 339–349.

Murphy, S.T. 2009. Atomistic simulation of defects and diffusion in oxides. Dissertation, Imperial College of London. http://abulafia.mt.ic.ac.uk/publications/theses/SMurphy_Thesis2-web.pdf (downloaded 20.12.2012).

Plimpton, S.J. 1995. Fast Parallel Algorithms for Short-Range Molecular Dynamics. Journal of Computational Physics vol. 117 pp. 1–19.

Salomonsen, G., Norman, N., Lønsjø, O. and Finstad, T.G. 1989. Kinetics and mechanism of oxide formation on Cr thin films. Journal of Physics: Condensed Matter vol. 1 pp. 7843–7850.

Su, M.Y. and Simkovich, G. 1987. Point defect structure of Cr_2O_3. Technical Report No. TR 87-008. The Pennsylvania State University, Applied Research Laboratory.

Tsai, S.C., Huntz, A.M. and Dolin, C. 1996. Growth mechanism of Cr_2O_3 scales: oxygen and chromium diffusion, oxidation kinetics and effect of yttrium. Materials Science and Engineering vol. A212, pp. 6–13.

Young, E.W.A., Gerretsen, J.H. and de Wit, J.H.W. 1987. The Oxygen Partial Pressure Dependence of the Defect Structure of Chromium(III) Oxide. Journal of the Electrochemical Society: Solid-State Science and Technology vol. 134 pp. 2257–2260.

7. μFEM modelling of wood cell deformation under pulping-type dynamic loads

Stefania Fortino, Petr Hradil & Lauri Salminen

VTT Technical Research Centre of Finland
P.O. Box 1000, FI-02044 VTT, Finland

7.1 Abstract

Compressive and shear loads applied to wet woodchips at high values of speed and temperature during thermo-mechanical (TM) pulping are aimed at separating wood fibres from the raw material in order to increase both the flexibility and the bonding ability of the fibres. This work proposes a computational approach for the simulation of wood cell deformation finalized to a deeper understanding of the most consuming mechanism during TM pulping, that is, the fibre cell wall opening. A flexible μFEM tool for Abaqus code has been developed which uses an automated script for parametric model generation. The use of the proposed numerical tool in the presence of different pulping-type loading conditions can provide suggestions for the energy saving during thermo-mechanical pulping processes.

7.2 Introduction

One of today's key objectives of the European forest industry is to decrease energy consumption during thermo-mechanical pulping. Pulping processes are aimed at separating fibres from the raw material by means of shear and compressive loads applied at high speed to wet woodchips biomass at high temperatures (60–160 ºC). During the refining of pulp, temperatures of 140–160 ºC are reached and there is a considerable increase of both the flexibility and the bonding ability of the wood fibres (De Magistris and Salmén 2006). The hardest and most consuming step during the process is the fibre cell wall opening. However, the scientific re-

search on the disintegration of wood cells is still in its infancy due to the fact that the mechanisms at the origin of this phenomenon are not well understood.

Wood biomass can be defined as a hierarchically structured composite characterized by a complex chemistry (Dvinskikh et al. 2011) due to the fact that its constituents (cellulose, hemicellulose and lignin) are polymers. Wood is a natural multiscale material very suitable to understand the interactions among different structural scales of the material itself. In particular softwood is a highly anisotropic material with both radial and tangential moduli of one order of magnitude lower than the longitudinal modulus (see literature in Qing and Mishnaevsky Jr. 2010). Following (Mishnaevsky Jr. and Qing 2008), softwood can be described at four different structural levels (see Figure 1): 1) at the macroscale level wood is composed of several annual rings that show different grade of darkness. The so-called earlywood zones are identified by lighter rings characterized by cells with large diameters and thin cell walls, while the so-called latewood zones are composed of darker rings characterized by cells with small diameters and thick cell walls (see also Modén and Berglund 2008). 2) At the mesoscale level wood shows a cellular structure, composed of hexagonal cells oriented in the direction of the stem. Due to this geometrical shape, wood is also considered as a material having honeycomb structure. 3) At the microscale level each cell wall is assumed to be composed of 4 layers with different microstructures and properties (usually named as S1, S2, S3, P), while a further layer (named M) works as bonding material, see (Mishnaevsky Jr. and Qing 2008) for the details. 4) At the nanoscale level, the first three layers in the tracheid cell are made of several hundred individual lamellae with different volume fractions and microfibril angles (MFAs). As explained in (Barnett and Bonham 2003), the microfibril angle of a wood cell layer represents the angle between the long axis of the wood fibre and the orientation of the cellulose microfibrils of the layer as they wind around the cell. The relation of MFA with the modulus obtained by nanoindentation techniques (Wimmer et al. 1997) and the stiffness tensor for the different cell wall layers is discussed in (Konnerth et al. 2010).

Several studies within recent COST actions (COST Action E35, 2004–2008, COST Action FP0802, 2009–2012) have pointed out the importance of both experimental and computational research at the microscale of wood to properly define its material properties as well as to understand the complex phenomena occurring in wood cells under different processes and environments (Salmén and Burgert 2009). In the last few years, theoretical micromechanics and numerical approaches based on the finite element method applied to microstructures (μFEM) have been developed to assess the macroscopic mechanical properties of wood material (Hofstetter and Gamstedt 2009, Mishnaevsky Jr. and Qing 2008, Qing and Mishnaevsky Jr. 2010). Some papers were also published on numerical models for defining the hygroscopic properties of wood (Eitelberger and Hofstetter 2010) as well as the viscoelastic properties of wood at the microscale (Eitelberger et al. 2012). However, the cited publications refer to dry wood while there is still a lack of information on the material properties for wet wood cells (De Magistris and Salmén 2008).

Since thermo-mechanical pulping is performed at very high speed and temperature, it is not possible to investigate the microscopic phenomena occurring in woodchips during the process. To solve this problem, a Swedish research conducted by De Magistris and Salmén during 2005–2008 provided interesting experimental results for wet wood at lower temperatures and low speed by using a specialized Arcan device (De Magistris and Salmén 2005, 2006). The performed tests gave interesting informations in regards of the optimal combination of compression and shearing loads to be used to improve the permanent deformation of wood fibres by reducing the needed work and, consequently, the energy consumption.

More research is needed to investigate the intrawall deformation. At this aim a flexible computational tool able to handle different geometries in earlywood, latewood and transition zones of wood cells composed of several layers with different orientations of fibrils and several contacts among cell walls during loading is required. Particle methods like the MPM (Material Point Method), used for example in the self-made code developed by Nairn'sgroup (Nairn 2006), are able to describe the complex geometries of wood cell layers by automatically defining the contacts among layers. However, the power of advanced FEM codes in the presence of nonlinear behaviour of materials (both constitutive and geometrical) suggests developing special μFEM algorithms for analysis of wood cells also within commercial codes for a wider range of applications (complex loading and boundary conditions, coupled hygro-thermo-mechanical analyses, etc.). A first version of such a computational tool is developed in Abaqus FEM code and introduced in the present paper.

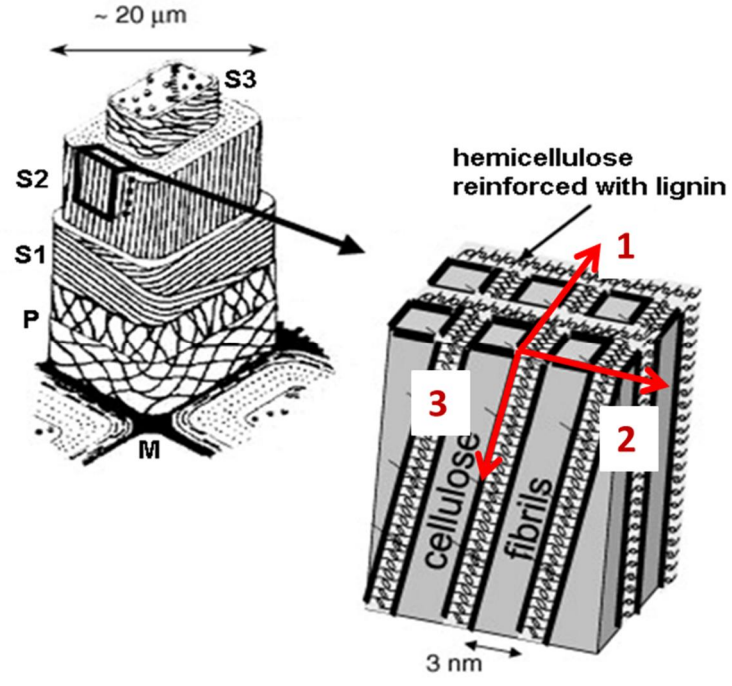

Figure 1. Structure of softwood and material coordinate system with axis 3 along the fibrils.

7.3 Short description of the research carried out by De Magistris and Salmén

In the following, the experimental and computational research on wood cell deformation carried out by De Magistris and Salmén is shortly summarized. For all the details the reader if referred to (De Magistris and Salmén 2005, 2006, 2008).

7.3.1 Experiments

Compared to the real conditions in the refiner during thermo-mechanical pulping, the tests were performed at lower temperatures (50 or 90 °C) and with a rate of deformation of 0.1 mm/min in the vertical direction by using a specialized Arcan device (De Magistris and Salmén 2005, 2006). The main idea of the experimental work was that by exploiting the principle of time-temperature superposition, the used test conditions can be considered equivalent to the real ones in the refiner, see references in (De Magistris and Salmén 2006).

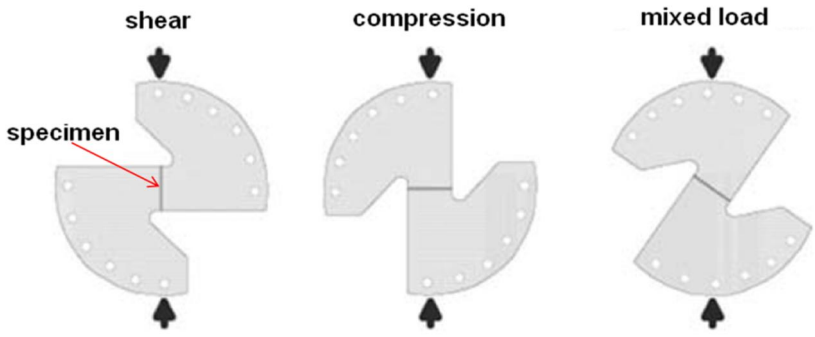

Figure 2. Scheme of Arcan plates, specimen and different loading conditions. Figure adapted from (De Magistris and Salmén 2006).

The tested specimens of Norway Spruce material had dimensions of 2 mm in the radial direction of wood, 40 mm in the tangential direction and 15 mm in the longitudinal direction. These were immersed into water at 4 °C for 1 day and then attached to the plates of the aluminiun Arcan device. During the application of the loading histories the specimens were immersed into water at 50 or 90 °C. The load was given in the vertical direction while the Arcan device was rotated in order to simulate different loading conditions from pure compression to shear to mixed compression-shear. In the performed tests, the specimens were loaded until collapse of the earlywood fibres but no fibre cracks were noticed.

Both the SEM images and the load-deformation curves registered during the performed experiments showed that the behaviour of wood cells under compressive or mixed compressive-shear loads is very different. Also earlywood and latewood zones deform in different ways. The following types of deformation were observed (De Magistris and Salmén 2005, 2006):

- During compression, earlywood fibres follow a characteristic ‘‘S’’ shape because of the tangential wall buckling, while the latewood fibres deformation follows the radial wall bending. The curve load-displacement under compression shows an initial elastic part, then a plateau region at almost constant load during buckling and finally a rising region.
- Under mixed compression-shear loading, the wood cells deform according to a “brick” shape. In this case the load-deformation curves do not show plateau.

The specimens were subjected to various cycles of loading and during each cycle there was a different loading condition. Based on the obtained experimental load-deformation curves, it was possible to evaluate the amount of work required under different types of loads and to draw the following main conclusions (De Magistracy and Salmon 2006):

- Less work is needed to deform wood cells under mixed compression-shear load compared to the pure compression case.
- In terms of energy consumption, the first load cycle is the more expensive to get an initial deformation. This suggests that the application of a combined load during the first loading cycle can represent an optimal choice to obtain permanent deformation in wood fibres by using less work.

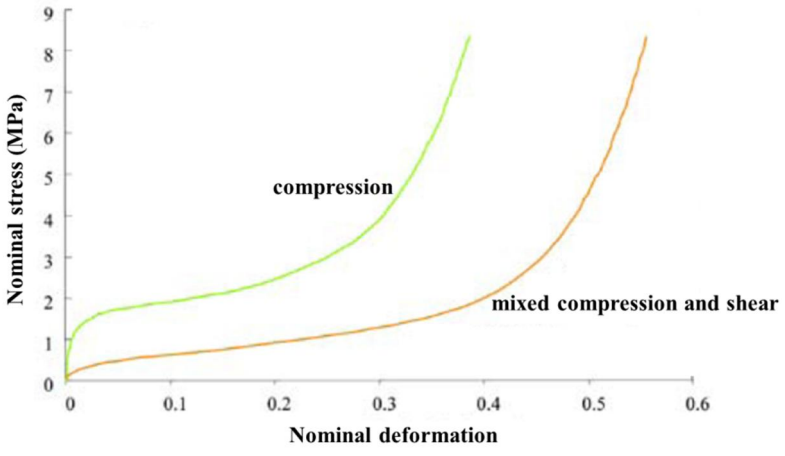

Figure 3. Typical curves obtained under compression and mixed loading. Figure adapted from (De Magistris and Salmén 2008). The nominal stress represents the total stress in the vertical direction (see Figure 2) and the Nominal deformation is the shortening of the sample in the vertical direction compared to the initial thickness. The curve corresponding to mixed load refers to the small shear experiment described in the results section.

7.3.2 Numerical modelling of wood cell

In (De Magistris and Salmén 2008) a three dimensional elastic FEM model in Abaqus code was proposed. Based on the geometry of a representative earlywood cell with dimensions taken from a SEM image, a set of three cell rows with four cells per row was studied. Each cell was composed of the five layers M,P,S1,S2,S3 characterising the softwood microstructure and each layer was attached to the adjacent ones by using the Abaqus option “contact TIE”. Cylindrical material orientations were assigned to each layer where the fibre axis was aligned with the microfibril (i.e. inclined with respect to the longitudinal axis of wood). Given displacements were applied trough plates posed at the top and bottom of the microstructure. The material properties (see Table 1) referred to dry wood and were calculated as follows:

- The concept of laminate theory was used. A cell wall can be considered as a laminate where the secondary layers S1, S2 and S3 represent 3 unidirectional laminae and the primary layer P is a randomly oriented lamina (see Figure 1). The chemical and elastic properties of cellulose, hemicellulose and lignin, were taken from earlier literature (see references in De Magistris and Salmén 2008).
- Using these properties, the orthotropic elastic coefficients for each layer were calculated by using the rule of mixture combined with a semi-empirical model from (Tsai and Hahn 1980).

The used FEM model was elastic and did not take into account the fact that the high temperature induces a softening that can provide different material properties for wet wood. However, the conclusions given in (De Magistris and Salmén 2008) are the following:

- The wood cell deformation simulated by using material properties for dry wood is almost the same as the one obtained for wet wood during the experiments.
- The use of orthotropic properties for the different layers provides a very similar wood cell deformation as the one provided by using isotropic properties.

It is worth to point out that in this research no comparison between numerical and experimental load-deformation curves was provided. Only the shape of the numerically obtained cell deformations were compared with the SEM images.

7.4 A μFEM model for woodchips biomass in Abaqus code

7.4.1 Description of the μFEM model

The finite element models are generated by using a script developed at VTT that is based on the unit cell geometry proposed in (Qing and Mishnaevsky Jr. 2010). The script is able to automatically create any number of cell wall layers; usually five (M, P, S1, S2 and S3) or less in simplified cases.

The geometry of the model is defined by its depth d, the layer thicknesses t_i, width of the internal layer T and angle θ. Optionally it is possible to specify the internal fillet radius r to avoid sharp corners between the connected walls. This was not used in the present paper. The basic model (unit cell) consists of one or two (in case of modelling earlywood and latewood) complete wood cells together with smaller parts of connected cells to form a rectangular pattern. It is very easy to extend the model horizontally and vertically if a larger simulation is needed. The complete model contains also self-contacts between cell walls that are not used in the present study because the analysis is stopped before the contacts occur.

Each cell wall layer is connected to a different orthotropic material model that can be also defined within the script including the material orientation that takes

into account the variation of microfiber angle in each layer. When combining earlywood and latewood, another cell is created between the full model cells that do not belong to any of the materials, and therefore its material properties and thicknesses are automatically calculated as averages of earlywood and latewood parameters (see Figure 2).

7.4.2 Dynamic analysis of microstructures by Abaqus

The Abaqus dynamic analyses are conducted on microstructures composed of a certain number a of unit cells. In the present study, a group of six cells (three on the top and three on the bottom), is identified as the smallest group suitable to capture the representative part of the microstructure that follows the characteristic shape reached during different types of loads. This representative part is composed of seven sub-cells (a central sub-cell and of six adjacent sub-cells), see Figure 3. The loads (or assigned displacements) are given through two plates (one on the top and the other on the bottom). Abaqus Explicit solver (version 6.11-1) and 8-node linear brick elements with reduced integration are used.

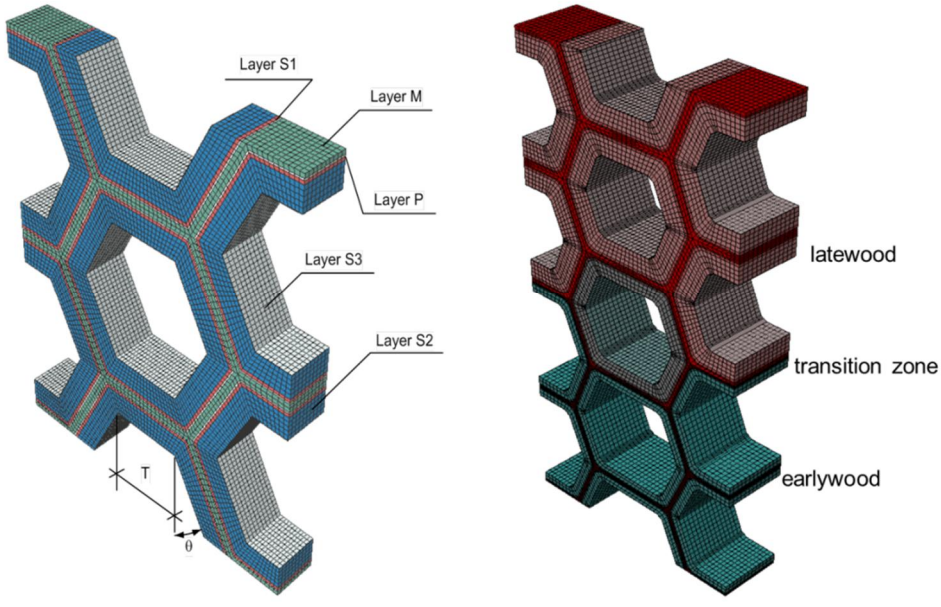

Figure 4. Left: unit cell with geometrical parameters (T and θ) and softwood layers. Right: model with earlywood, latewood and the transition zone.

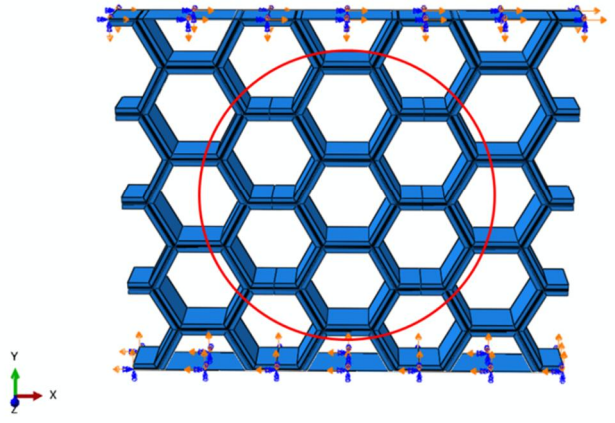

Figure 5. Abaqus model for an earlywood microstructure (θ = 30 deg). The red circle indicates the seven sub-cells composing the representative microstructure to be compared with the SEM images.

7.4.3 Case-study: mixed compression-shear load

In the present paper, the earlywood cell deformations under two different mixed compression-shear loads presented in (De Magistris and Salmén 2005) were numerically simulated by using the new computational tool described in the previous sub-section.

During the reference experimental tests, the specimens were immersed in water at 50 °C and the loads were applied with a rate of deformation of 0.1 mm/min in the vertical direction. The following combinations of compression and shear were numerically tested:

- Small shear: 74.6% of the total load in compression and 25.5% in shear;
- Large shear: 64% of the total load in compression and 46% in shear.

For both the performed numerical analyses, assigned displacements corresponding to an experimental vertical stress of 1.6 MPa (in the elastic range of the stress-deformation curve) were given on the top and on the bottom of the microstructure (see Figure 5). The geometry of the unit cell is slightly different than the one used in (De Magistris and Salmén 2008). The edge of the hexagonal cell is T = 24 μm and the initial cell angle θ=30º. The density is ρ~550 kg/m3. According to (De Magistris and Salmén 2008), the material properties for the secondary wall refer to the following microfibril angles: 50º for S3, 10° for S2, and –70° for S1, respectively. In the P layer the fibril angle can vary randomly. A depth d = 20 μm was considered in the longitudinal direction of wood. Orthotropic properties and cylindrical material orientations were used. Compared to the above reference paper, in the present work the axis 3 is the one in the fibril direction (see Figure 1). Due to this,

the Poisson's ratios were recalculated. The isotropic properties used for the plates were E=3500 MPa and υ=0.2.

Table 1. Thicknesses (th) and elastic properties for each layer.

	th	E_1	E_2	E_3	υ_{12}	υ_{13}	υ_{23}	G_{12}	G_{13}	G_{23}
	μm	(MPa)	(MPa)	(MPa)				(MPa)	(MPa)	(MPa)
M	0.45	1144	1144	2340	-0.35	-0.63	-0.63	890	890	890
P	0.15	10200	1560	10200	0.54	0.26	0.034	870	3910	1100
S1	0.225	2050	2050	41800	0.15	0.022	0.022	890	1330	1330
S2	2.4	3450	3450	70850	0.80	0.035	0.035	950	1910	1910
S3	0.045	3350	3350	68250	0.70	0.034	0.034	980	1890	1890

The simulated deformed shapes are compared with the SEM images taken during the reference experiments and the results show a good agreement (see Figs. 6 and 7). The stress-deformation curves for the two cases are shown in Figure 8. The deformation in the global y-direction is simply calculated as the displacement in the same direction divided by the initial height of the microstructure.

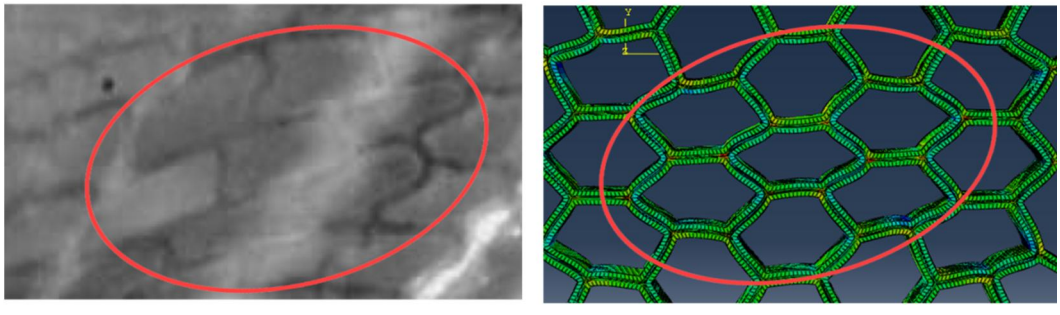

Figure 6. Small shear case**.** Left: wood cell deformation under the studied mixed compression-shear load. SEM image adapted from (De Magistris and Salmén 2008), max total stress ~ 1.6 MPa. Right: simulated wood cell deformation.

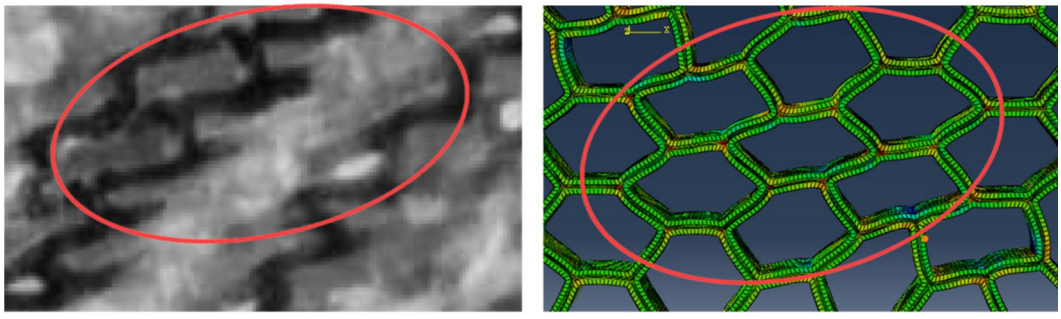

Figure 7. Large shear case**.** Left: wood cell deformation under the studied mixed compression-shear load. SEM image adapted from (De Magistris and Salmén 2008), max total stress ~ 2.4 MPa. Right: simulated wood cell deformation (max total stress =1.6 MPa).

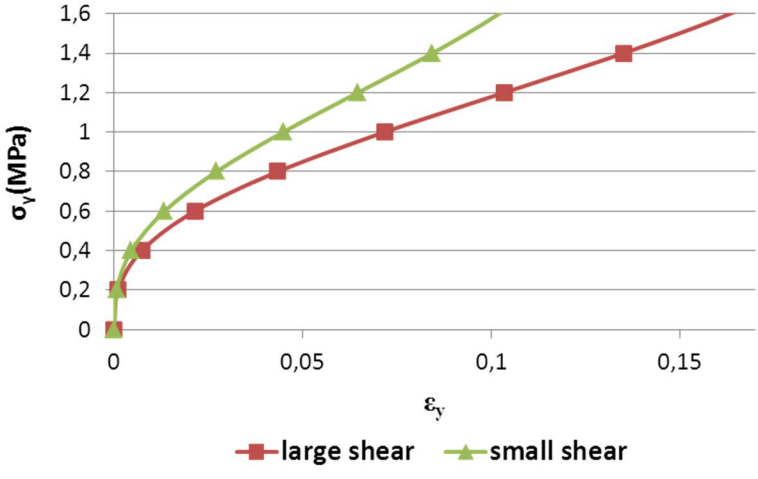

Figure 8. Stress-deformation curves for the studied cases (linear range).

7.4.4 Discussion and future steps

The results presented in the previous sub-section show that dynamic analyses under mixed compression-shear loading are able to simulate the “brick” shape of earlywood cells reached during the experiments. It can be noticed that in the case of small shear the values of vertical stresses are higher than the ones obtained for large shear (Figure 8). Even if these curves are only in the elastic range, this result already shows that the effect of a larger shear contribution is to reduce the work request. However, the reached stress values for both tests are higher than those

measured during the experiments due to the fact that the used material properties are for dry wood.

The next step of this research is to develop a more accurate material model capable to simulate the whole load-deformation curves as well as the permanent deformation attained at the end of each test sequence. To this aim, the following tools are needed:

1. A plastic model under compression to be integrated in the present model by using a subroutine of Abaqus code. A suitable model could be a variant of the plastic model for compression of wood cells introduced in (Nairn 2005).
2. The analysis of contacts between cell walls.

The assessment of the material properties for wet wood at process temperature is also important. This can be a difficult topic due to the fact that there is a lack of such information in the current literature.

7.5 Conclusions

This research work proposed a flexible computational tool for simulation of the wood cell deformation under pulping-type dynamic loads. The tool can automatically generate different geometries and can analyse representative microstructures under various loading conditions by using orthotropic elastic material properties. The numerical simulation of wood cell deformation is in agreement with the SEM images taken during experiments performed in a previous Swedish research.

The future extension of the methods consists in an improvement of the material model finalized to take into account also the plastic behaviour of wood cells. This represents an important step for the understanding of wood cell disintegration which is a challenging topic for both the European research and the forest industry.

The use of numerical virtual testing based on the development of the proposed model can give quantitative answers in regards of the work required during pulping-type tests and precious suggestions about the types of loads to be used for reducing the energy consumption.

7.6 References

Abaqus User's Manual. (2011). Version 6.11–1. 2011, Dassault Systèmes.

Barnett J.R. and Bonham V.A. (2004). Cellulose microfibril angle in the cell wall of wood fibres. Biol. Rev. 79, 461–472.

COST Action E35. (2004–2008). Fracture mechanics and micromechanics of wood and wood composites with regard to wood machining. http://www.boku.ac.at/physik/coste35/

COST Action FP0802. (2009–2012). Experimental and computational micro-characterization techniques in wood mechanics. http://cost-fp0802.tuwien.ac.at/

De Magistris F., Salmén L. (2005). Deformation of wet wood under combined shear and compression. *Wood Sci Technol* 39, 460–471.

De Magistris F., Salmén L. (2006). Mechanical behaviour of wet wood in sequences of compression and combined compression and shear. *Nordic Pulp and Paper Research Journal*, 21 (2), 231–236.

De Magistris F., Salmén L. (2008). Finite Element modelling of wood cell deformation transverse to the fibre axis. *Nordic Pulp and Paper Research Journal*, 23 (2), 240–246.

Dvinskikh SV, Henriksson M, Mendicino AL, Fortino S, Toratti T. (2011). NMR imaging study and multi-Fickian numerical simulation of the moisture transfer in Norway spruce samples. *Engineering Structures* 2011; 33:3079–3086.

Eitelberger J., Hofstetter K. (2010). Multiscale Homogenization of Wood Transport Properties: Diffusion Coefficients for Steady-State Moisture Transport. *Wood Material Science and Engineering* 5(2), 97–103.

Eitelberger J., Bader T.K., de Borst K., Jäger A. (2012). Multiscale prediction of viscoelastic properties of softwood under constant climatic conditions. *Computational Materials Science* 55*, 303–312*.

Hofstetter K., Gamstedt E. (2009). Hierarchical Modelling of Microstructural Effects on Mechanical Properties of Wood. A Review. *Holzforschung* 63, 130–138.

Konnerth J., Buksnowitz C., Gindl W., Hofstetter K., and Jäger A. (2010). Full Set of Elastic Constants of Spruce Wood Cell Walls Determined by Nanoindentation. Proceedings of the International Convention of Society of Wood Science and Technology and United Nations Economic Commission for Europe – Timber Committee October 11–14, 2010, Geneva, Switzerland.

Nairn J. A. (2006). Numerical simulations of transverse compression and densification in wood. *Wood and Fiber Science* 38(4): 576 – 591.

Mishnaevsky Jr. L., Qing H. (2008). Micromechanical modelling of mechanical behaviour and strength of wood: State-of-the-art review. *Computational Materials Science* 44, 363–370.

Moden C. S. and Berglund L. A. (2008). A two-phase annual ring model of transverse anisotropy in softwoods. *Composites Science and Technology* 68, 3020-3026.

Qing H., Mishnaevsky Jr. L. (2010). 3D multiscale micromechanical model of wood: From annual rings to microfibrils. *International Journal of Solids and Structures* 47, 1253–1267.

Salmén L. and Burgert I. (2009). Cell wall features with regard to mechanical performance. A review COST Action E35 2004-2008: Wood machining – micromechanics and fracture. *Holzforschung* 63(2), 121–129.

Tsai S.W. and Hahn H.T. (1980): Introduction to composite materials, In: Technomic pub. Lancaster.

Wimmer R., Lucas B.N., Tsui T.Y. and Oliver W.C. (1997) Longitudinal hardness and Young's modulus of spruce tracheid secundary walls using nanoindentation technique. *Wood Science and Technology* 31(2), 131–141.

8. MultiDesign innovation program

Tarja Laitinen

VTT Technical Research Centre of Finland
Sinitaival 6, P.O. Box 1300, FI-33101 Tampere

8.1 Abstract

The vision of the MultiDesign innovation programme is to create optimized and efficient machine components regarding material, design, manufacturing, performance, service and recycling by evolving multiscale modelling. Future vision of raw materials scarcity and energy efficiency integrated with increasing performance demands calls for totally novel solutions. Systematic, multiscale modelling is cost effective and fast way of producing and testing new solutions and concepts. Main obtained benefits are shorter R&D cycles, reduced time to market, less prototypes, raw materials savings and energy efficiency.

8.2 Introduction

The vision of the MultiDesign innovation programme is to create optimized and efficient machine components regarding material, design, manufacturing, performance, service and recycling by evolving multiscale modelling. The target is to be able to create a multiscale solver on any technical component or environment in a short time period (e.g., 2 months). Currently individual modelling tools are accepted and merely also used in research and development. Holistic approach, the need for comprehensive view instead of optimizing some parameters, is identified. Occasional multiscale linking takes place, but true multiscale, multidimensional, multiresolution approach is missing. Through development of modelling tools, model integration and operational platforms it is seen that in the coming 5–10 years modelling and simulation will be essential part of product development in

most companies. The anticipated technological and scientific benefits include the possibility to iterate and optimize the component behaviour as a part of a system starting from material development and ending up to recycling. Varying future scenarios can be simulated and evaluated, a profound understanding of multiscale and multidimensional problems achieved and tools for decision making developed.

8.3 Current project portfolio

The MultiDesign innovation program started in the beginning of 2012 and runs totally for 3 years. The volume of the MultiDesign project portfolio was at the end of year 2012 about 5 Me, corresponding to totally about 35 person years, including also significant amount of direct customer orders. Close co-operation with the customers is essential for the success of the programme. Models are always reductions of reality – in order to understand the main parameters affecting the phenomena and the importance of the phenomena in the business context the ongoing, open discussion with industry is fundamental.

One of the VTT spear head areas contributing to the programme is the whole powder technological value chain from modelling based material desing to powder manufacturing, consolidation and performance testing of the materials or components. A systematic material modelling approach ProperTune™ for material development to meet the performance requirements is currently globally acknowledged especially in wear research [1, 2, 3], Figure 1. VTT has profound performance and lifetime knowledge based on modelling and testing (fatigue, creep and fracture) as well as on thermodynamical modelling [4–7].

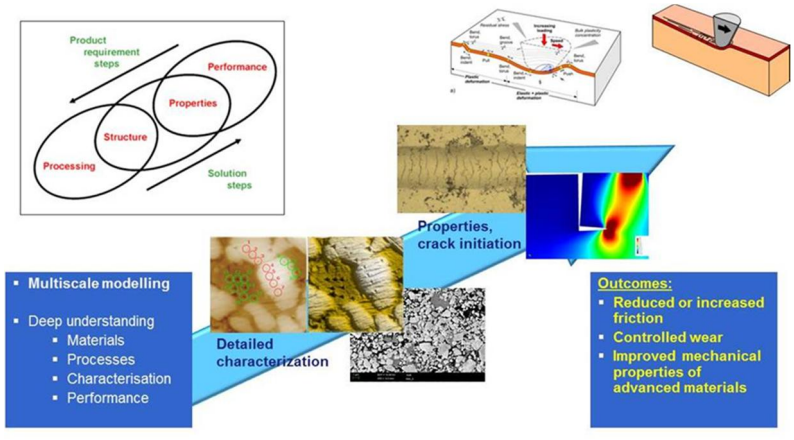

Figure 1. ProperTuneTM, systematic approach for controlled performance.

The high level scientific research work related to methodology, simulation and operational platforms aims to develop and combine the different simulators, e.g material models, varying manufacturing processes, component design rules, maintenance strategy, sustainability aspects and related life cycle costs, into common use environment. The ultimate target is automatic linking of heterogeneous simulation tools, which provide the results for customers in a collaborative interface with cost effective computational solutions. Existing integration solution for computational tools, Simantics, will be utilized and further developed in the program. [8]

Once digital manufacturing is introduced into the chain, the paradigm change from traditional design and labour intensive manufacturing to modelling based material development, digital design, virtual simulation and additive manufacturing is reality. New lean and agile supply chain based on additive manufacturing (AM) dramatically changes the logistics and distribution models for manufacturing. Since AM involves little human involvement to create a part, there is no longer need to concentrate manufacturing to a region of low-cost labor, but manufacturing can be performed as true just-in-time process near the end customer. Each and every part can be unique from the part created before or after, AM is truly manufacturing for design the products being typically customised, high-end products.

Key international partners are linked into the program, such as Karlsruhe Institute of Technology (KIT), Germany (powder metallurgy and performance), Stony Brook University, USA (thermal spraying), Argonne research lab USA (wear modelling), University of Sheffield and Saxonian Institute of Surface Mechanics (ProperTuneTM modelling), McGill University Canada (PhaseField modelling), Mesoscribe Inc, USA (Direct Write), University of Louisville, USA (additive manufacturing).

8.4 Impact

The global demand for any industrial manufacturing is cost efficiency. The designed and manufactured products need to fulfil the set design rules, but majority of the customers are not willing to pay extra on additional features or quality. Still the products are expected to perform perfectly. By multiscale modelling different scenarions can be built, simulated and verified, but physical prototypes need to be manufactured only on the optimised, best solutions. Thus the R&D cycles can be speeded up remarkably. Total cost of ownership (TCO) calculations related to different scenarios enlighten the cost efficiency throughout the whole product lifecycle.

As AM techniques make physical 3D objects directly from virtual 3D computer data, manufacturing can be localised near the end customer with mainly digital inventories. The component can be designed for function rather than for manufacturing with no additional tooling costs. AM techniques have the potential to ap-

proach zero waste material (or 100% utilisation) due to material ending only to the component being processed.

Energy efficiency is an established, global megatrend throughout the industries in order to secure energy supply, cut costs and mitigate greenhouse gas emissions. Resource efficiency is becoming the demand of industrial activity in sectors like construction, chemicals, automotive, aerospace, machinery or commodities. The alternatives to tackle the raw materials scarcity are either new primary (arctic, seabed) or secondary sources (reuse, recycling) or substitution. Multiscale modelling provides an efficient tool for testing out different material properties or design novel, performance based materials just for the case in question.

In Figure 2 is presented the current needs of industry and the impacts of MultiDesign innovation program. The benefitting customers/ customer groups include the whole value chain from material providers through manufacturing industry to equipment end users and service providers. New offering is based on identification and simulation of component and system level interactions resulting in optimized, sustainable products.

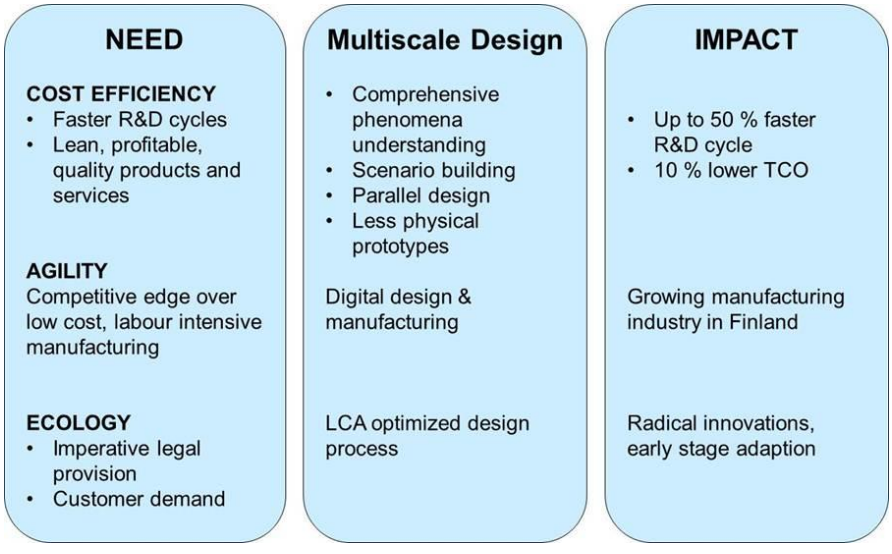

Figure 2. Current needs of industry and impact of MultiDesign innovation program.

8.5 References

1. Holmberg K, Ronkainen H, Laukkanen A, Wallin K, Friction and wear of coated surfaces – scales, modelling and simulation of tribomechnisms. Surface and Coatings Technology 202 (2007) 1034–1049

2. Holmberg K, Laukkanen A, Wear Models, In: Bruce, R. (ed.) Handbook on Lubrication and Tribology, Vol. II Theory and Design, 2nd edition, Chapter 13, CRC press, New York, USA, (2012), 13:1–21.

3. Holmberg K., Laukkanen A., Ghabchi A., Rombouts M, Turunen E., Waudby R., Suhonen T., Valtonen K. and Sarlin E. Computational modelling based wear resistance analysis of thick composite thermal sprayed and laser cladded coatings. To be submitted to Surface and Coatings Technology in February 2013.

4. Wallin, K. Simple distribution-free statistical assessment of structural integrity material property data. Engineering Fracture Mechanics. Elsevier, (2011), vol. 78, 9, pp. 2070–2081.

5. Holmström, S.; Rantala, J.; Laukkanen, A.; Kolari, K.; Keinänen, H.; Lehtinen, O. Modeling and verification of creep strain and exhaustion in a welded steam mixer. Journal of Pressure Vessel Technology, (2009), vol. 131, 6, pp. 061405.

5. Wallin, K. Statistical uncertainty in the fatigue threshold staircase test method. International Journal of Fatigue, (2011), vol. 33, 3, pp. 354–362.

6. Wallin, K. Structural integrity assessment aspects of the Master Curve methodology. Engineering Fracture Mechanics, (2010), vol. 77, 2, pp. 285–292.

7. Solin, Jussi; Nagel, G.; Mayinger, W. Cyclic behavior and fatigue of stainless surge line material. American Society of Mechanical Engineers, Pressure Vessels and Piping Division (Publication) PVP, vol. 3, pp. 611–619. 2009 ASME Pressure Vessels and Piping Conference, PVP 2009. Prague, Czech Republic, 26–30 July 2009.

8. Karhela, T.; Villberg, A.; Niemistö, H. Open Ontology-based Integration Platform for Modeling and Simulation in Engineering. International Journal of Modeling Simulation and Scientific Computing, Volume 3, Issues 2: (1250004), World Scientific Press, 2012.

9. Vertical multiscale modelling

Alejandro Revuelta

VTT Technical Research Centre of Finland
Tekniikantie 4 A, P.O. Box 1000, FI-02044 Espoo

9.1 Abstract

This paper stresses the need to go towards modelling and simulation solutions which combine together the different CAE tools available to practicioners. By doing this it is expected that results can be obtained which go beyond of what can be achieved with the current methodologies. And in this way we could reduce cost and increase performance through improved design. The different types of integration of tools are presented. In order to achieve this vision, a review of different knowledge areas which require further research is discussed. Finally, some of the current approaches done at VTT for the integration of different CAE tools are explained and briefly introduced.

9.2 Introduction

During the last decades, the usage of computer aided engineering (CAE) tools has seen an steady increased use in the technical and scientific world as the ratio of computational power to price has experienced an exponential growth. The use of numerical methods combined with this computational power has allowed us to create virtual models of physical phenomena which help in the understanding of nature. This models complement and in many cases enhance the analytical calculations and reduce the need of prototypes and empirical results.

VTT Technical Research Centre of Finland is a multitechnological applied research institute. In the last years we have observed how the use of CAE tools has permeated into most of its research areas, e.g., RF antenna design, manufactur-

ing technologies, electric machines design, biotechnology, and a long etcetera. In 2011, an internal survey was launched in order to identify the number of employees directly involved in material modeling. Results highlighted that in 2011 employees used nearly 100 menmonths in using and developing CAE tools in this area. About 20 different commercial modeling softwares were employed and near 60 codes which were either open source or in-house built (1). In other technological areas similar trends can be observed. This provides with an interesting picture of how important CAE tools have become in the scientific world.

But we would be mistaken in thinking that this kind of modeling is only the realm of research institutes or universities. The afore mentioned lower cost of computational hardware makes possible that a regular desktop PC runs powerful analyses and not only big companies but also SME use CAE tools regularly as part of their business workflow.

9.3 Advantages of integration of CAE tools in design

In the Mechanical Engineering context, Shigley defines design as: either to formulate a plan for the satisfaction of a specified need or to solve a problem. If the plan results in the creation of something having a physical reality, then the product must be functional, safe, reliable, competitive, usable, manufacturable, and marketable (2). For most products, especially so the more complex they are, there is no single individual with the know-how and capabilities to tackle all of those requirements at once. On (2) we can see a listing, which might be expanded even further, of 26 areas to be considered as part of the design process. Among others, strength/stress, corrosion, noise, maintenance or remanufacturability/resource recovery. Nowadays, for most of those areas a plethora a different CAE tools are available and actively used to help in analysing the component/system.

Designing is an innovative and very iterative process in which we create a set of feasible solutions and select the one which performs better for the intented task according to some specific metric. As more experience about the task performed is gained, modifications and improvements on the original design are done continuously. As an example, the basic design of an automobile hasn't changed much compared to the initial versions, but its performance and characteristics of both automobile and components have evolved significantly. CAE tools are a reality in the design process of many products nowadays and they have helped in reducing cost and time-to-market as well as increasing performance. But their use is still very compartmentalized and usually there is no transfer of information for one CAE tool to another or from one area of the design to another.

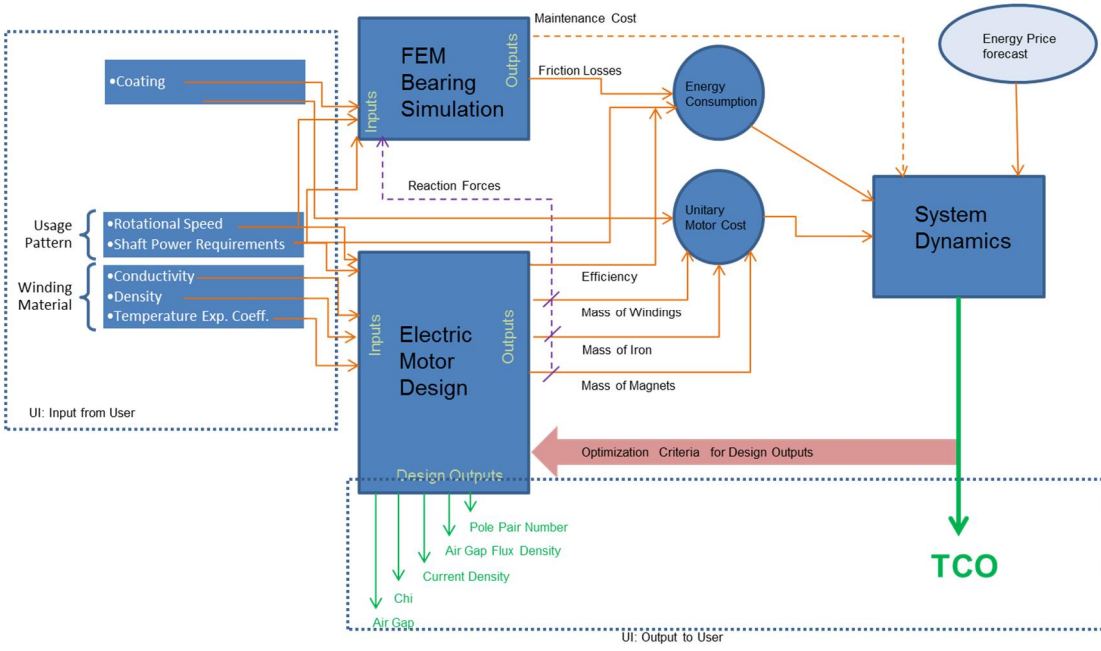

Figure 1. Example of benefit sought through integration of CAE tools.

It is obvious to understand that when designing, e.g., a load bearing component for a machine, the manufacturing process history of the component plays a role on the actual material properties of the manufactured part and on its final maximum admissible load or fatigue properties. And yet, still the most usual way to design this kind of component is to assume a history-free material status. Just nominal properties.

The integration of the different CAE tools involved at different levels on the design process shows an enormous potential. It would allow design solutions which go beyond what actual design methods and practises allow.

To illustrate this point let's consider a simple practical design exercise: An engineer has to select the best electric motor to run a certain equipment on his/hers factory. In order to solve this problem, he/she would typically take a catalogue of different motors provided by a manufacturer and select the one which better fits the task at the minimum cost. The design of the electric motor and the accompanying bearing would have been already done by the supplier using one CAE tool for the motor dimensioning and another for the bearing dimensioning and several options provided based on different usage scenarios. The total cost of ownership of the motor (TCO), the design metric, could be calculated for example with a System Dynamics model of the factory.

In Figure 1 we present an schematic of a design strategy in which all the CAE tools involved in the process are not used separately but integrated together. By following this approach, the TCO of the electric motor in the final installation could be considered during the design process of the electric motor itself. And whereas efficiency or cost might have been the metrics employed traditionally in the design of the motor, now we can provide a design customized for its final application. This approach garantees that the final TCO is at least as low as the one we would obtain with the traditional design method.

Anecdotically we have tested this approach with different usage scenarios and depending on the usage pattern we have managed to reduce the estimated TCO between 2–20% when using this integral approach when compared to selecting an electric motor with efficiency as the main design criteria.

This case is just an example of integration of a few modelling and simulation tools. Ideally, we could foresee an environment in which all the models and CAE tools involved would exchange data and results. In this utopic scenario, and combining the models with optimization algorithms, it would be possible to obtain very advanced designs in a reduced development time.

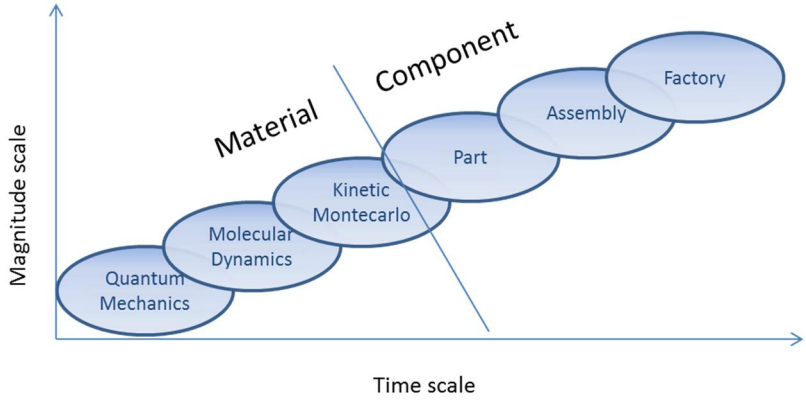

Figure 2. Representation of Multiscale integration

9.4 The directions of integration: multiscale, multidimension, multiresolution

When discussing the integration of different models and simulations we can classify this integration with respect to the directions in which it is done:

– Multiscale: In multiscale modelling the information travels from models representing phenomena occurring at very small scales of time and dimension towards models representing ever increasing scales on both time and dimensions (or viceversa). The scales can go from na-

nometres and nanoseconds and even smaller to kilometres and months or even years. Figure 2 represents this concept. Usually they are concerned about the same entity.

– Multidimension: This direction of integration refers to the combination of models which might be at similar scales of time or dimension but correspond to complete different entities. On the case represented on Figure 1 this could be exemplified by the combination of a motor design CAE tool with another for analysis of the bearings. Information from different systems and phenomena are combined together.

– Multiresolution: Most existing models treat any given phenomenon they represent at a particular level of resolution (3) (4). And as the resolution of the model we employ increases, so does usually its computational requirements. When we use a CAE tool, or a chain of tools, our objective might be different at different moments. If we are trying to get basic comprehension of how our system works or exploring the set of valid solutions to locate areas where those solutions are more optimal, we can use low-resolution models. If we want to understand better the underlying phenomenon or locate a more accurate result we would switch to a model with higher resolution. Figure 3 shows schematically this trade-off.

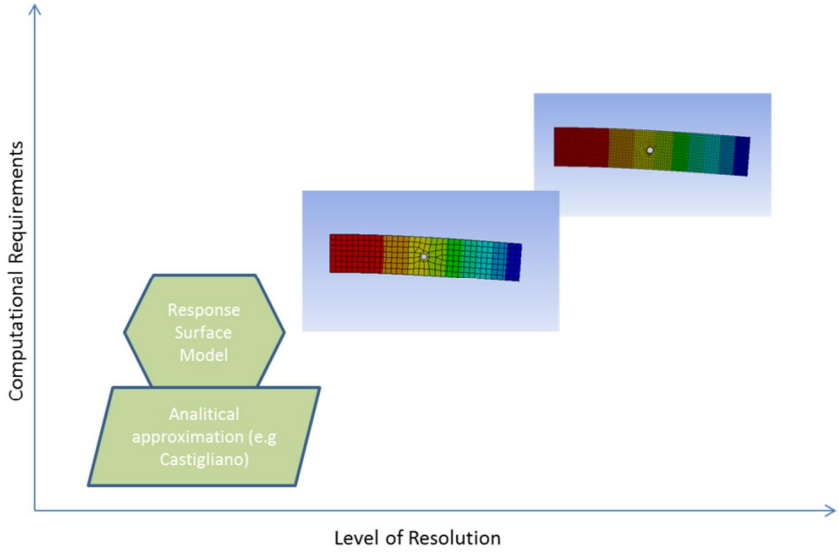

Figure 3. Representation of Multiresolution integration.

In order to create a successful integrated model which exploits the potential of the approach to the maximum, we can envision that we would need to produce this integration in all these directions. The multiscale and multidimensional integration would provide completeness to the scope of the integration while the multiresolution dimension could provide the necessary elements to make the whole simulation manageable.

9.5 The challenge of creating a complete system: putting everything together

As much as we can see a general CAE tool integration as a way to advance the state of the art on product and processes design, we must be realistic and understand the difficulty of the task. The variety of physical phenomena, dimensional and time scales, heterogeinity of tools and platforms and in general the particularities of each of the models and software implementations makes the integration a daunting objective.

If we are ever to achieve this goal of integration, there are many areas in which work needs to be focused and research done. Advances on this areas would contribute towards the final goal. As a non-exhaustive list we could present the following:

- Data exchange: Different CAE tools handle physical entities differently. Their representation of geometry, boundary conditions or input and output data usually difer. And despite several international standards are available and being developed for the exchange of simulation and modelling data (from organisms as SISO, IEEE or ISO). There seems not to be any clear option which is supported by the most common CAE tools. In general, support for those standards is limited at best. A lot of work has been done in this area and still needs to be done to achieve a universal solution.

- Validation and verification: In order to have a useful methodology we need to be sure that the results are reliable. This means that both the underlying mathematical models and their implementations have to be correct and suitable for the simulation task. Individual CAE tools and the models we run with them require already solid validation and verification plans. When we consider an integrated system, this becomes even more important since an error can propagate and magnify along the chain.

- Computational Resource Management: The factor that all CAE tools have in common is that all of them require computers to run. Some models and simulations can be as short as a fraction of a second on a regular desktop machine while others might require supercomputers to run in a reasonable amount of time. Advances in computer technology provide us with an ever increasing availability of computational resources, but still

these are finite and in many occasions the extent of what can be simulated and its level of detail is limited by our computational budget. When chaining different CAE tools together, this need of computational resources gets exacerbated.

    - A useful CAE integration must optimize its structure to the efficient use of all the forms of computation available: single thread solutions, Symmetric Multiprocessing (SMP), Massively Parallel (in clusters or GPU computing). Good queuing systems must be in place to distribute these resources optimally.

– User Interfacing: Connecting different CAE tools and making them work together is only as good as the results we can obtain from them. Most CAE tools, especially commercial ones, include preprocessing tools which help in setting up the problem and postprocessing tools that help in the task of printing and visualizing results. In many occasions this auxiliary tools become as important as the results themselves.

    - When considering an integrated environment, the same consideration is true. Preprocessing and postprocessing tools, as well as monitoring are very important. Work need to be done in creating an homogeneous interface to selected inputs and outputs for the models even if the individual CAE tools are very heterogeneous.

– Data enrichment: Carrying out simulations requires investment of resources. Preparing models and simulations is time consuming and as mentioned earlier some computations might require significant computational efforts. In many cases, simulations are deterministic and for a given set of inputs the outputs would be always the same. So, it only makes sense to keep a record of the simulation results so that computations don't need to be repited. This data can also serve as a basis to create metamodels of the model which can be used as a lower resolution model of the same phenomena with reduced computational cost.

    - Empirical tests are necessary to validate results or as inputs for some CAE tools. Those tests can be rather costly and in some cases even not repeatable at a later stage. So, the recording of results must be done thoroughly. Using historical data from previous simulations or empirical tests to improve the quality and accuracy of our results as well as to reduce the time needed to obtain a solution is what can be called *data enrichment*.

– The last cornerstone: The Methodogy: All the previously mentioned topics as well as a few other that we fail to mention are the building blocks

which we need to consider and study when building a successful multi-scale, multi-dimensional, multi-resolution integrative modelling solution. But the cornerstone of this infrastructure on top of which we have to build is the methodology. Methodology has to dictate what, when and how different CAE tools need to interact and to which level of resolution. If we are designing a mechanical support which will always be working under a static load in a high oxygen environment it wouldn't make sense to expend resources calculating the dynamic behaviour under a cyclic load of the support, but it could be completely sensible to make a corrosion analysis. A good methodology, with the help of the user, has to make use of all the mentioned building blocks to provide a useful solution with the minimum amount of resources invested in obtaining it. If we would build a huge chain of simulation without a proper methodology to exploit it we would found ourselves with an unmanageable system which would be impossible to run to termination with the current computational capabilities, and therefore with no utility.

As already mentioned; in our institute, with a little over 3000 employees, there are about 60 CAE tools employed just in material modelling of some kind. When considering all the disciplines at VTT, the number of codes would be in the hundreds. In the long run, our vision is having the capability to integrate all these tools together and be able to combine all the in-house multidisciplinary expertise in modelling. Already at the moment significant efforts towards that direction are being made. Multi-scale modelling of materials is common practise (1) and the Processing-Structure-Properties-Performance (PSPP) concept (5) is put in practice in areas like tribology.

An ontology based integration platform (6) called Simantics is being actively developed which already has the capability to integrate several different CAE tools, e.g. Apros, Balas or Fluent. Simantics also has the capabilities for creating nice user interfaces to control the models which are integrated. The platform is modular and open-source and can be used by the public which can also contribute to the development.

In addition to this, new concepts for integration based on MultiAgent systems (7) are being tested. In this approach, each model type is treated as an autonomous agent with models with different resolutions (which would include different CAE tools) and they should be capable of interacting with one another by cooperation, coordination and negotiation.

9.6 References

1. Materials Modelling Research in VTT. Yingfeng Shen, Merja Sippola, Kenneth Holmberg, Kim Wallin. Espoo : VTT Technical Research Centre of Finland, 2013. Multiscale modelling and design for engineering applications.

2. Shigley, et al. Mechanical Engineering Design. 7th. s.l. : McGraw-Hill, 2003.

3. Davis PK, Huber RK. Variable-resolution combat modeling: motivations, issues and principles. 1992. RAND Notes.

4. Specification of multi-resolution modeling space for multi-resolution system simulation. Hong, and Kim, Tag Gon. 89, 2012, Simulation.

5. Computational Design of Hierarchically Structured Materials. G.B. Olson, et al. 277, 1997, Science.

6. Open ontology-based integration platform for modeling and simulation in engineering. Karhela, , Niemistö, and Villberg, . 2012, International Journal of Modeling, Simulation and Scientific Computing, Vol. 3, p. 36.

7. Wooldridge. An Introduction to MultiAgent Systems. 2nd. s.l. : Wiley, 2009.

10. Combined CFD, material and system level analyses – Case Naantali power plant

Jari Lappalainen

VTT Technical Research Centre of Finland
Vuorimiehentie 3, P.O. Box 1000, FI-02044 Espoo

10.1 Abstract

This paper discusses the use of mathematical models in solving engineering problems. Undoubtedly there is a need for closer co-operation and co-use of different tools to enhance solving industrial engineering problems. This is shown through a recent case study, where thermal behaviour of evaporator pipes in a power plant was analysed. The main tool is the study was Apros, which is a software for dynamic modelling and simulation of industrial processes, and related automation and electrical systems. Additionally, the work was supported by CFD and thermal stress calculations. A model of a once-through evaporator of a coal power plant was developed, and used to analyse thermal behaviour of the evaporator tubes. Proper knowledge of the boundary conditions at the flue gas side were required. This information was obtained from the existing CFD results on the same evaporator. The main interest in simulations was the differences in pipe temperatures between two alternative control strategies of the evaporator: level control mode, and superheating mode. The simulation results were temperatures, and further interpretation was needed to draw the conclusions of the risk for the material. So yet another mathematical approach was needed to answer the original questions. The modelling part of the case is briefly described, the most interesting results are shown, and the combined use of modelling is discussed.

10.2 Introduction

Many different kinds of modelling and simulation related software tools are used for obtaining information about a new concept or plant under design, or analysing and developing an existing one. The common feature is supporting decision-making in engineering or production problems.

Steady state flow sheet simulators provide state information in various locations of the process system. The state comprises typically pressure, temperature, flow, enthalpy and fluid composition. Detailed dimensioning of the equipment, crucial part of an engineering project, is typically done using proprietary dimensioning programs, e.g. by a boiler manufacturer. These include steady state mass and energy balance solvers, and a great number of experience-based correlations. Computational Fluid Dynamics (CFD) is used to predict flow of fluids inside a piece of equipment. Heat transfer is often included in the studies. For example, boiler suppliers are interested in temperature and flow fields inside the furnace with different designs. The CFD programs help to optimize boiler geometry, and fuel and air feed locations for efficient combustion and heat transfer. In the existing plants, CFD can be used to optimise the operation. A dynamic process simulator differs from steady state simulation with its capability to predict dynamic behaviour. It differs from CFD by using coarser discretisation thus being able to capture larger scope of the process system. It aims to provide a virtual tool that can be operated similarly to the actual plant. However substantially more information about the system is obtained, than by normal process measurements.

Traditionally, the data in different engineering tools, such as P&ID, 3D, or simulation tools, are stored and presented in heterogeneous formats. For sure, deployment of simulation suffers from the fact that tools lay at separate islands which are hard to bridge with any ad-hoc way, within a tight time frame. Consequently, the work may be done with the tool that is the most familiar despite of the fact if is the best or adequete for the job.

During last years, there has been active development to improve tools interoperability in engineering. A key to interconnect and re-use data in different engineering tasks and phases is to apply common well-defined semantics for the data. The different software products must be open to enable export and import of the data contents and models. This need has been widely recognized and related development work is undergoing.

The Naantali case presented in the following was reported earlier by Lappalainen et al. (2012). The study was conducted without any software bridges between the different model based methods used. In other words, results by one tool was interpreted and moved manually into another tool. The case gives an example of the common need to use different tools to find the answers for a practical question from industry, thus highlighting the potential for combination of the tools at an appropriate level.

10.3 Tube damages at power plant

10.3.1 Motivation for the simulation study

The case study assesses conditions of evaporator pipes in a pulverized coal power plant in Naantali. History of the 315 MW power plant origins to the 1970's, with a number of small retrofits taken place during the years. One such a project was undergoing in summer 2010, including reconstruction of some evaporator tubes that had suffered damages, including tube burst, since the last plant maintenance shut-down (see Figure 1).

The damage followed timely by a recent change of control strategy. VTT studied some of the damaged tubes and material analysis suggested that the damaged part had experienced high temperatures (over 500 °C) for substantially long times. Questions arose of circumstances for excessive heating, and, their connection with the recent changes made in control strategy. The circumstances were too challenging for experimental study, so the plant engineers proposed analysis by modelling and simulation.

Figure 1. Some of the damaged evaporator tubes.

10.3.2 The modelling platform

The modelling and simulation platform Apros was used for building a dynamic model of the process area. Apros (www.Apros.fi) provides easy on-line access for configuring and running the simulation models, solution algorithms and model libraries for full-scale modelling and simulation of processes, including combustion power plants, nuclear power plants, and pulp and paper mills. Besides the pro-

cess, also automation and electrical systems can be modelled in detail. The extent of the applications varies from small computational experiments to models for full-scope training simulators. The model libraries have been comprehensively validated against data from physical process experiments.

The simulator offers predefined component models that are conceptually analogous with the actual devices, such as pipes, valves, pumps, heat exchangers, reactors, tanks, measurements, signal processing, controllers, electric devices, etc. The user drags and drops appropriate process components from model library palettes, draws connections, and enters process related input data. Parameterisation is straightforward, and most importantly, the tool hides all solution algorithms. The model libraries include models from simple to high fidelity. This way one can create an optimal model structure in respect of model fidelity needs, development time available, and simulation speed requirements. Several types of solvers for thermal hydraulic networks can be used, depending on the demanded fidelity level. The thermal hydraulics solvers provide means for solving of fluid flows, heat conduction in solid structures and between fluids and structures. In the solution, the model is considered as a network of nodes, i.e. control volumes, and branches, i.e. connections between the nodes. This calculation level network is managed automatically by the process component level, which is the level where user operates. The primary state variables of the thermal hydraulic nodes are pressure, enthalpy, and component mass fractions, and flow velocities for branches. Material property functions are used in calculating various quantities, such as density, viscosity, thermal conductivity and heat capacity according to the state variables. The equation solver processes the large systems of linear equations, which arise from the discretisation and linearisation of partial differential equations with respect to space and time. In addition to model configuration the modelling interface provides tools to manage simulation experiments, and to visualize the dynamic behaviour of the simulated system. The user can freely select any component variables to be displayed on the flowsheet diagrams as numerical values (monitor fields) or as trends in separate windows. During a simulation run, the model diagrams can be used for modifying component properties, e.g. controller set values, controller tuning parameters, starting/stopping devices. Any variable data can be logged to file for post-processing purposes.

10.3.3 The model building

In this case study, the scope of the modelling covers half of the evaporator, including 16 pipelines. The evaporator composes of two identical halves, which of the one with most pipe damages was selected. Model diagrams were used to organize the model configuration into suitable sub-processes, see the following figures for examples.

Most of the input data was taken from the original design drawings, including mainly locations and physical dimensions of process equipment and pipelines. The length and friction losses due to bends in the pipelines were studied and

modelled in detail from the design drawings, in order to show up any differences among the individual tubes due to their different routes at the boiler walls. Also appropriate data to define the model boundaries was needed, such as pressures, temperatures, and the heating power to the evaporator tubes.

The selected thermohydraulic model for this simulation study was the non-equilibrium separate phase flow (so-called 6-equation) model, which calculates the dynamic mass, energy, and momentum balances for both liquid and gas phases of water. This choice guaranteed that the modelling should capture any thermohydraulically meaningful phenomena taking place in the evaporator pipes.

The model starts from a point after the economizer, before the header that distributes the individual evaporator pipelines, see Figure 2. The length of each pipeline inside the evaporator is approximately 260 m, and this length was discretised into 65 pieces in the modelling. Additionally, there were two pipelines with more accurate discretisation.

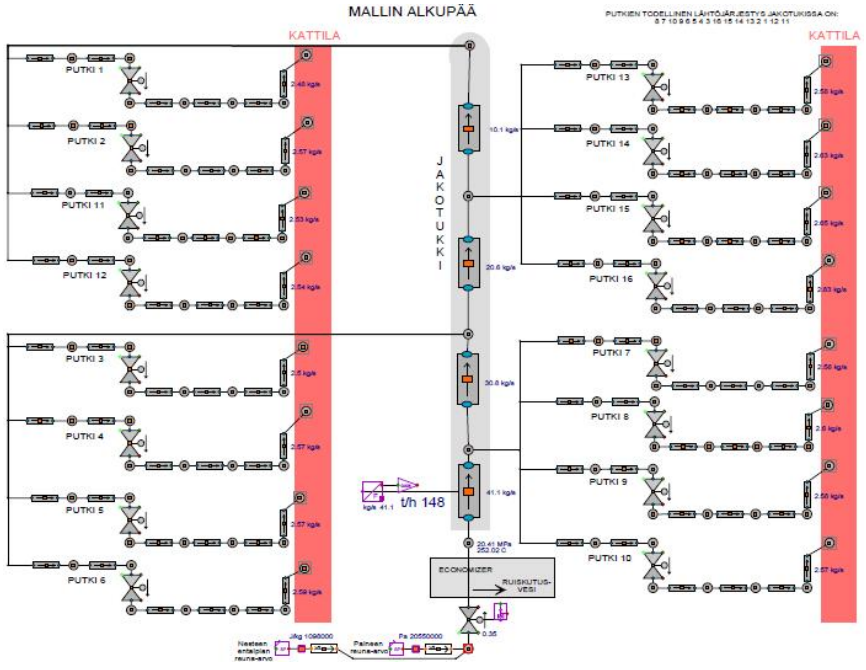

Figure 2. The model starts where the evaporator tubes separate out from the header after the economizer.

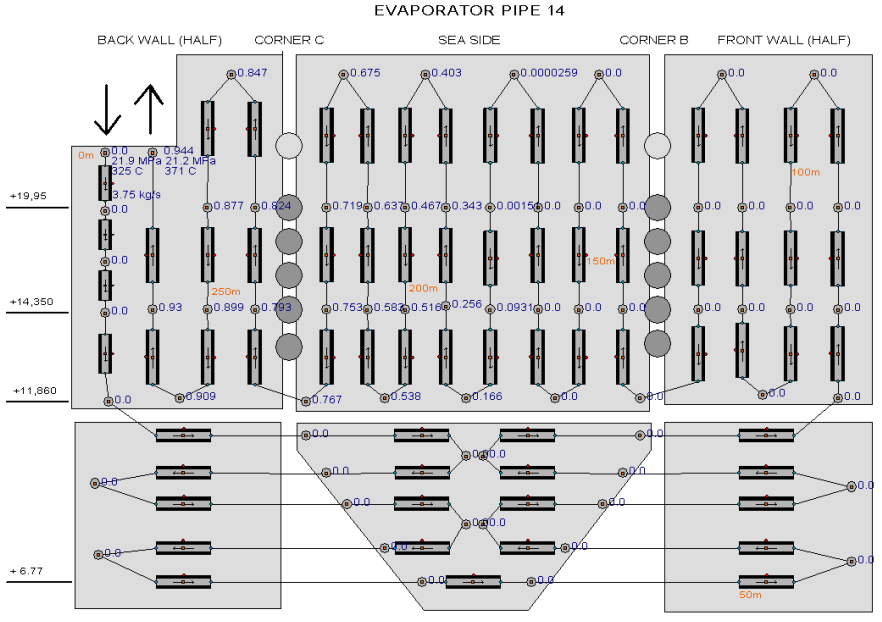

Figure 3. The route of each tube inside the evaporator was modelled like shown here.

Figure 3 is an example of a diagram showing an individual tube route inside the evaporator, as part of the water wall. In order to provide a realistic model for surface temperatures of the evaporator pipes inside the furnace, it was essential to model the pipeline's route on the walls including accurate positioning of turning points and elevations. The route of the pipeline starts at the back wall, it goes down to the cone, and starts to zigzag horizontally until the bottom part is fully covered. Then it rises upwards in the front wall, and zigzags the whole half of the furnace up and down, until comes back in the starting point and exits the furnace. The burners and air ports in the corners are marked in the figure too. The pipeline model composes of a series of heat pipe modules, having a thermohydraulic point in between. The heat pipe component includes also the pipe wall's heat structure. The average length of the pipe parts is 4 meters in this case. In addition, the heat structure of each pipe module is axially divided in two parts. There are 16 individual tubes that travel throughout the furnace half, installed next to each other. After the evaporator, these tubes are combined in a header, and the resulted flow is lead to a water steam separator (Sulzer bottle), which acts as the end boundary for the model.

The modelling did not include the burning and flue gas side of the boiler. Accordingly, the heating power from the combustion had to be defined as boundary condition to each heat pipe component that a tube model is constructed of. Initially, the heating power was considered as a constant value throughout the water

wall. The first simulation results revealed that this approximation was poor. Fortunately a CFD study of this same boiler had been conducted some time earlier. These CFD results were used to derive a more realistic heating power levels as a function of elevation. Additionally, the boiler corners were considered separately. Thus the heating power was transmitted to each heat pipe component by its position inside the furnace. The heating power levels ranged from 150 to 500 kW/m2. The bottom part of the evaporator, for example, was treated with the lowest power.

10.3.4 Results

The main interest in the simulation study was the peak temperatures and their localisation in the evaporator tubes in different situations. The study focused on comparing two different control strategies to operate the evaporator:

Control mode 1: Level control of the water-steam separation bottle

Control mode 2: Superheating state control

The traditional operation mode (Control mode 1) keeps part of the out coming water from the evaporator in liquid phase, and accordingly the water steam separator is run with liquid level in closed-loop control. In the other mode (Control mode 2) the out coming steam gets superheated, and the level of superheating is controlled. The reference states representing operation in these control modes were taken from historical data. To reach an operational state like this in the model, the boundary pressures and flow conditions were firstly set according to the reference state. Then, the heating power was adjusted to produce a proper match with the plant measurements. While the level of heating power was adjusted, its relative profile was not changed.

Besides the simulation of normal operation in these modes, also transients were simulated, such as throttling of a pipe, and reducing the feed flow. Special emphasis was put on simulation analysis to the part of the evaporator where the pipe damages had taken place. In the following, some illustrative samples of simulation results are described.

Simulation example A: Control modes 1 and 2, reference conditions. Power plants are operated long times in rather steady conditions, and it is important to analyze the system in these typical conditions, especially if there is suspicion of harmful condition for process equipment. Figure 4 illustrates conditions inside one evaporator tube (number 14) in control modes 1 and 2. Steam void fraction is presented, as well as pressure and temperature as function of the cumulative length of the tube. It is seen that the pressure and temperature are higher in Control mode 2, and evaporation starts earlier, than in Control mode 1. Furthermore, in Control mode 2, in the end of the tube, all liquid is evaporated and steam gets superheated.

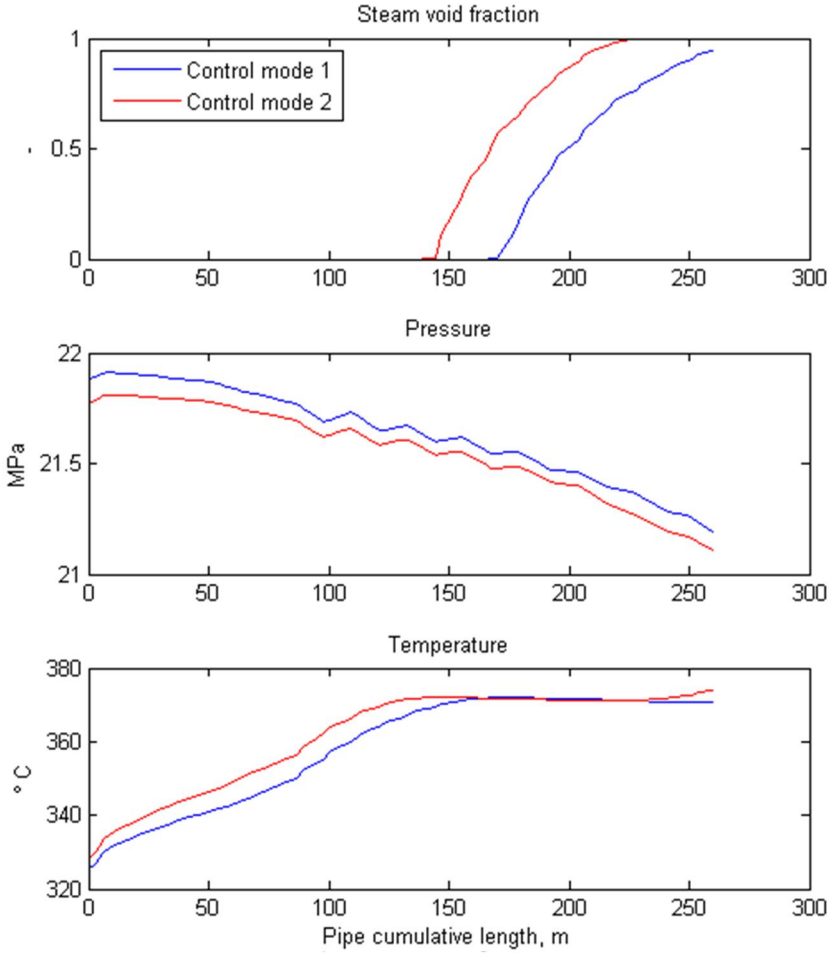

Figure 4. Simulation example A. Selected variables as profiles along one evaporator pipeline in different operation modes (system in steady state).

Simulation example B: Control mode 2, feed flow decreased with constant heating power. This simulation study illustrates the dynamics of the water wall piping in a disturbance, where the evaporator feed flow rate drops quickly but heating power stays constant. The feed flow was changed simply by setting 30% lower set point for the controller. The outer surface temperature of one tube (number 14) was selected to demonstrate the transient. Figure 5 shows the reference state for Control mode 2, and four time instants after the initiation of the disturb-

ance. The new steady state is reached in 4–5 minutes, and the end of the pipe heats up to over 500 °C.

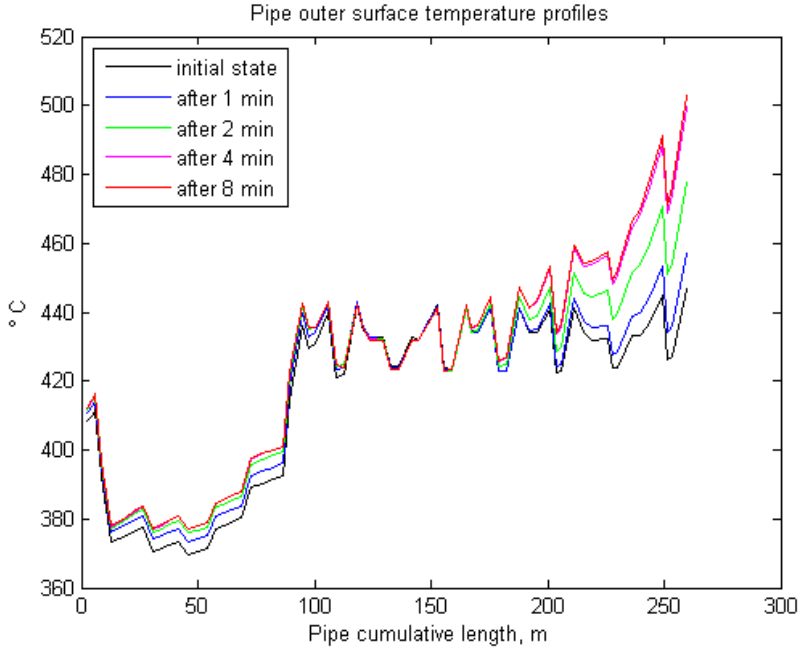

Figure 5. Simulation example B. Tube outer surface temperature profiles along one evaporator pipeline at different time instants after the disturbance.

10.3.5 Outcome of the simulation study

The simulation study was initiated due to the damages in the evaporator pipes, followed timely by a recent change of control strategy. The study showed that operation in superheating control mode does not stress these parts of the pipelines substantially more than level control mode. This was seen both in normal operation and in the transients simulated. In superheating control mode, end of the pipelines heated up more than in level control mode, but the risk for the pipe material was still considered low in normal long term operation conditions. In superheating control mode, however, the end side of the piping is clearly more sensitive for excessive high temperatures in case of power or flow disturbances. This must be addressed when planning operational practices. The major outcome was the obtained understanding of the practical meaning of different factors in the operation of the water steam side of the boiler.

10.4 Discussion

The strength of the Apros model build for this study is the rather detailed modeling of the pipelines, including the path on the walls, friction losses, heat transfer and thermohydraulic solution. The model scope was limited to just what was necessary to capture the two alternative operation modes that were compared. The simple approach used in modeling the heating power to the evaporator pipelines as static source terms can be considered as a weakness. There however the use of CFD results improved the accuracy of the approach. The heating power stayed constant regardless of the changing conditions inside the pipes, and in the pipe wall. One possible development step is to model the combustion and the flue gas flow in the furnace in Apros. The most sofisticated approach would be to combine the CFD simulation with the Apros model. Another useful link would be to transfer the Apros results into calculation of material lifetime. This would speed up the interpretation of the simulation results into practically and economically interesting figures, such as maintenance costs and prediction of operation life time.

10.5 Conclusions

This paper discussed combined use of model based methods in solving engineering problems, illustrated by a power plant case, where simulation was initiated due to the damages in the evaporator pipes. The major outcome was a good understanding of the practically meaningful factors in the problem case. To complete the study successfully, knowledge from two different model based calculations were utilised. The heating power form the combustion to different locations in the evaporator was estimated with the aid of CFD simulations. The simulation results in different operational conditions produced temperature profiles of the evaporator tubing, which were used to assess the risk for the tube material.

10.6 Acknowledgements

The author wish to thank Mechanical Maintenance Manager Harri Blom from Fortum Power and Heat Oy in Naantali who has greatly contributed to this study and its publishing.

10.7 Literature

Lappalainen, J., Blom, H, Juslin, K., Dynamic process simulation as an engineering tool – A case of analysing a coal plant evaporator, VGB Powertech – International Journal for Electricity and Heat Generation, 1/2 2012, pp. 62–68.

11. Combined structural analyses and system level simulation – Cases 1) Apros-TVO PAMS and 2) Apros-Abaqus Co-use

Pasi Laakso

VTT Technical Research Centre of Finland
Vuorimiehentie 3, P.O. Box 1000, FI-02044 Espoo

11.1 Abstract

This paper discusses about combined usage of structural analysis and system level simulation. Application area is continuous processes and their pipeline systems e.g. Power plants. Main idea is to base structural analysis on simulated transients. Simulation results include e.g. time dependant behaviour of pressures and temperatures. Simulation model can be done manually or automatically based on data read from plant databases or directly from the model taken from the structural analysis tool. Similarly structural analysis model can be either hand-made or based on information read from plant databases or simulation model. This paper concentrates on 2 recent cases that are done at VTT i.e. connecting Apros dynamic process simulator to TVO's Pams piping database and Abaqus commercial structural analyses tool.

11.2 Introduction

Structural analysis is important tool when analysing the endurance of the process plant equipment. It can be used to optimize operational procedures to minimize the load caused or alternatively to try to define how long equipment will last and when it should be replaced. This is especially important on safety critical systems like nuclear power plants. This analysis requires time series information concern-

ing the realistic process behaviour that occurs over the years. When measurement data is available it can be used. However there are also scenarios where measurements are not enough and more data needs to be generated using dynamic simulation e.g. when testing different operation procedures.

VTT has been integrating structural analysis and system level simulation in 2 recent projects. In both cases simulations has been done using Apros. In the earlier case TVO's (Teollisuuden voima) Pams database was the tool combined to Apros. In latter just started case Abaqus tool will be combined to Apros. Also few years back there was a project where Apros simulations were used as a basis for structural analysis done in Abaqus. This was mainly manual transfer. Now in the recent project data transfer will be automated.

Pams is not actually a structural analyser code. It is more like a database that stores plant model in a format that is useful for structural analyses purposes. It can take advantage of other tools like FPipe to perform structural analysis. It contains nodes that are coordinates in 3D space and elements that are connections (straight pipes, valves, bends...) between the nodes. Elements have also cross section definitions i.e. pipe diameter and wall thicknesses. Database has also detailed material properties tables for storing pipe materials, including insulation and plate. It also contains reference transients used for structural analysis. These transients are typically conservative i.e. describing the worst case scenario. They are typically done without simulations based on the experts manually defining the cases. Apros simulations best estimate type, meaning that they try to replicate the plant behaviour as closely as possible. Both conservative and best estimate transient still have their uses.

Abaqus is a tool made specifically for structural analysis. It can be used to analyse micro level cases like welds or alternatively macro level where larger pipeline system is under inspection. Its database structure closely resembles the Pams structure. Main components are nodes that are just dots in 3D space and elements between 2 nodes.

Database structure of Apros is pretty close to these. It has a concept of point that has very close resemblance for nodes and then there are pipes and valves that are very close to the elements in both Pams and Abaqus

11.3 Case Apros – TVO-Pams

The goal of the project was to enable using Apros to generate time series data to be used for structural analysis. TVO’s Pams software stores the plant model and can initiate other software to do e.g. structural analysis (like FPipe) and run dynamic simulation (Apros). One of the key ideas is that plant wide simulation model is used for running the transients. This way the boundaries of the load area under investigation behave realistically. If we would just model the area under inspection, defining realistic behaviour of the boundaries would be much more challenging task.

Tool called Pamros was developed to do the needed tasks. It gets Pams input file that contains a detailed description of a subprocess that it wants to be analysed e.g. nodes and elements, cross sections and materials. It also defines which initial state and transient should be executed. Project utilised also ready-made Apros simulation model of the Olkiluoto NPP. The idea is that small part of the whole plant model is replaced by the automatically generated detailed model. Automatic generation takes care of many details e.g. loss caused by bends, reducers and expanders is calculated and then used in simulation. The additions to existing model are based on the input data coming from Pams. Pams input data also specifies the output variables it expects to be collected during the transient.

After model improvements simulation model is stabilized and then the real simulation case i.e. transient is started. Pamros stores the predefined variables every time step while the simulation is running. After the run, results are gone through and excess data not necessary for structural analysis is removed and then finally results are given back to Pams that stores them to be used later for further analysis.

Pams is the initiator in this scenario. It generates the needed input file that contains detailed description of nodes and elements and gives it to Pamros. Pamros then makes the needed changes to the Apros model and calculates the results. Whole work flow is presented in Figure 1.

Currently couple of test cases has been executed and continuation for the project is under planning. It has been found out that using the plant wide simulation model is in some cases quite time consuming. This means that unless the value of getting realistic plant response is essential one can use smaller simulation models that just describe the area of intrest. Further projects will be focused on this approach.

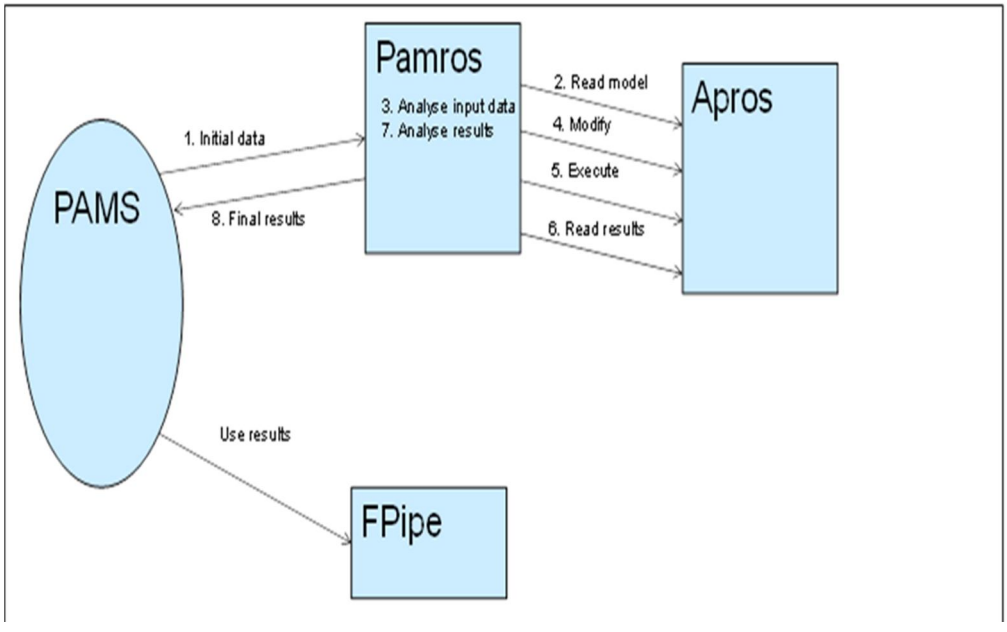

Figure 1. Pamros work flow.

11.4 Case Abaqus – Apros

This project has just been started. 1st manual excersice from generating input model from Abaqus and then making manually corresponding Apros model has been made. Goal has been to replicate the case from few years back where Apros was used in similar manner to generate input data for Abaqus. The eperiences gained from manual data transfer will then be basis for requirements analysis of the tool conencting the software together.

It is likely that the in this case tool is developed from the perspective of the system simulator. Here the simulation model is made before structural analysis and simulation model will be used to generate Abaqus model. Simulation results will be fed simultaneously to Abaqus.

Figure 2 shows the 1st simple example case that is a short pipeline having 3 corners. One detail from the corresponding hand-made Apros simulation model is in Figure 3. Also 1st transient has been executed using the model and Abaqus analysis will be next step. After this all the work phases are gone through manually.

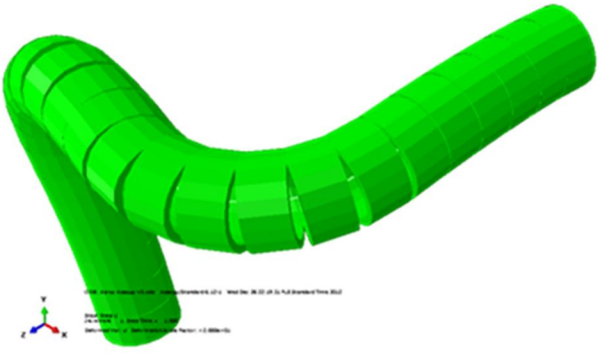

Figure 2. Abaqus pipeline.

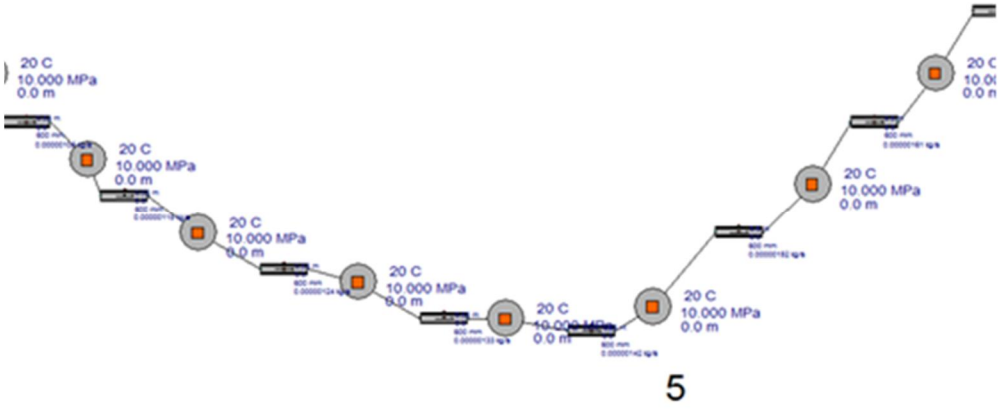

Figure 3. Detail from Apros simulation model.

11.5 Conclusions

Recently several software integration projects have been initiated. VTT has been implementing Open source integration platform called Simantics that has been basis when integrating e.g. CFD simulations to other simulation tools as well as integrating plant databases like Comos and Smartplant Foundation to simulator tools. Combining also structural analysis and dynamic simulation can be seen as a continuation to this ongoing trend.

New tools will enable using simulation results as a basis for structural analysis. Users of both tools can benefit from combination of simulation and structural analysis. This will give opportunities to analyse e.g. cases where the plant doesn't

even exist yet. Also not all the measurements needed are always available so simulation can be used to generate more data for analysis purposes. Other potential approach is that system level simulator has modelled a design he wants to verify using structural analysis. In this case the simulation model needs to be converted to a form suitable for structural analysis. It has been found out that all tools involved have pretty similar structures for storing data.

12. Optimizing life-cycle environmental performance of a value chain with MultiDesign approach

Tuomas Helin

VTT Technical Research Centre of Finland
Tekniikantie 2, P.O. Box 1000, FI-02044 Espoo

12.1 Abstract

To be competitive in today's society and business environment one needs to focus on overall acceptability of the activity and not only performance, properties and cost of the designed product or system. Sustainable business and design manages corporate social responsibility towards stakeholders, including environmental aspects. It addresses energy and resource efficiency, pollution prevention and air quality. VTT has the necessary knowhow and simulation platforms to introduce the modelling of environmental performance into Multiscale design of value chains.

Life cycle assessment (LCA) is an ISO 14040-14044 standardised methodology that has been developed to gain a better understanding of potential environmental impacts of product value chains. A life cycle approach ascertains that burden shifting of environmental impacts of studied value chain or system can be avoided: Partial optimisation that focuses on minimising environmental impacts of only one component or processing stage includes a risk that major impacts up or down the value chain are not identified and total impacts of the system may even increase. One example is a comparison of climate impacts of two stainless steel grades, austenitic and duplex, used in tanks for road transport of liquids (Ovaskainen 2011): Although manufacturing of duplex-grade steel causes more greenhouse gas (GHG) emissions per mass unit than manufacturing of austenitic steel, still the duplex steel causes less GHG emissions in road transport system due allowing lighter tanks and thus lower fuel consumption of the vehicle. Thus, it is advisable

model the whole system of interest with LCA to avoid burden shifting. VTT provides the necessary knowledge and software tools for carrying out LCA studies. LCA method and key integration potentials are presented in figure below.

VTT is active in developing LCA software tools on Simantics platform that will facilitate integration of LCA modelling with e.g. component, process and system level design tools. Output data from other modelling tools can be seamlessly integrated to be used as input data in LCA software to allow dynamic modelling of environmental impacts of different product system designs. The output from LCA software, environmental impact indicator result, can then be used as an input for e.g. component design tool as an additional design criteria. A component designer could get direct feedback on environmental impacts of individual decisions in such integrated modelling platform.

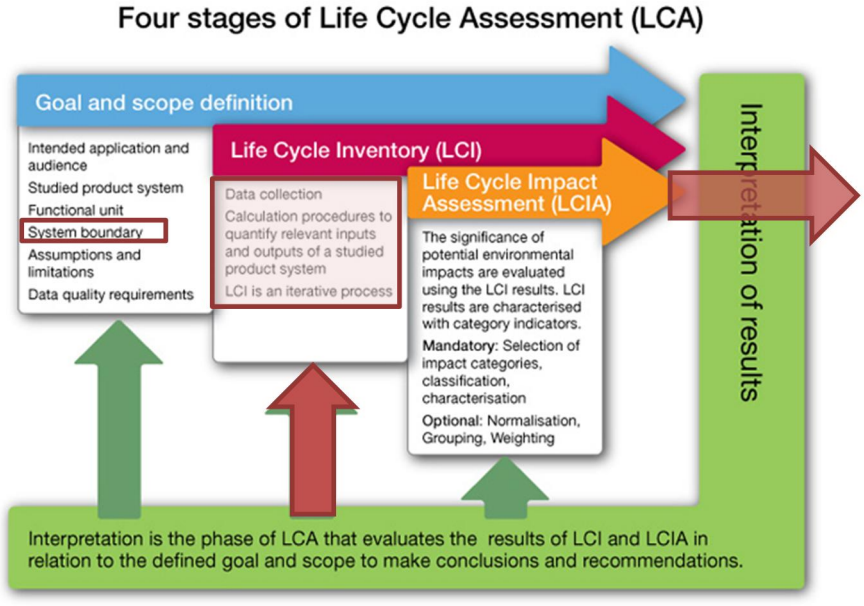

Figure 1. Structure of LCA method. Red arrows and squares show the potential data flows to be integrated to other modelling tools in MultiDesign platform.

Series title and number
VTT Technology 77

Title	**Multiscale modelling and design for engineering application**
Author(s)	Tarja Laitinen & Kim Wallin (Eds.)
Abstract	Utilizing 3D design procedures in manufacturing industry is well matured in industrial R&D. The shape of the components, design of the machine or the vehicle, assembly and finally the whole production are designed virtually through computational methods, which naturally offer flexibility and speed to the design phase. Simulation and virtual verification of the designed components is rapidly increasing and can further shorten R&D phase dramatically. However, virtual material values or models available for digital design and simulation are still limited. Due to the lack of digital material values the huge potential of tailoring performance cannot be fully exploited. VTT has recognized that for the economic and ecologic use of materials, digital design tools are a necessity of the digital design chain covering the whole region from material modelling to functional design. Development of new materials and understanding of material and process behaviour is always a complex equation of crossing interactions. Physical and chemical phenomena are affected from the nano- and/or molecular level up to macroscopic level. Interactions between the material performance, properties, microstructure and processing methods need to be understood more deeply. For this purpose, modelling skills have developed rapidly in recent decades both in industry and in academia, with the support of increased numerical calculation capacity and commercial multi-level and multi-physics software development. In this publication we are presenting some highlights from our current modelling activities obtained within VTT's MultiDesign innovation programme. We hope they will inspire new ideas on what could be done and obtained via digital approach to design.
ISBN, ISSN	ISBN 978-951-38-7913-6 (Soft back ed.) ISBN 978-951-38-7914-3 (URL: http://www.vtt.fi/publications/index.jsp) ISSN-L 2242-1211 ISSN 2242-1211 (Print) ISSN 2242-122X (Online)
Date	February 2013
Language	English
Pages	122 p.
Keywords	Multiscale modelling, design, material performance, simulation
Publisher	VTT Technical Research Centre of Finland P.O. Box 1000, FI-02044 VTT, Finland, Tel. 020 722 111

VTT Technical Research Centre of Finland is a globally networked multitechnological contract research organization. VTT provides high-end technology solutions, research and innovation services. We enhance our customers' competitiveness, thereby creating prerequisites for society's sustainable development, employment, and wellbeing.

Turnover: EUR 300 million
Personnel: 3,200

VTT publications

VTT employees publish their research results in Finnish and foreign scientific journals, trade periodicals and publication series, in books, in conference papers, in patents and in VTT's own publication series. The VTT publication series are VTT Visions, VTT Science, VTT Technology and VTT Research Highlights. About 100 high-quality scientific and professional publications are released in these series each year. All the publications are released in electronic format and most of them also in print.

VTT Visions

This series contains future visions and foresights on technological, societal and business topics that VTT considers important. It is aimed primarily at decision-makers and experts in companies and in public administration.

VTT Science

This series showcases VTT's scientific expertise and features doctoral dissertations and other peer-reviewed publications. It is aimed primarily at researchers and the scientific community.

VTT Technology

This series features the outcomes of public research projects, technology and market reviews, literature reviews, manuals and papers from conferences organised by VTT. It is aimed at professionals, developers and practical users.

VTT Research Highlights

This series presents summaries of recent research results, solutions and impacts in selected VTT research areas. Its target group consists of customers, decision-makers and collaborators.

Multiscale modelling and design for engineering application

Utilizing 3D design procedures in manufacturing industry is well matured in industrial R&D. The shape of the components, design of the machine or the vehicle, assembly and finally the whole production are designed virtually through computational methods, which naturally offer flexibility and speed to the design phase. Simulation and virtual verification of the designed components is rapidly increasing and can further shorten R&D phase dramatically.

However, virtual material values or models available for digital design and simulation are still limited. Due to the lack of digital material values the huge potential of tailoring performance cannot be fully exploited. VTT has recognized that for the economic and ecologic use of materials, digital design tools are a necessity of the digital design chain covering the whole region from material modelling to functional design.

Development of new materials and understanding of material and process behaviour is always a complex equation of crossing interactions. Physical and chemical phenomena are affected from the nano- and/or molecular level up to macroscopic level. Interactions between the material performance, properties, microstructure and processing methods need to be understood more deeply. For this purpose, modelling skills have developed rapidly in recent decades both in industry and in academia, with the support of increased numerical calculation capacity and commercial multi-level and multi-physics software development.

In this publication we are presenting some highlights from our current modelling activities obtained within VTT's MultiDesign innovation programme. We hope they will inspire new ideas on what could be done and obtained via digital approach to design.

ISBN 978-951-38-7913-6 (Soft back ed.)
ISBN 978-951-38-7914-3 (URL: http://www.vtt.fi/publications/index.jsp)
ISSN-L 2242-1211
ISSN 2242-1211 (Print)
ISSN 2242-122X (Online)